Washington University in St. Louis
Washington University Open Scholarship

Arts & Sciences Electronic Theses and Dissertations

Arts & Sciences

Summer 8-15-2010

Functional, degradable polyester materials synthesized from poly(epsilon-caprolactone-co-2-oxepane-1,5-dione): An investigation into the derivatization, self assembly, and degradation behavior of poly(epsilon-caprolactone)-based materials

Rhiannon K. Iha
Washington University in St. Louis

Follow this and additional works at: https://openscholarship.wustl.edu/art_sci_etds

 Part of the Chemistry Commons

Recommended Citation

Iha, Rhiannon K., "Functional, degradable polyester materials synthesized from poly(epsilon-caprolactone-co-2-oxepane-1,5-dione): An investigation into the derivatization, self assembly, and degradation behavior of poly(epsilon-caprolactone)-based materials" (2010). *Arts & Sciences Electronic Theses and Dissertations*. 503.
https://openscholarship.wustl.edu/art_sci_etds/503

This Dissertation is brought to you for free and open access by the Arts & Sciences at Washington University Open Scholarship. It has been accepted for inclusion in Arts & Sciences Electronic Theses and Dissertations by an authorized administrator of Washington University Open Scholarship. For more information, please contact digital@wumail.wustl.edu.

WASHINGTON UNIVERSITY IN SAINT LOUIS

Department of Chemistry

Dissertation Examination Committee:
Professor Karen L. Wooley, Co-Chair
Professor Joshua A. Maurer, Co-Chair
Professor Willam E. Buhro
Professor Garland R. Marshall
Professor Jacob Schaefer
Professor Jay R. Turner

Functional, degradable polyester materials synthesized from poly(ε-caprolactone-*co*-2-oxepane-1,5-dione): An investigation into the derivatization, self assembly, and degradation behavior of poly(ε-caprolactone)-based materials

by

Rhiannon K. Iha

A dissertation presented to the
Graduate School of Arts and Sciences
of Washington University
in partial fulfillment of the
requirements for the degree
of Doctor of Philosophy

August 2010

Saint Louis, Missouri

Copyright

Rhiannon K. Iha

2010

ABSTRACT OF THE DISSERTATION

Functional, degradable polyester materials synthesized from

poly(ε-caprolactone-*co*-2-oxepane-1,5-dione):

An investigation into the derivatization, self assembly, and degradation behavior of

poly(ε-caprolactone)-based materials

by

Rhiannon K. Iha

Doctor of Philosophy in Chemistry

Washington University in Saint Louis, 2010

Professor Karen L. Wooley, Chairperson

Biocompatible, degradable polymers possessing a high degree of complexity are an extremely desirable target for many applications. In order to further develop the range and utility of materials made from aliphatic polyesters, poly(ε-caprolactone-*co*-2-oxepane-1,5-dione) (P(CL-*co*-OPD)) was used as a polymeric precursor for the construction of a series of functional polyester-based materials. By taking advantage of the electrophilic ketone moieties characteristic of the OPD repeat unit, small molecule and polymer grafts were attached to the PCL backbone through the formation of both hydrazone and ketoxime ether linkages. This work has focused on both the synthesis and characterization of functional, degradable polyesters, including amphiphilic block graft copolymers, that possess significant potential for future use in diagnostic and therapeutic applications.

A dansyl-functionalized poly(ε-caprolactone) was synthesized by reacting (P(CL-*co*-OPD) with dansyl hydrazine. The resulting dansylated-PCL displayed interesting fluorescence behavior and showed solvent polarity dependance as the fluorescence emission maxima (λ_{em}) shifted from 494 nm in toluene to 526 nm in dimethyl sulfoxide (DMSO). Analysis of the λ_{em} of the dansyl-grafted polymer and a dansyl-functionalized small molecule analog with respect to three different solvent polarity parameters indicated that the fluorescence emission spectra of the dansylated polymer was influenced by solvent polarity, but that the dansyl fluorophore was overall less sensitive to the surrounding medium when grafted onto the polyester backbone.

Degradable, amphiphilic graft copolymers of poly(ε-caprolactone)-*graft*-poly(ethylene oxide), PCL-*g*-PEO, were synthesized *via* a "grafting onto" strategy taking advantage of the ketones presented along the backbone of the statistical copolymer (PCL-*co*-OPD). Through the formation of stable ketoxime ether linkages, 3 kDa poly(ethylene oxide) (PEO) grafts and *p*-methoxybenzyl (*p*MeOBn) side chains were incorporated onto the polyester backbone with a high degree of fidelity and efficiency, as verified by NMR spectroscopy and GPC analysis (90% grafting efficiency in some cases). The resulting block graft copolymers displayed significant thermal differences, specifically a depression in the observed melting transition temperature, T_m, in comparison to the parent PCL and PEO polymers. These amphiphilic block graft copolymers underwent self assembly in aqueous solution with the P(CL-*co*-OPD-*co*-(OPD-*g*-PEO)) polymer forming globular micelles and a P(CL-*co*-OPD-*co*-(OPD-*g*-PEO)-*co*-(OPD-*g*-*p*MeOBn)) forming cylindrical or rod-like micelles, as observed by transmission electron microscopy (TEM) and atomic force microscopy (AFM).

PCL-*g*-PEO copolymers synthesized from PCL-*co*-OPD that still contained free OPD units were found to undergo an early and rapid degradation upon being dispersed in aqueous solution. P(CL_{92}-*co*-OPD_5-*co*-(OPD-*g*-$PEO)_9$) showed immediate signs of degradation upon being dispersed in aqueous solution based upon both ^{1}H NMR spectroscopy and gel permeation chromatography (GPC) analysis. The solution state aggregates showed a minimal increase in aggregate size moving from a number-averaged hydrodynamic diameter (D_h) of 13 ± 3 nm at 0 h to 17 ± 3 nm at 24 h based upon analysis by dynamic light scattering (DLS). An increase in diameter upon degradation was corroborated by transmission electron microscopy (TEM) images showing circular particles that had a D_{av} of 15 ± 4 nm and 22 ± 5 nm at 0 and 24 h respectively. P(CL_{92}-*co*-(OPD-*g*-$PEO)_8$-*co*-(OPD-*g*-*p*$MeOBn)_6$), a polyester having no free OPD units, showed no signs of rapid degradation over 24 h by ^{1}H NMR or GPC analysis. Characterization of the solution state aggregates by DLS and TEM indicated that the circular particles formed by the PCL-*g*-PEO copolymer maintained both their size and morphology while being dispersed in aqueous solution for 24 h. P(CL_{327}-*co*-OPD_{22}-*co*-(OPD-*g*-$PEO)_{15}$-*co*-(OPD-*g*-*p*$MeOBn)_8$), a significantly larger PCL-PEO ketoxime ether conjugate possessing free OPD units, also showed signs of backbone degradation by ^{1}H NMR and GPC upon being transitioned into aqueous solution. DLS analysis, of the solution state aggregates formed by this amphiphilic block graft copolymer showed no substantial changes in the hydrodynamic diameter over time. However, characterization by TEM showed a transition from circular to rod-like or cylindrical aggregates as hydrolysis occurred.

To Starbucks and the many barristas that made this dissertation a reality.

ACKNOWLEDGEMENTS

I never know what to say in sections like this, whom to thank or how to thank them. So let's just make the most of this and see how it goes…

I would like to thank my advisor, Professor Karen L. Wooley, for her mentorship, advice, and for always being perplexed by my sense of humor. During my time at Washington University, Karen rarely told me what to do, but instead allowed me to hit my head against the wall, figure things out for myself, and grow as a chemist and as a person. Her knowledge, work ethic, and high expectations are something that I have always found impressive and hope to be able to emulate.

I would like to thank my committee Professor Jacob Schaefer and Professor Josh Maurer for their questions, advice, suggestions and support as I pursued research that at times felt impossible and inexplicable. I would also like to thank the other members of my dissertation examination committee, Professor Willam Buhro, Professor Garland Marshall, and Professor Jay Turner.

I am, of course, indebted to numerous members of the Department of Chemistry staff including Norma Taylor, Jessica Owens, Angie Stevens, and Phyllis Nolken. Without the help of these individuals I certainly would have been lost in the red-tape and seas of paper work. I would like to thank Dr. Andre D'Avignon for assistance with NMR spectroscopy as well as his generally sane and sound advice given during times of absolute insanity. Dr. Edwin Hiss deserves a special thank you, because without his help, I most assuredly would not have made it through graduate school alive.

The Wooley Group, past and present, deserves a significant amount of thanks, mostly for putting up with me and my antics, but also for good advice, academic discussions, criticism, and late night coffee. I of course need to thank all of my Wooley Group friends and colleagues: To Nam and Jeremy, my lab husbands—I don't know how this works exactly, but it really is the only way to explain it—thanks for understanding the need to have scotch in the desk drawer and for having the occasional drink with me. To David, for suggesting that I work on conducting polymers during my time at graduate school, and to Brooke for helping me find something else to work on when that fell through. To Ritu and Sandani, for their help getting through the end of this and helping me make it out of Texas alive. To Yali and Lily for their friendship and love of silly pop music.

Bryn. Thank you. It's never enough and never will be, but it's all that I have.

There are of course people outside of lab that deserve thanks simply for putting up with me—especially at the end of this journey. These are the friends that literally became family. Bryn, Chase, Cyller, Hank, Tiffany, Tristen, Kara, Tabbi, Tyler, Ryder, Nik, Ace, Randal, Mimi, Daniella, Shayna, Seth, Taylor, Becky, Nikita, Natasha, and Erin you guys were the glue that held my sanity together and chemically encouraged me to stay awake and see this through to the end.

I think that's everything and everyone, but if I forgot anyone, this thank you goes out to you.

~Cheers! It's been a wild ride~

TABLE OF CONTENTS

LIST OF FIGURES

Figure 3-2 (a) ^{1}H NMR spectra (300 MHz, $CDCl_3$) of the parent P(CL-*co*-OPD) polymer, **3** (red), P(CL-*co*-OPD-*co*-(OPD-*g*-PEO)), **4** (blue), a fully functionalized P(CL-*co*-OPD-*co*-(ODP-*g*-*p*MeOBn)) (purple), and P(CL-*co*-OPD-*co*-(OPD-*g*-PEO)-*co*-(OPD-*g*-*p*MeOBn)), **5** (green). **(b)** An overlay of GPC RI traces of the parent P(CL-*co*-OPD) polymer, **3** (red), P(CL-*co*-OPD-*co*-(OPD-*g*-PEO)), **4** (blue), P(CL-*co*-OPD-*co*-(OPD-*g*-PEO)-*co*-(OPD-*g*-*p*MeOBn)), **5** (green), and 3 kDa PEO (black).

Figure 3-3 (a) DSC thermograms from the third heating cycle of the melting transition region of the parent P(CL-*co*-OPD) polymer, **3** (red); 3 kDA PEO (black); a physical mixture of the parent P(CL-*co*-OPD) polymer, **3**, and 3 kDA PEO (orange); P(CL-*co*-OPD-*co*-(OPD-*g*-PEO)), **4** (blue); and P(CL-*co*-OPD-*co*-(OPD-*g*-PEO)-*co*-(OPD-*g*-*p*MeOBn)), **5** (green), and **(b)** DSC thermograms from the first heating cycle of the melting transition region of the parent P(CL-*co*-OPD) polymer, **3** (red); 3 kDA PEO (black); a physical mixture of the parent P(CL-*co*-OPD) polymer, **3**, and 3 kDA PEO (orange); P(CL-*co*-OPD-*co*-(OPD-*g*-PEO)), **4** (blue); and P(CL-*co*-OPD-*co*-(OPD-*g*-PEO)-*co*-(OPD-*g*-*p*MeOBn)), **5** (green).

Figure 3-4 (a) Intensity-averaged DLS histogram showing the bimodal size distribution of the aggregates **(b)** volume-averaged DLS histogram **(c)** and the number-averaged DLS histogram of the aggregates present in a 0.3 mg/mL solution of P(CL-*co*-OPD-*co*-(OPD-*g*-PEO)), **4**, a block graft copolymer containing 55 wt % PEO.

Figure 3-5 (a) Height image of tapping mode AFM image of P(CL-*co*-OPD-*co*-(OPD-*g*-PEO)), **4** (concentration 0.1 mg/mL) **(b)** TEM image of the micellar aggregates formed by P(CL-*co*-OPD-*co*-(OPD-*g*-PEO)), **4** (0.3 mg/mL solution).

Figure3-6 TEM image of the cylindrical aggregates formed by P(CL-*co*-OPD-*co*-(OPD-*g*-PEO)-*co*-(OPD-*g*-*p*MeOBn)), **5**, at 50000x magnification (0.3 mg/mL solution).

Figure 4-1 ^{1}H NMR spectra of (a) P(CL_{92}-*co*-OPD_5-*co*-(OPD-*g*-$PEO)_9$), 1, in $CDCl_3$, and (b) P(CL_{92}-*co*-(OPD-*g*-$PEO)_8$-*co*-(OPD-*g*-*p*$MeOBn)_6$), 2, a PCL-PEO ketoxime ether conjugate with no free OPD units present along the backbone.

Figure 4-2 (a)^{1}H NMR spectra of a 0.6 mg/mL solution of P(CL_{92}-*co*-(OPD-*g*-$PEO)_8$-*co*-(OPD-*g*-p$MeOBn)_6$), **2**, in 9:1 D_2O/ *d6*-THF (v/v) at 0 h (red), 12 h (blue) and 24 h (green) and **(b)** GPC chromatograms of lP(CL_{92}-*co*-(OPD-*g*-$PEO)_8$-*co*-(OPD-*g*-*p*$MeOBn)_6$), **2** (black), and lyophilized aliquots of a 0.6 mg/mL solution of P(CL_{92}-*co*-(OPD-*g*-$PEO)_8$-*co*-(OPD-*g*-*p*$MeOBn)_6$), **2**, in 9:1 D_2O/ *d6*-THF (v/v) taken at 0 h (red), 12 h (blue) and 24 h (green).

Figure 4-3 (a)^{1}H NMR spectra of a 0.6 mg/mL solution of P(CL_{92}-*co*-OPD_5-*co*-(OPD-*g*-$PEO)_9$), **1**, in 9:1 D_2O/ *d6*-THF/ (v/v) at 0 h (red), 12 h (blue) and 24 h (green); **(b)** GPC chromatograms of P(CL_{92}-*co*-OPD_5-*co*-(OPD-*g*-$PEO)_9$), **1** (black), and lyophilized aliquots of a 0.6 mg/mL solution of P(CL_{92}-*co*-OPD_5-*co*-(OPD-*g*-$PEO)_9$), **1**, in 9:1 D_2O/*d6*-THF (v/v) taken at 0 h (red), 6h (purple), and 12 h (blue); and **(c)** GPC chromatograms of P(CL_{92}-*co*-OPD_5-*co*-(OPD-*g*-$PEO)_9$), **1** (black), and lyophilized aliquots of a 0.6 mg/mL solution of P(CL_{92}-*co*-OPD_5-*co*-(OPD-*g*-$PEO)_9$), **1**, in 9:1 D_2O/ *d6*-THF (v/v) taken at 12 h (blue), 18 h (orange), and 24 h (green).

Figure 4-4 Intensity averaged, volume averaged, an number averaged histograms from dynamic light scattering analysis of a 0.6 mg/mL solution of P(CL_{92}-*co*-(OPD-*g*-$PEO)_8$-

co-(OPD-*g*-*p*MeOBn)$_6$), **2**, in 9:1 water/THF (v/v) at **(a)** 0 h incubation time, **(b)** 12 h incubation time and **(c)** 24 h incubation time.

Figure 4-5 TEM images and corresponding histograms for solution state aggregates formed in a 0.6 mg/mL solution of P(CL$_{92}$-*co*-(OPD-*g*-PEO)$_8$-*co*-(OPD-*g*-*p*MeOBn)$_6$), **2**, in 9:1 water/THF (v/v) at **(a)** 0 h incubation time, **(b)** 12 h incubation time and **(c)** 24 h incubation time. All samples were drop deposited onto glow treated TEM grids and were stained with a 2 % solution of uranyl acetate.

Figure 4-6 Intensity averaged, volume averaged, an number averaged histograms from dynamic light scattering analysis of a 0.6 mg/mL solution of P(CL$_{92}$-*co*-OPD$_5$-*co*-(OPD-*g*-PEO)$_9$), **1,** in 9:1 water/THF (v/v) at **(a)** 0 h incubation time, **(b)** 12 h incubation time, and **(c)** 24 h incubation time.

Figure 4-7 TEM images and corresponding histograms for solution state aggregates formed in a 0.6 mg/mL solution of P(CL$_{92}$-*co*-OPD$_5$-*co*-(OPD-*g*-PEO)$_9$), **1**, in 9:1 water/THF (v/v) at **(a)** 0 h incubation time, **(b)** 12 h incubation time and **(c)** 24 h incubation time. All samples were drop deposited onto glow treated TEM grids and were stained with a 2 % solution of uranyl acetate.

Figure 4-8 (a) ^{1}H NMR spectra of a 0.4 mg/mL solution of P(CL$_{327}$-*co*-OPD$_{22}$-*co*-(OPD-*g*-PEO)$_{15}$-*co*-(OPD-*g*-*p*MeOBn)$_8$), **3**, in 9:1 D$_2$O/*d6*-THF (v/v) at 0 h (red), 12 h (blue) and 24 h (green); **(b)** GPC chromatograms of P(CL$_{327}$-*co*-OPD$_{22}$-*co*-(OPD-*g*-PEO)$_{15}$-*co*-(OPD-*g*-*p*MeOBn)$_8$), **3**, (black), and lyophilized aliquots of a 0.6 mg/mL solution of P(CL$_{327}$-*co*-OPD$_{22}$-*co*-(OPD-*g*-PEO)$_{15}$-*co*-(OPD-*g*-*p*MeOBn)$_8$), **3** in 9:1 D$_2$O/*d6*-THF (v/v) taken at 0 h (red), 12 h (blue); and 24 h (green).

Figure 4-9 Intensity averaged, volume averaged, an number averaged histograms from dynamic light scattering analysis of a 0.4 mg/mL P(CL_{327}-*co*-OPD_{22}-*co*-(OPD-*g*-$PEO)_{15}$-*co*-(OPD-*g*-*p*$MeOBn)_8$), **3**, in 9:1 THF/H_2O (v/v) at **(a)** 0 h incubation time, **(b)** 6 h incubation time, **(c)** 12 h incubation time, and **(d)** 18 h incubation time.

Figure 4-10 TEM images of the solution state aggregates and corresponding histograms for the spherical particles present in a 0.4 mg/mL solution of P(CL_{327}-*co*-OPD_{22}-*co*-(OPD-*g*-$PEO)_{15}$-*co*-(OPD-*g*-*p*$MeOBn)_8$), **3** in 9:1 water/THF (v/v) **(a)** 0 h incubation time, **(b)** 6 h incubation time **(c)** 12 h incubation time, and **(d)** 18 h incubation time. All samples were drop deposited onto glow treated TEM grids and were stained with a 2 % solution of uranyl acetate.

LIST OF SCHEMES

LIST OF TABLES

CHAPTER ONE

INTRODUCTION

Chapter One

Introduction

In 1967 at the beginning of the landmark movie, *The Graduate,* someone giving career advice to the main character, the recently graduated Benjamin Braddock, declared, "I want to say one word to you. Just one word… Plastics…There's a great future in plastics."[1] The last fifty years has demonstrated both the wisdom and accuracy of this quotation to the point that the modern era has frequently been labeled "The Plastic Age." Plastics play such an enormous role in everyday existence that it would be next to impossible to imagine life without them. Currently the chemical industry consumes 12% of the fossil feed stocks generated per year; of that 12% almost half is used as raw materials for synthesis, most of which is used to manufacture polymeric materials.[2, 3] As of 2007, in a given year, the worldwide production of plastics exceeded 150 million tons.[4] The success of plastics can in part be attributed to the low cost of manufacturing, processability, utility in numerous applications, and thermal and chemical stability.[2, 4] It is this last quality, however, that also makes commodity plastics somewhat problematic. Many synthetic polymers are resistant to aging and decomposition making them useful for long term applications, but this resistance to degradation also inhibits their breakdown by natural mechanisms once the plastic product is no longer in use. This attribute is a problem in applications where the materials are either by choice or by need used for a short amount of time before becoming waste or becoming unnecessary. Issues regarding the long term disposal of plastics combined with mounting concerns regarding the environmental footprint caused by using fossil fuels as a resource for the generation of

polymeric materials have promoted an exploration into polymeric materials that are biologically compatible, biodegradable, and renewable.

In the investigations into substitutes for traditional plastics, aliphatic polyesters have been a major focus in the search for renewable materials and seem to provide a promising sustainable alternative. Commercially, the greatest interest thus far has focused on using the aliphatic polyester, poly(lactide) (PLA), due to its mechanical and physical properties, its processability, and naturally its hydrolytic degradability.[2, 3, 5] Currently, PLA is manufactured on a large scale in the United States, Europe and Japan.[4] In the United States, Cargill in conjunction with Dow has started operation of a PLA plant under the name NatureWorks® which uses corn, starch, and plant wasted as a raw material for PLA production, and this particular plant has the capacity to produce 140,000 tons of PLA per year.[2, 4] At present, Natureworks® has developed its Ingeo™ biopolymer and fibers—all PLA-based—which have been used to manufacture goods ranging from plastic packaging and bottles to shirts.[6]

Degradable polyesters are clearly applicable from a commercial and manufacturing standpoint, and there is an obvious environmental motivation for using degradable polymers as alternative materials for commodity applications. However, the medical and biomedical fields were amongst the first to actively pursue the use of aliphatic polyesters as synthetic alternatives to commonly used materials.[7] Surgical implants and sutures were meant to be temporary medical solutions, and as such degradability of the materials used for these applications was a highly desirable characteristic. Consequently, synthetic polymers with the ability to degrade and be eliminated from a biological system were ideal for applications of this nature. In the 1960s, studies on aliphatic polyester

homopolymers and copolymers were researched for use in surgical and biomedical applications.[5, 7, 8] Poly(glycolic acid) (PGA), an aliphatic polyester which does not require an enzyme to degrade in the human body, became the first degradable polymer used as a suturing material in the 1962, which was eventually manufactured under the name Dexon®.[9] Another suture, developed shortly thereafter was Vicryl®, a suture made from a copolymer of PGA and PLA.[10] Aliphatic polyesters have also found use in many areas requiring resorbable polymeric materials[11] and have been employed as prosthetic devices;[5, 12] as scaffolds for soft and hard tissue engineering;[13-15] and as bone screws, pins, and plates.[16-18]

Macroscopic employment of devices produced from degradable copolymers and homopolymers are still being employed in the medical field with Dexon® and Vicryl® still being two of the most commonly used sutures,[5] and polyester-based materials are still under investigation to further optimize their characteristics for use in biomedical applications. These polyesters are well known to be biocompatible and upon degradation produce benign, resorbable degradation products,[19] and because of their prior use in surgical applications, using polyesters for *in vivo* drug delivery applications was also considered.[7, 8] Despite the wide variety of aliphatic polyesters available, PGA and PLA are the most universally used because their degradation rate is both rapid and tunable.[5] Both of these polymers have been explored as potential systems for drug delivery and have been investigated for the long term sustained release of anti-malarials[20] and as narcotic antagonist delivery systems.[21] There have also been commercially successful ventures using aliphatic polyesters as drug delivery systems: Lupron Depot, which employs a PLA-PGA polymer for endometriosis and prostate cancer treatments,[22, 23] and

Capronor, a 1-year implantable contraceptive device that uses poly(caprolactone) (PCL).[5, 24]

However, as investigations into the creation of significantly more complex materials progressed, there has been a focus on the preparation of well-defined and highly functional biocompatible and degradable polymers. Synthetic polyesters of a specific molecular weight possessing a narrow molecular weight distribution can be produced *via* ring opening polymerization (ROP) of cyclic monomers (i.e. lactides and lactones), and is typically initiated and mediated by metal-containing catalysts.[25] Tin-[26-29] and aluminum-based[30-37] catalysts are amongst the most common catalysts employed for ROP, but catalysts employing other metals[38-41] have also been developed for use in the ROP of cyclic monomers to produce polyesters. If these materials were designed for use in biomedical applications, the residual metals remaining in the polyester material after synthesis could pose a risk. This concern about residual heavy metal contamination has encouraged the development of methods for removing excess metal remaining in the polymer samples from the mediation of the polymerization process. One method employing thiols was developed to reduce and remove excess tin from polyester materials designed for biomedical applications, and proved successful in reducing the amount of tin present in PCL samples to levels acceptable for *in vivo* applications.[42] This method does not, however, remove all of the residual metal and also introduces an extra step in production.

There, are also alternative approaches for synthesizing polyesters by ROP that avoid metal contamination altogether. One method that is receiving considerable attention is the synthesis of polyesters *via* organocatalytic ROP.[43] This method provides many of the

same advantages as metal-mediated ROP by producing well-defined polymers of a specified molecular weight combined with the ability to polymerize a diversity of monomers. Another method that circumvents the use of metals and has been promoted as a greener polymerization technique is the use of enzymatic polymerization, and specifically the use lipases for the synthesis of polyesters.[44-46] This method, while promising, does have limitations compared to more traditional synthetic methods when it comes to efficiency, monomer selection, and polymerization control.[45]

The numerous synthetic methods available for preparing a variety of well-defined polyesters, is amongst the key reasons that aliphatic homopolyesters and copolyesters comprise an area receiving considerable scientific emphasis in terms of further synthetic development and exploration into the integration of polyesters into significantly more complex materials. Synthetic polyesters—despite their successful employment in early biomedical devices and drug delivery systems—are still limited in application due to two major draw backs: an inherent hydrophobicity and a deficiency of chemical functionality beyond the ester groups present in the backbone. In order to broaden the utility of synthetic aliphatic polyesters, it is necessary to develop strategies for the incorporation of functional ligands and hydrophilic components to construct polyester-based systems that are better suited for *in vivo* applications including targeted nanoscale delivery agents for therapeutic and diagnostic agents[47, 48] and more intricate tissue engineering scaffolds that can induce migration and regeneration or be used as a matrix to support and organize cell growth.[49, 50]

One possibility for incorporation of functionality into polyesters is the inclusion of reactive groups at the chain ends. This strategy has been employed for the incorporation

of vitamins and hormones,[51] saccharides,[52] polysaccharides,[53] cholesterol,[54] and chromophores[55]. However, this method only allows for a limited degree of functionalization, and with linear polymers is restricted to the incorporation of two functional moieties—one at each chain end. The addition of reactive groups along the polyester back bone for the incorporation of functional side chains provides a strategy that overcomes this limitation. Functional groups presented at multiple locations along the backbone allows for the incorporation of numerous ligands of the same type, but also provides a polymeric precursor for the attachment of a variety of different molecules to a single polyester backbone.

The preparation of aliphatic polyesters with the ability to support multiple pendant functional groups has been an area of extensive research, and initially two major strategies were proposed for achieving derivatization of the polyester backbone (**scheme 1-1**).[56, 57] The first method is based on the polymerization of lactone monomers bearing functionalities,[58] while the second strategy involves post-polymerization modification using a "grafting onto" approach for the attachment of pendant groups and ligands.[59]

The employment of functional lactide and lactone monomers provides a controlled route for the synthesis of functional, degradable polyesters, and from there can be

Scheme 1-1. Major strategies for the functionalization of aliphatic polyesters.[82]

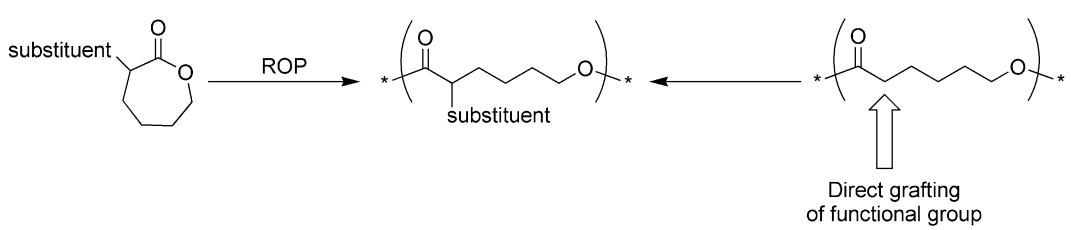

extended to the preparation of multifunctional nanoscale particles and materials.[60] Much research has focused on the preparation of cyclic diester monomers that can be directly polymerized or copolymerized to yield polylactides and polyglycolides presenting unique pendant groups along the polyester backbone.[61, 62] Some of the most exploited diester monomers possessed alkene[63]and alkyne[64] functionalities. There has also been considerable work investigating the synthesis and polymerization of substituted ε-caprolactone monomers, which upon ROP afford PCL-based polymers with functional groups incorporated along the backbone.[56, 57] Using these substituted lactone monomers, polyesters possessing bromides,[65, 66] chlorides,[67, 68] acrylates,[69] olefins,[70] protected hydroxyl groups,[71] protected carboxyl groups,[72] and even poly(ethyene oxide) (PEO) side chains[73] have been produced.

The direct functionalization of pre-formed polyesters is attractive because it avoids the synthesis of complex monomers, and a single polyester can provide for the creation of a variety of functionalized materials. Additionally, using this strategy there is the ability for multiple derivatives to be incorporated in a single step. An illustrative example is the functionalization of PCL or PLA backbones in the α-position *via* enolate generation with an alkyl lithium base.[59] These enolates are highly reactive towards electrophiles, including CO_2, benzaldehyde, and iodine, which eventually generate polyester backbones presenting carboxylic acids,[74] hydroxyl,[75] and iodo moieities[76] respectively. This chemical strategy has also been employed for the direct grafting of hydrophilic polymer chains like PEO[77] and poly-(L-lysine)[78] onto a polyester back bone to generate amphiphilic block graft copolymers. While enolate formation clearly provides an elegant method using polyesters as a platform for the preparation of a diversity of materials, this

strategy is limited because chain scission is unavoidable under the reaction conditions necessary for enolate generation.

These two strategies provide a strong foundation for polyester derivatization, but a combination of the two methods into a two-step process has proven to be the most powerful tool for the synthesis of complex polyester-based materials. The polymerization of a monomer possessing a pendant group with latent functionality allows the resulting polyester to be used as a modular system for the generation of a series of multifunctional materials (**Scheme 1-2**). This strategy is most effective when the substituted monomer can be synthesized easily, undergo controlled polymerization, and the latent functionality is reactive enough to ensure sufficient incorporation of the desired moieties. The derivatization of polymers can be a challenging process for many reasons, and reactions designed for the attachment of molecules on onto a polyester is an even

Scheme 1-2. ROP of a substituted caprolactone followed by its chemical derivatization to generate various functional polyesters.[56]

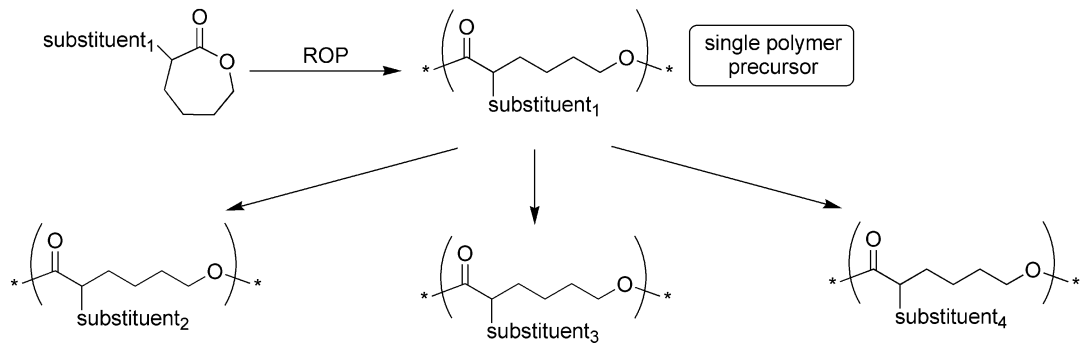

more sensitive endeavor as the chemistries used must avoid harsh conditions to avoid premature degradation of the polyester backbone. In order to achieve polyester functionalization while minimizing backbone degradation, robust, efficient, and

orthogonal chemistries are often used as they are quantitative, chemoselective, and proceed under mild reaction conditions.[79-81]

One of the most prevalent chemistries currently employed for the modification of aliphatic polyesters, is the copper-catalyzed alkyne-azide cycloaddtion (CuAAC) "click" reaction. While the topic of polyester modification by "click" chemistry has been extensively reviewed in the literature,[79, 82, 83] There are some seminal and unique studies that illustrate the versatility of this chemistry and its utility in transforming aliphatic polyesters into complex, multifaceted materials. For example, α-azido derivatives have been prepared by reaction of poly(α-chloro-ε-caprolactone-*co*-ε-caprolactone) with sodium azide, and these polymers can subsequently be reacted with alkynes to afford functionalized PCL *via* triazole formation.[67, 68] This synthetic strategy has been used to prepare PCL-based glycolpolymers[84] and amphiphilic PEO-grafted PCL.[67, 68] Another strategy employed for the creation of tailor-made polyester-based materials was the incorporation of acetylene groups onto the polyester back bone, after which the alkyne moities could be reacted with azide-bearing molecules. This approach was used to generate PEO- and peptide-grafted aliphatic polyesters[85] and was also found to be effective in the conjugation of azido-camptothecin to a polyester backbone for the preparation of a hydrolytically degradable polymer-drug conjugate.[86]

While the CuAAC has become the prevailing reaction for use in polyester functionalization, other robust, efficient,and orthogonal (REO) chemistries have also proven to be practical methods for the creation of a variety of distinct polymeric materials from polyesters. Some of the more common REO reactions that have been recently

employed include Michael additions[87-89] and thiolene reactions,[90] both of which take advantage of polyesters possessing pendant alkene moieties.

Another functional group that has been incorporated into polyesters and has been generally exploited for the creation of derivatized materials is the ketone moiety. Ketones presented along a polyester backbone provide a site for the integration of numerous small molecules, and are known to undergo selective and efficient reaction with *O*-substituted hydroxylamines, or aminooxy compounds, to form stable ketoxime ether linkages. Poly(epsilon-caprolactone-*co*-2-oxepane-1,5-dione) (P(CL-*co*-OPD) is a PCL-based polymer with electrophilic ketone groups.[91-93] Previous work investigating the chemistry of this polyester system has produced grafted materials,[94, 95] crosslinked networks,[95] and amphiphilic graft copolymers.[96, 97]

This system has been generally studied for its utility in generating degradable materials based upon PCL, though the chemistry for incorporating functional small molecules and polymeric grafts deserves further study and optimization. Additionally, the polyester-based materials generated from P(CL-*co*-OPD), require additional characterization to understand their physical characteristics and degradation profile to advance the quality of the materials prepared and make them relevant for applications. The purpose of this dissertation work is to further investigate the use of P(CL-*co*-OPD) as a modular platform system, and to analyze the characteristics of the resultant polyester-based materials.

Initial work, which is discussed in **Chapter 2**, focused on the functionalization of the PCL-*co*-OPD system with the chromophore, 5'-dimethyaminonapthylene-1-sulfohydrazide, commonly known as dansyl hydrazine. While hydrazone formation has

been previously shown to be a less efficient conjugation strategy in comparison to using aminooxy compounds,[94] the commercial availability of dansyl hydrazine and its well documented use as a chromophore and fluorophore make it an ideal system for the investigation of a PCL-dye conjugate. In order to obtain a better understanding of the spectral behavior of polyester-dye conjugates, the covalent integration of multiple fluorescent probes along a PCL-based copolymer was investigated through the attachment of dansyl hydrazine to multiple sites along the P(CL-*co*-OPD) backbone *via* acid-catalyzed hydrazone formation. The resulting solvatochromic behavior of the dansylated-polymer in a series of organic solvents is described, and was compared to the solution state fluorescence of a dansyl-bearing small molecule analog.

In **Chapter 3**, the electrophilic ketone moiety present in the OPD units of P(CL-*co*-OPD) was used as a reactive chemical handle for the incorporation of hydrophilic polymer grafts and small molecule ligands to generate functional amphiphilic block graft copolymers. Aminooxy-PEO chains were incorporated along the PCL backbone by acid-catalyzed oxime condensation to afford PCL-PEO ketoxime ether conjugates with a high degree of grafting efficiency. To further demonstrate the modularity of the P(CL-*co*-OPD) system, aminooxy-PEO and a small molecule ligand, *p*-methoxy-*O*-benzylhydroxylamine (*p*MeOBn) were simultaneously grafted onto the polymer backbone in a in a one-pot reaction with a demonstrated grafting efficiency of greater than 75%. The resulting amphiphilic block graft copolymers were characterized by differential scanning calorimetry (DSC) and were found to have unique thermal transitions relative to the parent P(CL-*co*-OPD) and PEO polymers. Incorporation of hydrophilic grafts onto the otherwise hydrophobic PCL backbone allowed for dispersion

of these polymers in aqueous solution. Upon dissolution the block graft copolymers self-assembled to produce distinctive solution state morphologies.

Chapter 4 serves as an extension of the work discussed in **Chapter 3** and characterizes the unique hydrolytic degradation behavior associated with PCL-PEO ketoxime ether conjugates prepared from P(CL-*co*-OPD). This chapter focuses on the early and rapid degradation associated with PCL-g-PEO copolymers still possessing unfunctionalized OPD repeat units, and seeks to document this degradation process to obtain a better understanding of the mechanism of hydrolysis. Additionally, to thoroughly characterize the amphiphilic block graft copolymers and their resultant hydrolytic degradation, changes in the size and shape of solution state aggregates were tracked while the polymer was dispersed in aqueous solution. Analysis of the self-assembled structures revealed changes in size and alterations in morphology as a function of polyester backbone hydrolysis.

References

1. Nichols, M., The Graduate. Embassy Pictures: United States, 1967.

2. Mecking, S. Nature or petrochemistry? - Biologically degradable materials. *Angewandte Chemie International Edition* **2004,** *43*, 1078-1085.

3. Guillet, J., Plastics and the Environment. In *Degradable Polymers Principles and Applications*, 2nd ed.; Scott, G., Ed. Kluwer Academic Publishers: Boston, 2002; pp 413-448.

4. Williams, C. K. Synthesis of functional biodegradable polyesters. *Chemical Society Reviews* **2007,** *36*, 1573-1580.

5. Pişkin, E., Biodegradable Polymers in Medicine. In *Degradable Polymers Principles and Applicatinos*, 2nd ed.; Scott, G., Ed. Kluwer Academic Publishers: Boston, 2002; pp 413-448.

6. http://www.natureworksllc.com/.

7. Albertsson, A.-C.; Varma, I. K. Recent developments in ring opening polymerization of lactones for biomedical applications. *Biomacromolecules* **2003,** *4*, 1466-1486.

8. Vert, M. Aliphatic polyesters: Great degradable polymers that cannot do Everything. *Biomacromolecules* **2004,** *6*, 538-546.

9. Schmitt, E. E.; Polistina, R. A. Surgical Sutures. 3297033, 1967.

10. Schneider, A. K. Polylactide Sutures. 3636956, 1972.

11. Vert, M. Bioresorbable polymers for temporary therapeutic applications. *Angewandte Makromolekulare Chemie* **1989,** *166*, 155-168.

12. Schmitt, E. E.; Polistina, R. A. Polyglycolic Acid Prosthetic Devices. 3463158, 1969.

13. Maquet, V.; Martin, D.; Malgrange, B.; Franzen, R.; Schoenen, J.; Moonen, G.; Jérôme, R. Peripheral nerve regeneration using bioresorbable macroporous polylactide scaffolds. *Journal of Biomedical Materials Research* **2000,** *52*, 639-651.

14. Gogolewski, S.; Pineda, L.; Michael Büsing, C. Bone regeneration in segmental defects with resorbable polymeric membranes: IV. Does the polymer chemical composition affect the healing process? *Biomaterials* **2000,** *21*, 2513-2520.

15. Marra, K. G.; Szem, J. W.; Kumta, P. N.; DiMilla, P. A.; Weiss, L. E. In vitro analysis of biodegradable polymer blend/hydroxyapatite composites for bone tissue engineering. *Journal of Biomedical Materials Research* **1999,** *47*, 324-335.

16. Furukawa, T.; Matsusue, Y.; Yasunaga, T.; Shikinami, Y.; Okuno, M.; Nakamura, T. Biodegradation behavior of ultra-high-strength hydroxyapatite/poly (L-lactide) composite rods for internal fixation of bone fractures. *Biomaterials* **2000,** *21*, 889-898.

17. Bergsma, J. E.; de Bruijn, W. C.; Rozema, F. R.; Bos, R. R. M.; Boering, G. Late degradation tissue response to poly(-lactide) bone plates and screws. *Biomaterials* **1995,** *16*, 25-31.

18. Leenslag, J. W.; Pennings, A. J.; Bos, R. R. M.; Rozema, F. R.; Boering, G. Resorbable materials of poly(L-lactide): VII. In vivo and in vitro degradation. *Biomaterials* **1987,** *8*, 311-314.

19. Pitt, G. G.; Gratzl, M. M.; Kimmel, G. L.; Surles, J.; Sohindler, A. Aliphatic polyesters II. The degradation of poly(DL-lactide), poly (epsilon-caprolactone), and their copolymers in vivo. *Biomaterials* **1981,** *2*, 215-220.

20. Wise, D. L.; McCormick, G. J.; Willet, G. P.; Anderson, L. C. Sustained release of an antimalarial drug using a copolymer of glycolic/lactic acid. *Life Sciences* **1976,** *19*, 867-873.

21. Schwope, A. D.; Wise, D. L.; Howes, J. F. Lactic/glycolic acid polymers as narcotic antagonist delivery systems. *Life Sciences* **1975,** *17*, 1877-1885.

22. Okada, H.; Yamamoto, M.; Heya, T.; Inoue, Y.; Kamei, S.; Ogawa, Y.; Toguchi, H. Drug delivery using biodegradable microspheres. *Journal of Controlled Release* **1994,** *28*, 121-129.

23. Okada, H.; Ogawa, Y.; Yashiki, T. Prolonged Release Microcapsule and its Productons. 4652441, 1994.

24. Pitt, C. G.; Jeffcoat, A. R.; Zweidinger, R. A.; Schindler, A. Sustained drug delivery systems. I. The permeability of poly(epsilon-caprolactone), poly(D,L-lactic acid), and their copolymers. *Journal of Biomedical Materials Research* **1979,** *13*, 497-507.

25. Dechy-Cabaret, O.; Martin-Vaca, B.; Bourissou, D. Controlled ring-opening polymerization of lactide and glycolide. *Chemical Reviews* **2004,** *104*, 6147-6176.

26. Kowalski, A.; Libiszowski, J.; Biela, T.; Cypryk, M.; Duda, A.; Penczek, S. Kinetics and Mechanism of cyclic esters polymerization initiated with tin(II) octoate. Polymerization of epsilon-caprolactone and L,L-Lactide co-initiated with primary amines. *Macromolecules* **2005,** *38*, 8170-8176.

27. Kowalski, A.; Duda, A.; Penczek, S. Mechanism of cyclic ester polymerization initiated with tin(II) octoate. 2. Macromolecules fitted with tin(II) alkoxide species observed directly in MALDI-TOF spectra. *Macromolecules* **2000,** *33*, 689-695.

28. Kemnitzer, J. E.; McCarthy, S. P.; Gross, R. A. Preparation of predominantly syndiotactic poly(beta-hydroxybutyrate) by the tributyltin methoxide catalyzed ring-opening polymerization of racemic beta-butyrolactone. *Macromolecules* **1993,** *26*, 1221-1229.

29. Kricheldorf, H. R.; Sumbel, M. V.; Kreiser-Saunders, I. Polylactones. 20. Polymerization of epsilon-caprolactone with tributyltin derivatives: a mechanistic study. *Macromolecules* **1991**, 1944-1949.

30. Mosnacáček, J.; Duda, A.; Libiszowski, J.; Penczek, S. Copolymerization of L,L-lactide at its Living polymer-monomer equilibrium with epsilon-caprolactone as comonomer. *Macromolecules* **2005,** *38*, 2027-2029.

31. Liao, T.-C.; Huang, Y.-L.; Huang, B.-H.; Lin, C.-C. Alcoholysis of methyl aluminium biphenoxides: Excellent initiators for the ring opening polymerisation of epsilon-caprolactone. *Macromolecular Chemistry and Physics* **2003,** *204*, 885-892.

32. Mecerreyes, D.; Jérôme, R. From living to controlled aluminium alkoxide mediated ring-opening polymerization of (di)lactones, a powerful tool for the macromolecular engineering of aliphatic polyesters. *Macromolecular Chemistry and Physics* **1999,** *200*, 2581-2590.

33. Kowalski, A.; Duda, A.; Penczek, S. Polymerization of L,L-Lactide initiated by aluminum isopropoxide trimer or tetramer. *Macromolecules* **1998,** *31*, 2114-2122.

34. Duda, A.; Penczek, S. Polymerization of epsilon-caprolactone initiated by aluminum isopropoxide trimer and/or tetramer. *Macromolecules* **1995,** *28*, 5981-5992.

35. Ropson, N.; Dubois, P.; Jérôme, R.; Teyssié, P. Macromolecular engineering of polylactones and polylactides. 20. Effect of monomer, solvent, and initiator on the ring-opening polymerization as Initiated with aluminum alkoxides. *Macromolecules* **1995,** *28*, 7589-7598.

36. Degee, P.; Dubois, P.; Jérôme, R.; Teyssié, P. Macromolecular engineering of polylactones and polylactides. 9. Synthesis, characterization, and application of omega-primary amine poly(epsilon-caprolactone). *Macromolecules* **1992**, 4242-4248.

37. Dubois, P.; Jérôme, R.; Teyssié, P. Macromolecular engineering of polylactones and polylactides. 3. Synthesis, characterization, and applications of poly(epsilon-caprolactone) macromonomers. *Macromolecules* **1991,** *24*, 977-981.

38. Kricheldorf, H. R. Syntheses of biodegradable and biocompatible polymers by means of bismuth catalysts. *Chemical Reviews* **2009,** *109*, 5579-5594.

39. Rieth, L. R.; Moore, D. R.; Lobkovsky, E. B.; Coates, G. W. single-site beta-diiminate zinc catalysts for the ring-opening polymerization of beta-butyrolactone and beta-valerolactone to poly(3-hydroxyalkanoates). *Journal of the American Chemical Society* **2002,** *124*, 15239-15248.

40. Agarwal, S.; Mast, C.; Dehnicke, K.; Greiner, A. Rare earth metal initiated ring-opening polymerization of lactones. *Macromolecular Rapid Communications* **2000,** *21*, 195-212.

41. Dobrzynski, P.; Li, S.; Kasperczyk, J.; Bero, M.; Gasc, F.; Vert, M. Structure-property relationships of copolymers obtained by ring-opening polymerization of glycolide and epsilon-caprolactone. Part 1. Synthesis and characterization. *Biomacromolecules* **2004,** *6*, 483-488.

42. Stjerndahl, A.; Wistrand, A. F.; Albertsson, A.-C. Industrial utilization of tin-initiated resorbable polymers: Synthesis on a large scale with a low amount of initiator residue. *Biomacromolecules* **2007,** *8*, 937-940.

43. Kamber, N. E.; Jeong, W.; Waymouth, R. M.; Pratt, R. C.; Lohmeijer, B. G. G.; Hedrick, J. L. Organocatalytic ring-opening polymerization. *Chemical Reviews* **2007,** *107*, 5813-5840.

44. Kobayashi, S.; Makino, A. Enzymatic polymer synthesis: An opportunity for green polymer chemistry. *Chemical Reviews* **2009,** *109*, 5288-5353.

45. Kobayashi, S.; Uyama, H.; Kimura, S. Enzymatic polymerization. *Chemical Reviews* **2001,** *101*, 3793-3818.

46. Gross, R. A.; Kumar, A.; Kalra, B. Polymer synthesis by in vitro enzyme catalysis. *Chemical Reviews* **2001,** *101*, 2097-2124.

47. Hiroaki, O.; Masaki, Y.; Toshiro, H.; Yayoi, I.; Shigeru, K.; Yasuaki, O.; Hajime, T. Drug delivery using biodegradable microspheres. *Journal of Controlled Release* **1994,** *28*, 121-129.

48. Holland, S. J.; Tighe, B. J.; Gould, P. L. Polymers for biodegradable medical devices. 1. The potential of polyesters as controlled macromolecular release systems. *Journal of Controlled Release* **1986,** *4*, 155-180.

49. Langer, R.; Peppas, N. A. Advances in biomaterials, drug delivery, and bionanotechnology. *Bioengineering, Food, and Natural Products* **2003,** *49*, 2990-3006.

50. Place, E. S.; George, J. H.; Williams, C. K.; Stevens, M. M. Synthetic polymer scaffolds for tissue engineering. *Chemical Society Reviews* **2009,** *38*, 1139-1151.

51. Kricheldorf, H. R.; Kreiser-Saunders, I. Polylactones: 30. Vitamins, hormones and drugs as co-initiators of $AlEt_3$-initiated polymerizations of lactide. *Polymer* **1994,** *35*, 4175-4180.

52. Xu, N.; Lu, F.-Z.; Du, F.-S.; Li, Z.-C. Synthesis of saccharide-terminated poly(epsilon-caprolactone) via michael addition and "click" chemistry. *Macromolecular Chemistry and Physics* **2007,** *208*, 730-738.

53. Gref, R.; Rodrigues, J.; Couvreur, P. Polysaccharides grafted with polyesters: Novel amphiphilic copolymers for biomedical applications. *Macromolecules* **2002,** *35*, 9861-9867.

54. Klok, H.-A.; Hwang, J. J.; Iyer, S. N.; Stupp, S. I. Cholesteryl-(L-lactic acid)$_n$ building blocks for self-assembling biomaterials. *Macromolecules* **2002,** *35*, 746-759.

55. Carstens, M. G.; Bevernage, J. J. L.; van Nostrum, C. F.; van Steenbergen, M. J.; Flesch, F. M.; Verrijk, R.; de Leede, L. G. J.; Crommelin, D. J. A.; Hennink, W. E. Small oligomeric micelles based on end group modified mPEG-oligocaprolactone with monodisperse hydrophobic blocks. *Macromolecules* **2006,** *40*, 116-122.

56. Jérôme, C.; Lecomte, P. Recent advances in the synthesis of aliphatic polyesters by ring-opening polymerization. *Advanced Drug Delivery Reviews* **2008,** *80*, 1056-1076.

57. Lecomte, P.; Riva, R.; S., S.; Riegrr, J.; Van Butsels, K.; Jérôme, R. New prospects for the grafting of functional groups onto aliphatic polyesters. Ring-opening polymerization of alpha- or gamma-substituted epsilon-caprolactone followed by the chemical derivitization of the substituents. *Macromolecular Symposia* **2006,** *240*, 157-165.

58. Lou, X.; Detrembleur, C.; Jérôme, R. Novel aliphatic polyesters based on functional cyclic (di)esters. *Macromolecular Rapid Communications* **2003,** *24*, 161-172.

59. Ponsart, S.; Coudane, J.; Vert, M. A novel route to poly(epsilon-caprolactone)-based copolymers via anionic derivatization. *Biomacromolecules* **2000,** *1*, 275-281.

60. Pounder, R. J.; Dove, A. P. Towards poly(ester) nanoparticles: recent advances in the synthesis of functional poly(ester)s by ring-opening polymerization. *Polymer Chemistry* **2010,** *1*, 260-271.

61. Noga, D. E.; Petrie, T. A.; Kumar, A.; Weck, M.; García, A.; Collard, D. M. Synthesis and modification of functional poly(lactide) copolymers: Toward biofunctional materials. *Biomacromolecules* **2008,** *9*, 2056-2062.

62. Gerhardt, W. W.; Noga, D. E.; Hardcastle, K. I.; García, A.; Collard, D. M.; Weck, M. Functional Lactide Monomers: Methodology and Polymerization. *Biomacromolecules* **2006,** *7*, 1735-1742.

63. Leemhuis, M.; Akeroyd, N.; Kruijtzer, J. A. W.; van Nostrum, C. F.; Hennink, W. E. Synthesis and characterization of allyl functionalized poly(alpha-hydroxy)acids and their further dihydroxylation and epoxidation. *European Polymer Journal* **2008,** *44*, 308-317.

64. Jiang, X.; Vogel, E. B.; Smith, M. R.; Baker, G. L. "Clickable" polyglycolides: Tunable synthons for thermoresponsive, degradable polymers. *Macromolecules* **2008,** *41*, 1937-1944.

65. Detrembleur, C.; Mazza, M.; Halleux, O.; Lecomte, P.; Mecerreyes, D.; Hedrick, J. L.; Jérôme, R. Ring-opening polymerization of gamma-bromo-epsilon-caprolactone: A novel route to functionalized aliphatic polyesters. *Macromolecules* **1999,** *33*, 14-18.

66. Mecerreyes, D.; Atthoff, B.; Boduch, K. A.; Trollsas, M.; Hedrick, J. L. Unimolecular combination of an atom transfer radical polymerization initiator and a lactone monomer as a route to new graft copolymers. *Macromolecules* **1999,** *32*, 5175-5182.

67. Riva, R.; Schmeits, S.; Jérôme, C.; Jérôme, R.; Lecomte, P. Combination of ring-opening polymerization and "Click Chemistry" : Toward functionalization and grafting of poly(epsilon-caprolactone). *Macromolecules* **2007,** *40*, 796-803.

68. Riva, R.; Schmeits, S.; Stoffelbach, F.; Jérôme, C.; Jérôme, R.; Lecomte, P. Combination of ring-opening polymerization and "click" chemistry towards functionalization of aliphatic polyesters. *Chemical Communications* **2005,** *5334-5336*.

69. Mecerreyes, D.; Humes, J.; Miller, R. D.; Hedrick, J. L.; Detrembleur, C.; Lecomte, P.; Jérôme, R.; Roman, J. S. First example of an unsymmetrical difunctional monomer polymerizable by two living/controlled methods. *Macromolecular Rapid Communications* **2000,** *21*, 779-784.

70. Lou, X.; Detrembleur, C.; Lecomte, P.; Jérôme, R. Controlled synthesis and chemical modification of unsaturated aliphatic (Co)polyesters based on 6,7-dihydro-2(3*H*)-oxepinone. *Journal of Polymer Science Part A: Polymer Chemistry* **2002,** *40*, 2286-2297.

71. Stassin, F.; Halleux, O.; Dubois, P.; Detrembleur, C.; Lecomte, P.; Jérôme, R. Ring opening copolymerization of epsilon;-caprolactone, gamma-(triethylsilyloxy)-epsilon;-caprolactone and gamma-ethylene ketal-epsilon-caprolactone: a route to hetero-graft copolyesters. *Macromolecular Symposia* **2000,** *153*, 27-39.

72. Vert, M. Chemical routes to poly(beta-malic acid) and potential applications of this water-soluble bioresorbable poly(beta-hydroxy alkanoate). *Polymer Degradation and Stability* **1998,** *59*, 169-175.

73. Rieger, J.; Bernaerts, K. V.; Du Prez, F. E.; Jérôme, R.; Jérôme, C. Lactone End-Capped Poly(ethylene oxide) as a New Building Block for Biomaterials. *Macromolecules* **2004,** *37*, 9738-9745.

74. Gimenez, S.; Ponsart, S.; Coudane, J.; Vert, M. Synthesis, properties and in vitro degradation of carboxyl-bearing PCL. *Journal of Bioactive and Compatible Polymers* **2001,** *16*, 32-46.

75. Coulembier, O.; Mespouille, L.; Hedrick, J. L.; Waymouth, R. M.; Dubois, P. Metal-Free Catalyzed Ring-Opening Polymerization of Î²-Lactones: Synthesis of Amphiphilic Triblock Copolymers Based on Poly(dimethylmalic acid). *Macromolecules* **2006,** *39*, 4001-4008.

76. Nottelet, B.; Coudane, J.; Vert, M. Synthesis of an X-ray opaque biodegradable copolyester by chemical modification of poly (epsilon-caprolactone). *Biomaterials* **2006,** *27*, 4948-4954.

77. Huang, M. H.; Coudane, J.; Li, S.; Vert, M. Methylated and pegylated PLA-PCL-PLA block copolymers via the chemical modification of di-hydroxy PCL combined with ring opening polymerization of lactide. *Journal of Polymer Science Part A: Polymer Chemistry* **2005,** *43*, 4196-4205.

78. Nottelet, B.; Ghzaoui, A. E.; Coudane, J.; Vert, M. Novel amphiphilic poly(epsilon-caprolactone)-*g*-poly(L-lysine) degradable copolymers. *Biomacromolecules* **2007,** *8*, 2594-2601.

79. Iha, R. K.; Wooley, K. L.; Nyström, A. M.; Burke, D. J.; Kade, M. J.; Hawker, C. J. Applications of orthogonal "Click" chemistries in the synthesis of functional soft materials. *Chemical Reviews* **2009,** *109*, 5620-5686.

80. Hawker, C. J.; Fokin, V. V.; Finn, M. G.; Sharpless, K. B. Brining efficiency to materials synthesis: The philosophy of click chemistry. *Austrailian Journal of Chemistry* **2007,** *60*, 381-383.

81. Hawker, C. J.; Wooley, K. L. The convergence of synthetic organic chemistry and polymer chemistries. *Science* **2005,** *309*, 1200-1205.

82. Lecomte, P.; Riva, R.; Jérôme, C.; Jérôme, R. Macromolecular engineering of biodegradable polyesters by ring-opening polymerization and "click" chemistry. *Macromolecular Rapid Communications* **2008,** *29*, 982-997.

83. Lutz, J.-F. 1,3-Dipolar cycloadditions of azides and alkynes: A universal ligation tool in polymer and materials science. *Angewandte Chemie International Edition* **2007,** *46*, 1018-1025.

84. Xu, N.; Wang, R.; Du, F.-S.; Li, Z.-C. Synthesis of amphiphilic biodegradable glycocopolymers based on poly(epsilon-caprolactone) by ring-opening polymerization and click chemistry. *Journal of Polymer Science Part A: Polymer Chemistry* **2009,** *47*, 3583-3594.

85. Parrish, B.; Breitenkamp, R. B.; Emrick, T. PEG- and peptide grafted aliphatic polyesters by click chemistry. *Journal of the American Chemical Society* **2005,** *127*, 7404-7410.

86. Parrish, B.; Emrick, T. Soluble captothecin derivatives prepared by click cycloaddtion chemistry on functional aliphatic polyesters. *Bioconjugate Chemistry* **2006,** *18*, 263-267.

87. Ozturk, G.; Long, T. E. Michael addition for crosslinking of poly(caprolactone)s. *Journal of Polymer Science Part A: Polymer Chemistry* **2009,** *47*, 5437-5447.

88. Hu, X.; Chen, X.; Liu, S.; Shi, Q.; Jing, X. Novel aliphatic poly(ester-carbonate) with pendant allyl ester groups and its folic acid functionalization. *Journal of Polymer Science Part A: Polymer Chemistry* **2008,** *46*, 1852-1861.

89. Rieger, J.; Van Butsele, K.; Lecomte, P.; Detrembleur, C.; Jérôme, R.; Jérôme, C. Versatile functionalization and grafting of poly(epsilon-caprolactone) by Michael-type addition. *Chemical Communications* **2005**, 274-276.

90. Campos, L. M.; Killops, K. L.; Sakai, R.; Paulusse, J. M. J.; Damiron, D.; Drockenmuller, E.; Messmore, B. W.; Hawker, C. J. Development of thermal and photochemical strategies for thiol-ene click polymer functionalization. *Macromolecules* **2008,** *41*, 7063-7070.

91. Tian, D.; Dubois, P.; Jérôme, R. Poly(2-oxepane-1,5-dione): A highly crystalline modified poly(epsilon-caprolactone) of a high melting temperature. *Macromolecules* **1998,** *31*, 924-927.

92. Latere, J.-P.; Lecomte, P.; Dubois, P.; Jérôme, R. 2-Oxepane-1,5-dione: A precursor of a novel class of versatile semicrystalline biodegradable (co)polyesters. *Macromolecules* **2002,** *35*, 7857-7859.

93. Latere Dwan'Isa, J.-P.; Lecomte, P.; Dubois, P.; Jérôme, R. Synthesis and characterization of random copolyesters of epsilon-caprolactone and 2-oxepane-1,5-dione. *Macromolecules* **2003,** *36*, 2609-2615.

94. Van Horn, B. A.; Iha, R. K.; Wooley, K. L. Sequential and single-step, one-pot strategies for the transformation of hydrolytically degradable polyesters into multifunctional systems. *Macromolecules* **2008,** *41*, 1618-1626.

95. Van Horn, B. A.; Wooley, K. L. Crosslinked and functionalized polyester materials constructed using ketoxime ether linkages. *Soft Matter* **2007,** *3*, 1032-1040.

96. Taniguchi, I.; Kuhlman, W. K.; Mayes, A. M.; Griffith, L. G. Functional modification of biodegradable polyesters through a chemoselective approach: application to biomaterial surfaces. *Polymer International* **2006,** *55*, 1385-1397.

97. Taniguchi, I.; Mayes, A. M.; Chan, E. W.; Griffith, L. G. A Chemoselective approach to grafting biodegradable polyesters. *Macromolecules* **2005,** *38*, 216-219.

CHAPTER TWO

STUDY OF SOLVENT EFFECTS ON THE FLUORESCENCE OF DANSYL-DERIVATIZED POLY(ε-CAPROLACTONE)

CHAPTER TWO

Study of solvent effects on the fluorescence of dansyl-derivatized poly(ε-caprolactone)

Abstract

A dansyl-functionalized poly(ε-caprolactone) was synthesized by reacting poly(ε-caprolactone-*co*-2-oxepane-1,5 dione) (P(CL-*co*-OPD)) with dansyl hydrazine. The resulting dansylated-PCL displayed interesting fluorescence behavior and showed solvent polarity dependance as the fluorescence emission maxima (λ_{em}) shifted from 494 nm in toluene to 526 nm in dimethyl sulfoxide (DMSO). Analysis of the λ_{em} of the dansyl-grafted polymer and a dansyl-functionalized small molecule analog with respect to three different solvent polarity parameters indicated that while the fluorescence emission spectra of the dansylated polymer was influenced by solvent polarity the dansyl fluorophore was overall less sensitive to the surrounding medium when grafted onto the polyester backbone.

Introduction

The covalent labeling of polymers with chromophores and fluorophores is a technique that has been applied for probing both the physical characteristics of polymers and the way in which they interact with their surroundings.[1] Polymer-[2-4], biomolecule-[5-8], and nanoparticle-dye[9-11] conjugates are useful for tracing the location of nanoscale objects and for probing the chemical and physical environment in both intra- and extra-cellular settings. Non-covalently incorporated dyes, due to their low molecular weight and mobility, may provide misleading information regarding the location of the labeled

species; consequently, polymeric materials bearing covalently bonded chromophores and fluorophores that do not suffer from dye leaching or dye-coupling are amongst some of the most promising materials for use in biomedical and imaging applications[12, 13]

Among the variety of potential fluorescent molecules that can be covalently incorporated into macromolecules, the 5-dimethylaminonaphtylsulfonamide group, or dansyl moiety, is one of the most attractive due to the accessibility of numerous commercially available derivatives that can be used for the chemoselective conjugation of the dansyl chromophore onto a variety of synthetic and biological substrates. As the dansyl fluorophore exhibits strong solvatochromic behavior, it has a rich history of being employed in the study of polymer surfaces and films,[14-17] exploring the behavior of polymeric materials in solution,[18-20] and examining the penetration of solvents into polymer networks.[21, 22]

While the development of well-defined nanoscale materials bearing chromophores and fluorophores is an active area of research, there are very few examples investigating polyester dye conjugates. Work in this area has typically focused on attaching only one or two chromophores per polymer chain to the chain ends,[23-26] or the dye is incorporated as part of a multi-functional core.[27] In order to further extend the utility of polyester-dye conjugates, the covalent integration of multiple fluorescent probes along a poly(ε-caprolactone)-based copolymer was explored. The direct attachment of 5'-dimethyaminonapthylene-1-sulfohydrazide, commonly known as dansyl hydrazine to poly(ε-caprolactone-*co*-2-oxepane-1,5-dione) (P(CL-*co*-OPD) through hydrazone formation and the resulting solvatochromic behavior of the dansylated-polymer in a series of organic solvents is described.

Results and discussion

Synthesis of a dansylated polyester and small molecule dansyl adduct

A dansylated polyester, P(CL_{148}-*co*-OPD_8-*co*-(OPD-*g*-dansyl)$_{14}$), **1**, was obtained by reaction of P(CL_{148}-*co*-OPD_{22}) with excess dansyl hydrazine to afford a copolymer partially derivatized with dansyl moieties *via* a hydrazone formation using a procedure previously described in the literature (**Scheme 2-1**).[28] The reaction afforded a 72% yield of the dansylated polymer, but the coupling efficiency of the danysl hydrazine was, at 58%, not as efficient as other coupling methods employing aminooxy derivatives.[28]

The derivatized polymer, **1**, was analyzed by both ^{1}H NMR and ^{13}C NMR

Scheme 2-1. Synthesis of P(CL_{148}-*co*-OPD_8-*co*-(OPD-*g*-dansyl)$_{14}$), **1**.

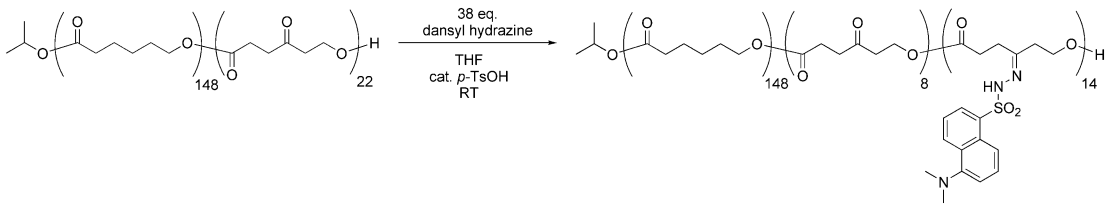

spectroscopies (**Figure 2-1 (a)**). The ^{1}H NMR spectrum exhibited resonances characteristic of the dansyl group in the aromatic region of the spectrum and a singlet at 2.90 ppm corresponding to the dimethylamino protons. The spectrum also showed a decrease in the intensity of signals associated with unfunctionalized OPD units at 4.35 ppm corresponding to the C***H***$_2$OCO protons in the OPD subunit, and the appearance of a multiplet at 4.00 ppm representative of the C***H***$_2$OCO protons in the dansyl-grafted OPD unit, thus demonstrating that the dansyl functionality was incorporated at the ketone units along the polyester backbone. ^{13}C NMR spectroscopy of the resulting fluorescent polymer, **2**, also supported incorporation of the dansyl hydrazine through hydrazone

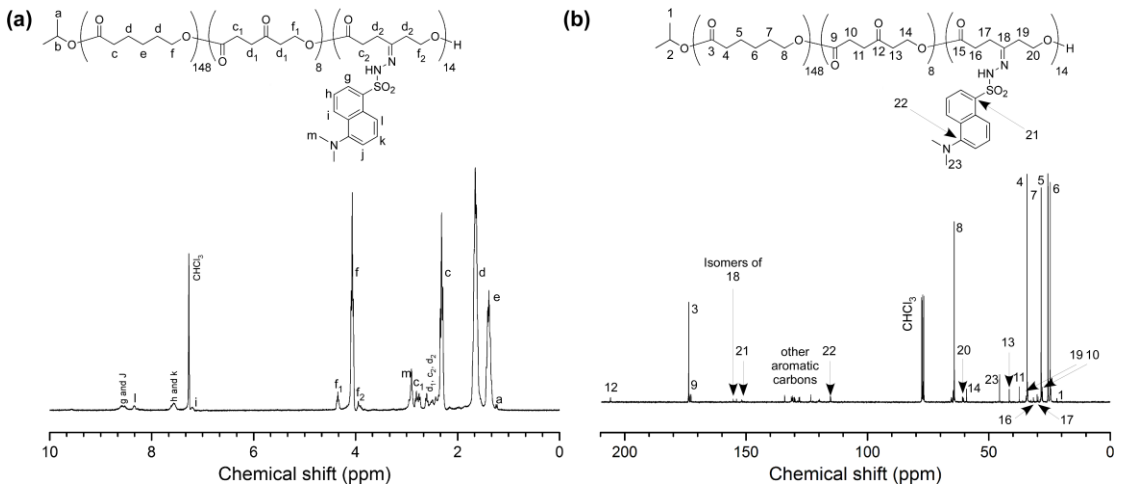

Figure 2-1(a) ^{1}H NMR spectrum and **(b)** ^{13}C NMR spectrum of P(CL_{148}-*co*-OPD_{8}-*co*-(OPD-*g*-dansyl)$_{14}$), **1**, in $CDCl_3$.

formation. Signals corresponding to the two hydrazone isomers formed were observed at 155 and 154 ppm, and signals associated with the carbons in the functionalized OPD unit could also be observed (**Figure 2-1 (b))** Resonances diagnostic of the dansyl group itself were also present, with the aromatic carbon signals occurring from 115-135 ppm, and the peak indicative of the dimethylamino carbons visible at 44.5 ppm (**Figure 2-1 (b)**).

In addition to NMR spectroscopy, the dye-polymer conjugate, **1**, was analyzed by gel permeation chromatography (GPC). The GPC traces showed a slight increase in the peak molecular weight, which supported the addition of small molecule grafts onto the polymer backbone and produced a symmetric chromatogram with a molecular weight distribution of 1.5 that was similar to that of the starting P(CL-*co*-OPD) polymer indicating that little to no degradation of the backbone occurred.

To further verify the conjugation of dansyl chromophores onto the PCL backbone, P(CL_{148}-*co*-OPD_8-*co*-(OPD-*g*-dansyl)$_{14}$), **1**, was characterized by GPC instrumentation equipped with an inline UV-vis photodiode array detector (UV-PDA). The absorption maximum observed at 29 min—the retention time associated with the polymer—was 339 nm, a reasonable absorption for the dansyl moiety (**Figure 2-2 (a) and (b)).** The RI response from the polymer and the detected UV-vis absorption due to the dansyl chromophore can be clearly associated. **Figure 2-2(c)** depicts a three dimensional plot

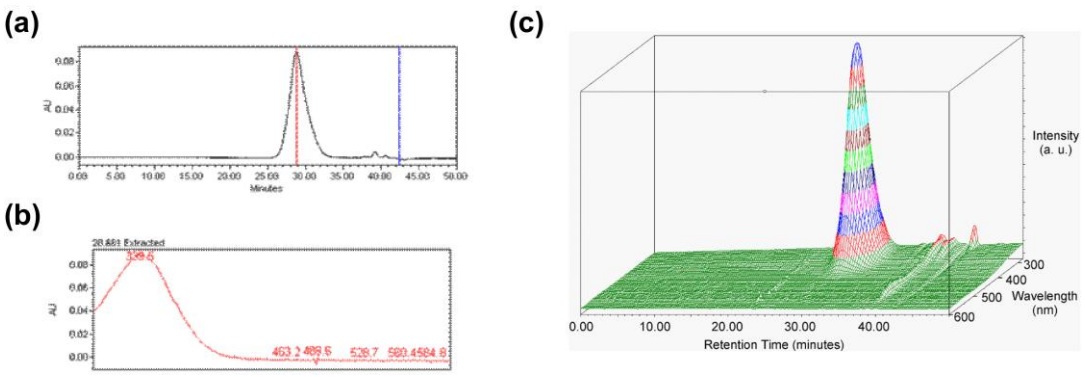

Figure 2-2. GPC UV-PDA characterization of P(CL_{148}-*co*-OPD_8-*co*-(OPD-*g*-dansyl)$_{14}$), **1**, showing **(a)** the RI detector response, **(b)** the UV absorption spectrum at a retention time of 29 min that corresponded to the peak retention time of the polyester, and **(c)** three dimensional plot of detector response as a function of wavelength and retention time.

showing detector response as a function of UV-vis absorbance and retention time. This graphic representation confirmed that that the significant UV-vis absorption occurs in conjunction with the elution of the polymer, substantiating the covalent attachment of the chromophore to the PCL backbone (**Figure 2-2 (c)).**

A small molecule analog to the dansylated copolymer, **1**, 4-(5'-dimethylaminonapthylsulfonyl)-methyl-pentanoate, **2**, was produced by the reaction of dansyl hydrazine with methyl levulinate (**Scheme 2-2**). The reaction went to completion

Scheme 2-2. Synthesis 4-(5'-dimethylaminonapthylsulfonyl)-methyl-pentanoate, **2.**

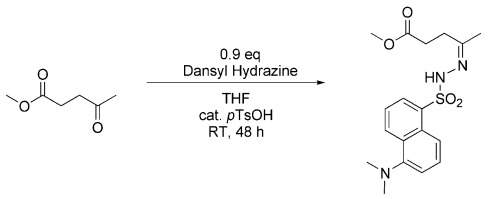

over a 48 h period at room temperature and produced the desired dansyl-conjugated small molecule analog, **2**, in high yield.

^{1}H NMR characterization of 4-(5'-dimethylaminonapthylsulfonyl)-methyl-pentanoate, **2**, confirmed that attachment of the dansyl through hydrazone formation was successful. **Figure 2-3 (a)** shows the anticipated aromatic signals associated with the protons of the dansyl moiety from 8.60-7.15 ppm and diplayed resonances corresponding the dimethylamino groups at 2.90 ppm (**Figure 2-3 (a)**). Hydrazone formation was confirmed by the absence of a signal at 2.1 ppm corresponding to the terminal methyl group α to the ketone in methyl levulinate, which upon hydrazone formation shifted upfield to 1.76 ppm. This compound forms *cis* and *trans* isomers of the hydrazone which can be observed by the dual signals for the methyl ester protons at 3.58 and 3.52 ppm and the proton signals for the methyl group alpha to the ketone at 1.79 and 1.76 ppm. The ^{13}C NMR spectrum also supports complete functionalization of the ketone based upon signals at 115-135 ppm indicative of the aromatic carbons of the dansyl chromophore, the presence of resonances at 156.9 and 154.9 ppm representative of the newly formed hydrazone, and the absence of a peak at 205 ppm corresponding to unreacted ketone group (**Figure 2-3 (b)).** The formation of *cis* and *trans* isomers is made very clear in ^{13}C spectrum, as there are dual signals present for each carbon in the molecule.

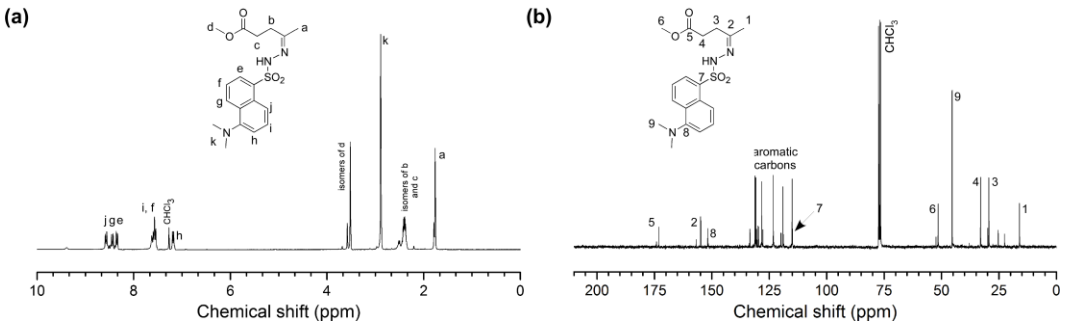

Figure 2-1(a) ^{1}H NMR spectrum and **(b)** ^{13}C NMR spectrum of 4-(5'-dimethylaminonapthylsulfonyl)-methyl-pentanoate, **2**, in $CDCl_3$

Absorption and Emission Spectra

The chromophore-bearing polymer, **1**, and small molecule analog, **2**, were analyzed by UV-vis and fluorescence emission spectroscopy in a series of six organic solvents to assess the solvatochromic behavior of the dansyl moiety when it has freedom to interact freely with the solvent *vs.* when it is covalently tethered to a polyester chain (**Table 2-1**) The absorption band maxima, λ_{abs}, of both the dansylated polymer, **1**, and small molecule-dye conjugate, **2**, were nearly constant in all six solvents, and in all cases the λ_{abs} was a single band with a wavelength close to 345 nm. The absorption observed for the dansyl hydrazone is also significantly different than the 330 nm λ_{abs} reported for dansyl hydrazine[29] and closely matches the λ_{abs} that have been previously reported in the literature for an assortment of small molecule dansyl hydrazones.[30]

The fluorescence emission spectra of polymer, **1**, and the small molecule, **2**, showed the anticipated stokes shift of approximately 150 nm traditionally associated with the dansyl fluorophore (**Figure 2-4).** [29, 30] Dansyl groups are known to exhibit dual

Table 2-1. Summary of the refractive index (*n*), dielectric constant (ε), Dimroth's $E_T(30)$, π*, and the λ_{abs} and λ_{em} of the dansylated polymer, **1,** and small molecule analog, **2**, in tested solvents at room temperature.

					Small Molecule Analog, 1		Functionalized Polymer, 2	
Solvent	n[a]	ε[a]	$E_T(30)$[b,c]	π*[b]	λ_{abs} (nm)	λ_{em} (nm)	λ_{abs} (nm)	λ_{em} (nm)
Toluene	1.49	2.4	34	--	346	488	346	494
Ethyl acetate	1.37	6.0	38	0.55	342	503	344	512
Tetrahydrofuran	1.40	7.6	37	0.58	342	501	344	502
Dichloromethane	1.42	9.1	41	0.82	348	513	348	514
N,N-dimethylformamide	1.43	36.7	44	1.0	346	522	346	527
Dimethyl sulfoxide	1.48	46.6	45	1.0	346	530	342	526

[a] From *The Handbook of Organic Solvent Properties*[31]
[b] From *Modern Physical Organic Chemistry*[32]
[c] From *Solvent Effects in Organic chemistry*[33]

fluorescence with one band occurring at high energy that corresponds to the non-charge transfer state (b* band) and the other being a lower energyband representative of the intramolecular charge transfer state (a* band), which is the band known to be responsive to the polarity or polarizability of the surrounding medium. For the fluorophore-derivatized polymer, **1**, and the fluorescent small molecule, **2**, the fluorescence observed was typically a singular fluorescence corresponding to emission from the intramolecular charge transfer state (**Figure2-4 (a) and (b)**).

The dansylated small molecule, **1**, shows the anticipated solvatochromic trend where the emission maximum (λ_{em}) increases in wavelength with increasing solvent polarity with the greatest red shift occurring when the emission spectrum is taken in dimethyl sulfoxide (DMSO) (**Figure 2-4 (a)**). While the λ_{em} is similar for both the polymer and the small molecule analog in many solvents, there are distinct differences in the λ_{em}, for ethyl acetate (EtOAc). In EtOAc, λ_{em} occurs at 512 nm and 503 nm for the functionalized PCL and small molecule fluorophore respectively. Additionally, the dansyl-bearing polymer, **1**, does not clearly exhibit the traditionally observed increase in λ_{em} with solvent

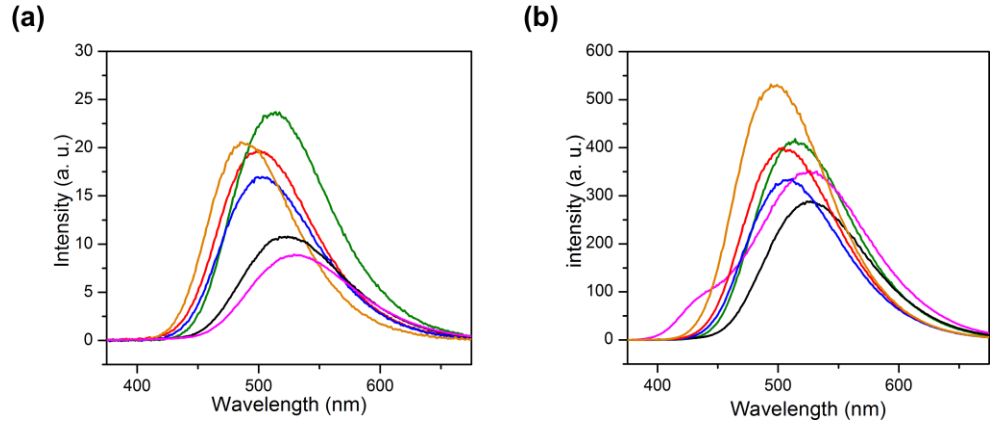

Figure 2-4. Fluorescence emission spectra for **(a)** the small-molecule dansyl conjugate, **2** and **(b)** P(CL_{148}-*co*-OPD_8-*co*-(OPD-*g*-dansyl)$_{14}$), **1**, in toluene (orange), ethyl acetate (blue), tetrahydrofuran (red), dichloromethane (green), N,N-dimethylformamide (black), and dimethyl sulfoxide (pink).

polarity observed in the emission spectra of the dansylated methyl levulinate. The series of emission spectra show one major deviation for the dansylated polymer: the λ_{em} for the polyester-dye conjugate, **2**, in EtOAc is significantly greater than the λ_{em} in tetrahydrofuran (THF) despite the fact that THF is generally considered to be the more polar solvent based upon the dielectric constant and should provide greater stabilization for the excited state of the dansyl fluorophore, (**Table 2-1, Figure 2-4 (b)** (blue)). Another unique characteristic of the dansylated polymer is observed in the emission spectrum taken in DMSO, where the dansyl fluorophore appears to be exhibiting dual fluorescence showing emission bands associated with both the non-charge transfer state and intramolecular charge transfer state (**Figure 2-4 (b)** (pink)). The λ_{em}, was, as in the other spectra obtained, still representative of the a* band or the fluorescence emission from the charge transfer state.

Scale of solvent polarity

In order to better understand how solvent polarity affected the dansyl fluorophore for the functionalized polymer, **1**, and small molecule, **2**, the λ_{em} observed in each solvent

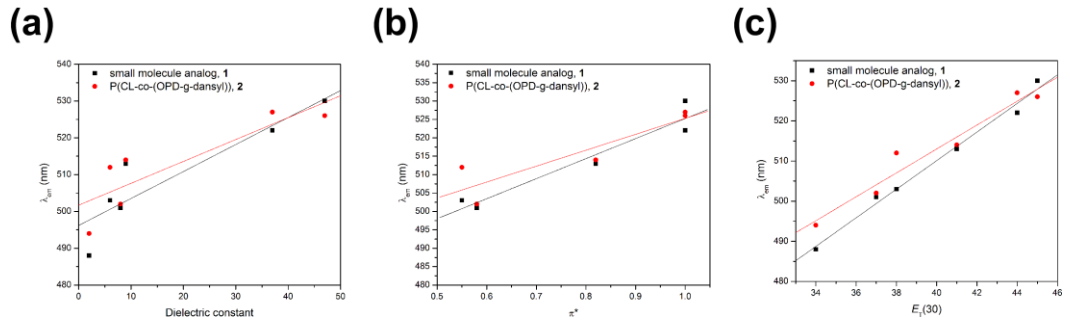

Figure 2-5. λ_{em} for the small-molecule dansyl conjugate, **2** (black) and P(CL_{148}-*co*-OPD_8-*co*-(OPD-*g*-dansyl)$_{14}$), **1** (red), plotted against **(a)** solvent dielectric constant, **(b)** π* and **(c)** Dimroth's E_T(30).

series was correlated with three different solvent polarity parameters. The first was a comparison of the dielectric constant of the solvents used with the λ_{em} (**Figure 2-5 (a)**). The polymeric and small molecule hydrazone conjugates, **1** and **2** respectively, show a linear relationship between λ_{em} and the dielectric constant. However, the slope observed in the plot for the polymer is less than the slope observed in the plot for the small molecule. This would suggest that the excited state of the dansyl fluorophore when attached to the polyester backbone is not affected as greatly by the polarity of the medium in which it is dissolved. Alternatively, the excited state of the small molecule dansyl hydrazone, **2**, with its greater slope appeared to be more sensitive to its surroundings, suggesting that the solvent playe a more pronounced role in with respect to stabilizing the excited state of the dansyl moiety in the less sterically hindered small molecule analog.

This same trend was also observed when λ_{em} was correlated with two empirical solvent polarity scales: π^*, which is based upon observed transition energies from several different dyes, [34, 35] and Dimroth's $E_T(30)$, a scale based upon the transition energy for pyridinium-N-phenol betaine.[33] Kowsower's *Z*, though a commonly used empirical solvent parameter was not employed in this analysis due to the lack of Z values available for the solvents used in this study.[36] When λ_{em} was plotted against π^* (**Figure 2-5 (b)**) and $E_T(30)$ (**Figure 2-5 (c)**), the fluorophore-bearing polymer, **1,** showed a red shift that correlated with solvent polarity, but again both solvent parameters demonstrated that the fluorescence behavior of the dansyl groups covalently associated with the PCL backbone were not affected as dramatically by solvent polarity or polarizability as the dansylated methyl levulinate (**Figure 2-5**). Ultimately, the fluorescence behavior of

P(CL_{148}-*co*-OPD_8-*co*-(OPD-*g*-dansyl)$_{14}$), **1**, correlates best with Dimroth's $E_T(30)$, in which the empirically determined polarity of EtOAc is slightly greater than that of THF, which may partially explain what previously appeared to be an anomaly associated with the λ_{em} in that solvent (**Table 2-1, Figure 2-5 (b)**)

Experimental

Materials

The synthesis of 1,4,8-trioxaspiro-9-undecanone (TOSUO)[37-40] and P(CL-co-OPD) has been described previously.[41, 42] ε-Caprolactone c(CL) (Aldrich Chemical Company) was distilled from CaH_2 and stored under argon. Toluene and tetrahydrofuran (Aldrich Chemical Company) were dried by heating at reflux over sodium and distilled under argon prior to use. Aluminum triisopropoxide $Al(OiPr)_3$ (Aldrich Chemical Company) was purified by sublimation and dissolved in dry toluene prior to use. The dimethyl sulfoxide and N, N,-dimethyl formamide used in spectral experiments were distilled under vacuum from molecular sieves. All other reagents (solvents, *p*-toluenesulfonic acid (*p*-TsOH), dansyl hydrazine, methyl levulinate, *etc*.) were purchased from Aldrich and used as received**.**

Instrumentation

^1H NMR (300 MHz) and ^{13}C NMR (75 MHz) spectra were acquired in $CDCl_3$ unless otherwise noted on a Varian Mercury 300 spectrometer using the residual solvent signal as the internal reference. Infrared spectra were recorded on a Perkin-Elmer Spectrum RX FT-IR system by film deposition onto NaCl salt plates. Differential

scanning calorimetry was performed under nitrogen atmosphere using 40 μL aluminum pans on a Mettler Toledo DSC822 with heating and cooling at 10 °C/min from –100 °C to 100 °C. T_m values were obtained from the third heating scan as the peak values from the thermogram. Gel permeation chromatography was performed on a Waters Chromatography, Inc., 1515 isocratic HPLC pump equipped with an inline degasser, a model PD2020 dual-angle (15° and 90°) light scattering detector (Precision Detectors, Inc.), a model 2414 differential refractometer (Waters, Inc.), and four PL_{gel} polystyrene-*co*-divinylbenzene gel columns (Polymer Laboratories, Inc.) connected in series: 5 μm Guard (50 × 7.5 mm), 5 μm Mixed C (300 × 7.5 mm), 5 μm 10^4 (300 × 7.5 mm), and 5 μm 500 Å (300 × 7.5 mm) using the Breeze (version 3.30, Waters, Inc.) software. The instrument was operated at 35 °C with THF as eluent. Data collection was performed with Precision Acquire 32 Acquisition program (Precision Detectors, Inc.) and analyses were carried out using Discovery32 software (Precision Detectors, Inc.) with a system calibration curve generated from plotting molecular weight as a function of retention time for a series of broad polydispersity poly(styrene) standards. UV-vis spectroscopy data were collected on a Varian Cary 1E UV-vis spectrophotometer. Fluorescence spectroscopy was performed using a Varian Cary Eclipse fluorescence spectrophotometer. Solutions used for UV-vis and fluorescence emission experiments for the small molecule were approximately 1.8 x 10^{-4} M. Solutions used for UV-vis and fluorescence emission experiments for the polymer had a concentration of approximately 0.30 mg/mL, corresponding to a 2.0 x 10^{-4} M concetration of dansyl functionalities in solution.

Synthesis

P(CL-*co*-OPD) Copolymer Synthesis

Random copolymers of ε-caprolactone (CL) and 2-oxepane-1,5-dione (OPD) were prepared by ring opening polymerization of CL and the synthetic monomer TOSUO by initiation with $Al(OiPr)_3$, and the resulting P(CL-*co*-TOSUO) was subsequently deprotected using triphenylcarbenium tetrafluoroborate as previously reported.[41, 42]

P(CL_{148}–*co*-OPD_{22}) GPC: M_n= 31400 Da, M_w= 45200 Da, PDI = 1.4. M_n (^{1}H NMR) = 19800 Da. ^{1}H NMR (300 MHz, $CDCl_3$) δ 5.0 (septet, J = 6.3 Hz, 1 H of initiated chain end, $(CH_3)C\boldsymbol{H}_2O$), 4.25 (t, J = 7.2 Hz, 2 H of OPD units, $C\boldsymbol{H}_2OCO$), 4.05 (t, J = 6.6 Hz, 2H of CL units, $C\boldsymbol{H}_2OCO$), 3.65(t, J = 6.3 Hz, 2H of terminated chain end, $C\boldsymbol{H}_2OH$), 2.82 (t, J = 7.2 Hz, 2 H OPD units, $C(O)CH_2C\boldsymbol{H}_2COO$), 2.75 (t, J = 7.2 Hz, 2 H OPD units 2H OPD units, $C(O)C\boldsymbol{H}_2CH_2COO$), 2.62 (t, J = 7.5 Hz, 2 H OPD units, $C\boldsymbol{H}_2CH_2OCO$) 2.3 (t, J = 7.5 Hz, 2 H of CL units, $C\boldsymbol{H}_2COOCH_2$), 1.65 (m, 4 H of CL units, $OCH_2C\boldsymbol{H}_2$and $C\boldsymbol{H}_2CH_2COO$), 1.45 (m, 2 H of CL units, $C\boldsymbol{H}_2CH_2CH_2COO$), 1.25 ppm (d, J = 6.3 Hz, 6 H of initiated chain end, $(C\boldsymbol{H}_3)_2CHO$). ^{13}C NMR (75 MHz, $CDCl_3$) δ 205.9, 173.4, 172.7, 64.6, 64.2, 59.2, 41.6, 37.5, 34.2, 34.0, 28.4, 27.9, 25.6, 24.7, 24.5 ppm. IR (cm^{-1}) 3600-3000, 2946, 2866, 1727 (str, multiple modes), 1471, 1419, 1397, 1366, 1239, 1296, 1242, 1191, 1108, 1061, 1046, 962, 934, 842, 806, 771, 733, 707.

P(CL_{148}-co-OPD_8-*co*-(OPD-*g*-dansyl)$_{14}$) (1). A solution of dansyl hydrazine (67.1 mg, 0. 253 mmol) in THF (0.5 g) was added to a vial containing a solution of P(CL_{148}-*co*-OPD_{22}) (131.6 mg, 0.00665 mmoles)in THF (0.5 g). The solution was stirred at RT for

ten minutes to ensure complete mixing of the two chemicals, after which 2 drops of a solution of *p*-toluenesulfonic acid (75 mg in 2.0 mL of THF) was added to the reaction. The reaction was allowed to proceed at RT for 6 h and reaction progress was monitored by ^{1}H NMR spectroscopy. The product was isolated by precipitation into cold hexanes, was collected by vacuum filtration, and was dried *in vacuo* for 24 h to yield a lightly yellow (120.1 mg, 72 %. Yield) GPC: $M_{n,\,PS}$ = 27600 Da, $M_{w,\,PS}$ = 40100 Da, PDI_{PS} = 1.5. M_n (^{1}H NMR) = 21700 Da. ^{1}H NMR (300 MHz, CDCl) δ 8.6-7.15 (four m, 6 H, aromatic of dansyl), 4.35 (t, J = 7.2 Hz, 2 H of OPD units,C***H***$_2$OCO), 4.05 (t, J = 6.6 Hz, 2 H of CL units, C***H***$_2$OCO), 4.00 (m, J = 7.2 Hz, 2 H of OPD-*g*-dansyl, C***H***$_2$OCO), 2.90 (broad singlet, 6 H of dansyl units, N(C***H***$_3$)$_2$), 2.82 (t, J = 7.2 Hz, 2 H of OPD units, C(O)CH$_2$C***H***$_2$COO), 2.75 (t, J = 7.2 Hz, 2 H of OPD units, C(O)C***H***$_2$CH$_2$), 2.70-2.4 (t, J = 7.5 Hz, 2 H of OPD units; 4 H of OPD-*g*-dansyl), 2.3 (t, J = 7.5 Hz, 2 H of CL units, C***H***$_2$COOCH$_2$), 1.65 (m, 4 H of CL units, OCH$_2$C***H***$_2$and C***H***$_2$CH$_2$COO), 1.45 (m, 2 H of CL units, C***H***$_2$CH$_2$CH$_2$COO), 1.25 ppm (d, J = 6.3 Hz, 6 H of initiated chain end, (C***H***$_3$)$_2$CHO). ^{13}C NMR (75 MHz, $CDCl_3$) δ 205.9, 173.8, 173.7, 173.4, 173.3, 172.8, 172.7, 155.3, 154.0, 151.8, 134-128, 123.5, 120.2, 119.8, 115.4, 115.2, 77.5, 65.6, 65.2, 64.6, 61.0, 60.6, 59.2, 45.6, 42.6, 37.6, 36.0, 34.6, 34.0, 33.8, 32.0, 30.2, 29.8, 28.2, 28.0, 25.7, 24.7, 24.4, 22.0 ppm.

4-(5'-dimethylaminonapthylsulfonyl)-methyl-pentanoate (2). Dansyl Hydrazine (110 mg, 0.377 mmol, 1.0 eq) was dissolved in THF (0.5 mL), and a solution of methyl levulinate (72.9 mg, 0.56 mmol, 1.5 eq) in THF (2.5 mL) was added to the reaction mixture. The reaction was stirred at room temperature for 5 min. to ensure complete

dissolution, after which 5 drops of a solution of *p*-toluenesulfonic acid (75 mg in 20 mL of THF) was added to the reaction. The reaction was allowed to proceed at RT, and was monitored by ^{1}H NMR spectroscopy to determine completion. After stirring for 48 h, solvent was removed by rotary evaporation, and the sample was dried *in vacuo* for 12 h. 100% conversion of the dansyl hydrazine to the equivalent hydrazone was observed based upon ^{1}H NMR analysis. Resulting samples were subsequently used for UV-vis and fluorescence experiments. (138 mg, 0.365 mmol, 96% yield). ^{1}H NMR (300 MHz, CDCl) δ 8.56 (d, J = 8.5 Hz, 1H, aromatic of dansyl), 8.56 (d, J = 8.5 Hz, 1H, aromatic of dansyl), 8.54 (d, J = 8.8 Hz, 1H, aromatic of dansyl), 8.35 (d, J = 7.7 Hz, 1H, aromatic of dansyl), 7.57 (t, J = 7.9 Hz, 2 H, aromatic of dansyl), 7.19 (d, J = 7.4 Hz, 1H, aromatic of dansyl), 3.58 and 3.52 (s, 3 H, isomers of C***H***$_3$OCO), 2.89 (s, 6H, (C***H***$_3$)$_2$N), 2.55-2.35 (two m, isomers of $CH_2C\boldsymbol{H}_2C(O)CH_3$ and $OCOC\boldsymbol{H}_2CH_2$), 1.79 and 1.76 (s, 3H, C(O)C***H***$_3$). ^{13}C NMR (75 MHz, $CDCl_3$) δ 174.2, 173.1, 156.9, 154.9, 151.8, 151.5, 133.9, 133.4, 131.2, 130.9, 130.5, 129.9, 129.7, 128.3, 127.8, 123.3, 119.9, 119.0, 115.1, 114.9, 52.4, 51.5, 45.4, 33.0, 29.9, 29.4, 25.4, 22.6, 16.1 ppm.

Conclusions

Conjugation of multiple dansyl chromophores to the backbone of P(CL-*co*-OPD) was completed *via* acid-catalyzed hydrazone formation. Derivatization of the polyester backbone with the dansyl moiety was established by the appearance of aromatic resonances in the ^{1}H NMR spectrum combined with a shift in the resonances associated with the OPD subunits; the appearance of aromatic resonances and new signals corresponding to the newly formed hydrazone functionalities in the ^{13}C NMR spectrum

of the polyester further substantiated the covalent attachment of the chromophore. Analysis of the resulting polymer by GPC UV-PDA verified that the resulting fluorescence of the polyester sample was caused by covalently bound dansyl groups conjugates.

The dansylated polyester, **1**, was characterized by UV-vis and fluorescence emission spectroscopy in a series of solvents. The dansylated-PCL showed solvatochromic behavior and exhibited an increase in the λ_{em} with increasing solvent polarity. The λ_{em} of the dansylated- P(CL-*co*-OPD), **1**, and the λ_{em} of a dansyl-derivatized small molecule analog, **2**, were plotted against the dielectric constant as well as two empirical solvent polarity parameters—Dimroth's $E_T(30)$ and π^*. From these analyses it was observed that the λ_{em} of the dansyl fluorophore, when covalently bound to the P(CL-*co*-OPD) backbone, was not as sensitive to the polarity of the surrounding solvent, and that Dimroth's $E_T(30)$ appeared to be the empirical polarity scale that best correlated with the spectral behavior of the polymer-bound fluorophore. This work demonstrated that attachment to a macromolecule can appreciably change the behavior of a fluorophore or chromophore. Consequently, spectroscopic analysis of polymer-dye conjugates should be performed as a essential part of characterization process, because analysis of a monomer or small molecule analog may not provide a complete picture of the solvatochromic behavior of polymeric materials carrying covalently bound dyes.

Acknowledgements

This material is based upon work supported in part by the National Science Foundation under Grant No. DMR-0451490 and Grant No. DMR-0906815, by the Department of

Energy under Grant No. DE-FG02-08ER64671, and by the National Heart Lung and Blood Institute of the National Institutes of Health as a Program of Excellence in Nanotechnology (HL080729). Additional thanks go out to Dr. Benjamin Beck and Professor Craig J. Hawker at the University of California Santa Barbara for the acquisition of GPC UV-PDA data for the dansyl-functionalized PCL polymers. GPC analysis was performed through the Materials Facilities Network, www.mfrn.org.

References

1. Winnik, F. M., Photophysics of preassociated pyrenes in aqueous polymer solutions and in other organized media. *Chemical Reviews* **1993,** *93*, 586-614.

2. Flemming, C.; Maldijian, A.; Da Costa, D.; Rullay, A. K.; Haddleton, D. M.; St. John, J.; Penny, P.; Noble, R. C.; Cameron, N. R.; Davis, B. G., A carbohydrate-antioxidant hybrid polymer reduces oxidative damage in spermatozoa and enhances fertility. *Nature Chemical Biology* **2005,** *1*, 270-274.

3. Droumaguet, B. L.; Mantovani, G.; Haddleton, D. L.; Velonia, K., Formation of giant amphiphiles by post-functionalization of hydrophilic protein–polymer conjugates. *Journal of Materials Chemistry* **2007,** *17*, 1916-1922.

4. Nicolas, J.; Khoshde, E.; Haddleton, D. M., Bioconjugation onto biological surfaces with fluorescently labeled polymers. *Chemical Communications* **2007**, 1722-1724.

5. Sawa, M.; Hsu, T.-L.; Itoh, T.; Sugiyama, M.; Hanson, S. R.; Vogt, P. K.; Wong, C.-H., Glycoproteomic probes for fluorescent imaging of fucosylated glycans in vivo. *Proceedings of the National Academy of Sciences* **2006,** *103*, 12371-12376.

6. Toutchkine, A.; Nguyen, D.-V.; Hahn, K. M., Simple one-pot preparation of water-soluble, cysteine-reactive cyanine and merocyanine dyes for biological imaging. *Bioconjugate Chemistry* **2007,** *18,* 1344-1348.

7. Bai, M.; Rone, M. B.; Papadopoulos, V.; Bornhop, D. J., A novel functional translocator protein ligand for cancer imaging. *Bioconjugate Chemistry* **2007,** *18,* 2018-2023.

8. Bai, M.; Wyatt, S. K.; Han, Z.; Papadopoulos, V.; Bornhop, D. J., A novel conjugable translocator protein ligand labeled with a fluorescence dye for in vitro imaging. *Bioconjugate Chemistry* **2007,** *18*, 1118-1122.

9. Opsteen J. A; Brinkhuis, R. P.; Teeuwen, R. L. M.; Löwik, D. W. P. M.; van Hest, J. C. M., Clickable polymersomes. *Chemical Communications* **2007**, 3136 - 3138.

10. Samuelson, L. E.; Dukes, M. J.; Hunt, C. R.; Casey, J. D.; Bornhop, D. J., TSPO targeted dendrimer imaging agent: synthesis, characterization, and cellular internalization. *Bioconjugate Chemistry* **2009,** *20* (11), 2082-2089.

11. Park, J.; Yang, J.; Lee, J.; Lim, E. K.; Suh, J. S.; Huh, Y. M.; Haam, S., Synthesis and characterization of fluorescent magneto polymeric nanoparticles (FMPNs) for bimodal imaging probes. *J. Colloid Interface Sci.* **2009,** *340,* 176-181.

12. Stewart, W. W., Lucifer dyes-highly fluorescent dyes for biological tracing. *Nature* **1981,** *292*, 17-21.

13. Harm-Anton Klok, H.-A.; Becker, S.; Schuch, F.; Pakula, T.; Müllen, K., Synthesis and solid state properties of novel fluorescent polyester star polymers. *Macromolecular Bioscience* **2003,** *3*, 729-741.

14. Holmes-Farley, S. R.; Whitesides, G. M., Fluorescence properties of dansyl groups covalently bonded to the surface of oxidatively functionalized low-density polyethylene film. *Langmuir* **1986,** *2*, 266-281.

15. González-Benito, J.; Aznar, A.; Baselga, J., Solvent and temperature effects on the polymer-coated glass fibers. Fluorescence of the dansyl moiety. *Journal of Fluorescence* **2002,** *11*, 307-314.

16. Ding, L.; Fang, Y.; Jiang, L.; Gao, L.; Yin, X., Twisted intra-molecular electron transfer phenomenon of dansyl immobilized on chitosan film and its senseing property to the composition of ethanol/water mixtures. *Thin Solid Films* **2005,** *478*, 318-325.

17. Kang, J.; Ding, L.; Lü, F.; Zhang, S.; Fang, Y., Dansyl-based fluroescent flim sensor for nitroaromatics. *Journal of Physics D: Applied Physics* **2006,** *39*, 5097-5102.

18. Chen, H.-L.; Morawetz, H., Kinetics of polymer complex interchange in poly(acrylic acid)-poly(oxyethylene) solutions. *Macromolecules* **1982,** *15*, 1445-1447.

19. Strauss, U. P.; Vesnaver, G., Optical probes in polyelectrolyte studies. II. Fluorescence spectra of dansylated copolymers of maleic anhydride and alkyl vinyl ethers. *The Journal of Physical Chemistry* **1975,** *79*, 2426-2429.

20. Wang, B.-B.; Zhang, X.; Jia, X.-R.; Li, Z.-C.; Ji, Y.; Yang, L.; Wei, Y., Fluorescence and aggregation behavior of poly(amidoamine) dendrimers peripherally modified with aromatic chromophores: The effect of dendritic architectures. *Journal of the American Chemical Society* **2004,** *126*, 15180-15194.

21. Shea, K. J.; Sasaki, D. Y.; Stoddard, G. J., Fluorescence probes for evaluating chain solvation in network polymers. An analysis of the solvatochromic shift of the dansyl probe in macroporous styrene-divinylbenzene and styrene-diisopropenylbenzene copolymers. *Macromolecules* **1989,** *22*, 1722-1730.

22. Hoffmann, D. A.; Anderson, J. E.; Frank, C. W., Solvent partitioning in fluorescent polydimethylsiloxane networks. *Journal of Materials Chemistry* **1995,** *5*, 13-25.

23. Ciardelli, G.; Saad, B.; Lendlein, A.; Neuenschwander, P.; Suter, U. W., Synthesis of fluorescence-labled short-chain polyester segments for the investigation of bioresorbable poly(ester-urethane)s. *Macromolecular Chemistry and Physics* **1997,** *198*, 1481-1498.

24. Ciardelli, G.; Kojima, K.; Lendlein, A.; Neuenschwander, P.; Suter, U. W., Synthesis of biomedical, fluorescence-labled polyurethanes for the investigation of their degradation. *Macromolecular Chemistry and Physics* **1997,** *198*, 2667-2688.

25. Carstens, M. G.; Bevernage, J. J. L.; van Nostrum, C. F.; van Steenbergen, M. J.; Flesch, F. M.; Verrijk, R.; de Leede, L. G. J.; Crommelin, D. J. A.; Hennink, W. E., Small oligomeric micelles based on end group modified mPEG-oligocaprolactone with monodisperse hydrophobic blocks. *Macromolecules* **2006,** *40*, 116-122.

26. Picarra, S.; Martinho, J. M. G., Viscoelastic effects on dilute polymer solutions phase demixing: Fluorescence study of a poly(epsilon-caprolactone) chain in THF. *Macromolecules* **2000,** *34*, 53-58.

27. Klok, H.-A.; Becker, S.; Schuch, F.; Pakula, T.; Müllen, K., Synthesis and solid state properties of novel fluorescent polyester star polymers. *Macromolecular Bioscience* **2003,** *3*, 729-741.

28. Van Horn, B. A.; Iha, R. K.; Wooley, K. L., Sequential and single-step, one-pot strategies for the transformation of hydrolytically degradable polyesters into multifunctional systems. *Macromolecules* **2008,** *41*, 1618-1626.

29. Haugland, R. P., *Handbook of Fluorescent Probe Probes and Research Chemicals*. Molecular Probes, Inc.: USA, 1992.

30. Binding, N.; Kläning, H.; Karst, U.; Pötter, W.; Czeschinski, P. A.; Witting, U., Analytical realiability of carbonyl compound determination using 1,5-dansylhydrazine-derivatization. *Fresenius Journal of Analytical Chemistry* **1998,** *362*, 270-273.

31. Smallwood, I. M., *Handbook of Organic Solvent Properties*. Halsted Press: New York, 1996.

32. Anslyn, E. V.; Dougherty, D. A., *Modern Physical Organic Chemistry*. University Science Books: Sausalito, CA, 2006.

33. Reichardt, C., *Solvent Effects in Organic Chemistry*. Verlag Chemie: New York, 1979; Vol. 3.

34. Kamlet, M. J.; Abboud, J. L.; Taft, R. W., The solvatochromic comparison method. 6. The .pi.* scale of solvent polarities. *Journal of the American Chemical Society* **1977,** *99* (18), 6027-6038.

35. Abboud, J. L.; Kamlet, M. J.; Taft, R. W., Regarding a generalized scale of solvent polarities. *Journal of the American Chemical Society* **1977,** *99*, 8325-8327.

36. Kosower, E. M., The effect of solvent on spectra. I. A new empirical measure of solvent polarity: Z-values. *Journal of the American Chemical Society* **1958,** *80,* 3253-3260.

37. Tian, D.; Dubois, P.; Grandfils, C.; Jérôme, R., Ring-opening polymerization of 1,4,8-trioxospiro[4.6]-9-undecanone: A new route to aliphatic polyesters bearing functional pendant groups. *Macromolecules* **1997,** *30,* 406-409.

38. Tian, D.; Dubois, P.; Jérôme, R., Macromolecular engineering of polylactones and polylactides 23. Synthesis and characterization of biodegradable and biocompatible homopolymers and block Copolymers based on 1,4,8-trioxa[4.6]spiro-9-undecanone. *Macromolecules* **1997,** *30,* 1947-1954.

39. Tian, D.; Dubois, P.; Jérôme, R., Macromolecular engineering of polylactones and polylactides. 22. Copolymerization of 1,4,8-trioxaspiro[4.6]-9-undecanone initiated by aluminum isopropoxide. *Macromolecules* **1997,** *30,* 2575-2576.

40. Tian, D.; Dubois, P.; Jérôme, R., Poly(2-oxepane-1,5-dione): A highly crystalline modified poly(epsilon-caprolactone) of a high melting temperature. *Macromolecules* **1998,** *31,* 924-927.

41. Latere Dwan'Isa, J.-P.; Lecomte, P.; Dubois, P.; Jérôme, R., Synthesis and characterization of random copolyesters of epsilon-caprolactone and 2-oxepane-1,5-dione. *Macromolecules* **2003,** *36,* 2609-2615.

42. Latere, J.-P.; Lecomte, P.; Dubois, P.; Jérôme, R., 2-Oxepane-1,5-dione: A precursor of a novel class of versatile semicrystalline biodegradable (co)polyesters. *Macromolecules* **2002,** *35,* 7857-7859.

CHAPTER THREE

COMPLEX, DEGRADABLE POLYESTER MATERIALS *VIA* KETOXIME ETHER-BASED FUNCTIONALIZATION: AMPHIPHILIC, MULTIFUNCTIONAL GRAFT COPOLYMERS AND THEIR RESULTING SOLUTION-STATE AGGREGATES

CHAPTER THREE

Complex, degradable polyester materials *via* ketoxime ether-based functionalization: Amphiphilic, multifunctional graft copolymers and their resulting solution-state aggregates

[This work has been submitted and accepted for publication as Iha, R.; Van Horn, B. A.; Wooley, K. L. Complex, degradable polyester materials *via* ketoxime ether-based functionalization: Amphiphilic, multifunctional graft copolymers and their resulting solution-state aggregates, *Journal of PolymerScience Part A: Polymer Chemistry*, **2010**, *accepted*]

Abstract

Degradable, amphiphilic graft copolymers of poly(ε-caprolactone)-*graft*-poly(ethylene oxide), PCL-*g*-PEO, were synthesized *via* a grafting onto strategy taking advantage of the ketones presented along the backbone of the statistical copolymer poly(ε-caprolactone)-*co*-(2-oxepane-1,5-dione), (PCL-*co*-OPD). Through the formation of stable ketoxime ether linkages, 3 kDa PEO grafts and *p*-methoxybenzyl side chains were incorporated onto the polyester backbone with a high degree of fidelity and efficiency, as verified by NMR spectroscopies and GPC analysis (90% grafting efficiency in some cases). The resulting block graft copolymers displayed significant thermal differences, specifically a depression in the observed melting transition temperature, T_m, in comparison to the parent PCL and PEO polymers. These amphiphilic block graft copolymers undergo self assembly in aqueous solution with the P(CL-*co*-OPD-*co*-(OPD-*g*-PEO)) polymer forming spherical micelles and a P(CL-*co*-OPD-*co*-(OPD-*g*-PEO)-*co*-(OPD-*g*-*p*MeOBn)) forming

cylindrical or rod-like micelles, as observed by transmission electron microscopy (TEM) and atomic force microscopy (AFM).

Introduction

When investigating chemistries for the functionalization of polymeric materials, it is critical to consider reactions that are quantitative, chemoselective, and functional group tolerant, especially when performing chemistry in the presence of biological molecules or macromolecules that may contain sensitive or reactive groups. Consequently, synthetic strategies used in the creation or modification of well-defined structurally- and compositionally-complex materials must, by necessity, employ reactions that exhibit a high degree of fidelity and that proceed under mild reaction conditions.[1-3] In terms of transformations that are efficient yet orthogonal to a multiplicity of chemical centers, those involving carbonyls demonstrate great breadth, due to the uniqueness and high reactivity of aldehydes and ketones. Hydrazide, (thio)semicarbizide, and aminooxy compounds are all nitrogen-containing nucleophiles that are capable of specific reaction with ketones and aldehydes, and have been used in the construction of complex bioconjugates.[4, 5] Recent literature indicates that this same set of nucleophiles and their utility in polymer synthesis and post-polymerization modification are being investigated for the preparation of functional materials,[6-9] with special attention being given to their effectiveness in the modification and fabrication of biocompatible polymer systems.[10-12]

Aliphatic polyesters are one class of polymers that offer an attractive platform for biomedical, drug delivery, and tissue engineering applications, due to the ability

to synthesize well-defined polymers[13] and oligomers[14] as well as a variety of architectures[15-17] that produce benign degradation products.[18-20] Despite this advantageous attribute, their lack of chemical handles for further derivatization and inherent hydrophobicity necessitate the development of strategies for the incorporation of functional ligands and hydrophilic segments in order to construct polyester systems that are better suited for *in vivo* applications. Recent literature documents the incorporation of functional molecules including folic acid,[21] RGD peptide[22], and sugars[23] into aliphatic polyester systems to make the polymers more effective as therapeutic or diagnostic agents. In addition to ligands and targeting moieties, amino groups have been grafted onto the backbone to generate cationic, water-soluble polyesters.[24] Another strategy for making aliphatic polyesters water-dispersible involves the synthesis of polyesters bearing hydophilic polymer grafts to generate amphipilic block graft copolymers. Poly(L-lysine)[25, 26] and PEO grafts have been the primary polymer systems for study as hydrophilic grafts. A variety of chemistries including anionic modification,[27] atom transfer radical addition,[28] and "click" cycloaddition[29-31] have been used for attachment of the grafts onto polyester backbones with varying degrees of grafting efficiency.

Our strategy for the transformation of degradable aliphatic polyesters into functional materials for biomedical applications centers upon their outfitting with multiple moieties, including hydrophilic polymer grafts, to afford amphiphilic block graft copolymers that are capable of assembly into well-defined, multi-functional nanostructures. Our efforts in this area focus on poly(ε-caprolactone-*co*-2-oxepane-1,5-dione) (P(CL-*co*-OPD)),[32] an aliphatic polyester with reactive ketones presented

along the polyester backbone. The chemical approach exploits the inherent electrophilicity of the ketone carbonyls to achieve economical and orthogonal incorporation of multiple functionalities through ketoxime ether formation, while minimizing exposure to reaction conditions that could lead to premature degradation. Aminooxy chemistry affords a convenient and efficient method for the construction of functional and crosslinked polyester materials using P(CL-*co*-OPD).[33, 34] Analogously, using a "grafting onto" approach, hydrophilic polymers with an aminooxy-terminus can be employed as nucleophiles to obtain amphiphilic graft copolymers *via* reaction with the ketones on the hydrophobic P(CL-*co*-OPD) backbone. Mayes and co-workers employed ketoxime ether formation for the chemoselective incorporation of PEO grafts ranging from 150 Da to 2 kDa,[35] and have used these graft copolymers to create functional biocompatible surfaces.[36] While the approach yielded the desired graft copolymers, the method of conjugation employed required long reaction times (days), high stoichiometry (up to 25 equivalents of hydroxylamine to ketone) and heat to maximize the number of PEO grafts.

Due to the versatility of the ketone moiety and the potential indicated by previous research, we are interested in further developing and optimizing the P(CL-*co*-OPD) system for use in the creation of functional, water-soluble, nanoscale particles through the combined incorporation of various chemical handles and hydrophilic PEO grafts. Herein, we report a highly efficient method for the addition of 3 kDa PEO-grafts and small molecule probes onto the P(CL-*co*-OPD) backbone *via* acid-catalyzed ketoxime ether formation at room temperature using low

stoichiometric equivalents of PEO. The resulting amphiphilic graft block copolymers display unique thermal characteristcs relative to their parent copolymers, and were found to self assemble in aqueous solution yielding aggregates of varying morphology.

Results and discussion

To create multi-functional amphiphilic copolymers, having a high degree of versatility in their structure and composition, and involving the coupling of small molecules to hydrolytically-degradable macromolecules and/or of macromolecules to each other (*i.e.* grafting of poly(ethylene oxide) (PEO) and a PCL backbone), a few criteria must be met regarding the types of chemistries employed and reaction conditions utilized. For example, the reaction environment should be sufficiently mild to avoid premature degradation of the polymer, while still allowing for the economical incorporation of numerous polymer and small molecule ligands onto the polymer backbone. It is often difficult to remove free polymer remaining in the desired graft polymeric material; the choice of a highly-efficient grafting chemistry would improve the consumption of the polymer reagents and would produce a more pure product. Additionally, when working with a hydrolytically degradable polymer system, the ability to incorporate both hydrophilic polymer grafts and other units in a single step to afford a functional amphiphilic copolymer is beneficial, as it minimizes the premature degradation of the polyester backbone that may result from sequential functionalization reactions. Consequently, the modification of P(CL-*co*-OPD) with aminooxy-functionalized PEO was studied independently and with a small molecule

ligand, *p*-methoxy-*O*-benzylhydroxylamine, in order to obtain a high degree of grafting density and multi-functionality efficiently, under mild reaction conditions.

Synthesis of PCL-*g*-PEO ketoxime ether conjugates

A α-methoxy-ω-aminooxy-poly(ethylene oxide), **1**, was synthesized by a two-step process, adapting a procedure reported by Gajewiak and co-workers (**Scheme 3-1**).[37] The first step involved a Mitsunobu displacement of the hydroxyl chain end on a 3 kDA α-methoxy-poly(ethylene oxide) to give the ω-phthalimido compound, **2**. Removal of the phthalimide group was accomplished through hydrazinolysis to yield the desired aminooxy-terminated poly(ethylene oxide), **1**.

^{1}H nuclear magnetic resonance (NMR) spectra were collected for **2** and **1**, in both $CDCl_3$ and acetone-d_6 (**Figure 3-1**), to confirm their structures, spectroscopically and chemically. As expected, there was almost no difference for the spectra of **2** in the two solvents, whereas **1** underwent reaction with acetone to afford a ketoxime product that allowed for further differentiation of the proton signals adjacent to the ω-terminal functional group. The ^{1}H NMR spectrum of **2**, taken in $CDCl_3$, had signals at 7.80 ppm and 4.38 ppm, corresponding to the aromatic protons on the phthalimide (Phth)

Scheme3- 3. Synthesis of α-methoxy-ω-aminooxy-poly(ethylene oxide), **1**.

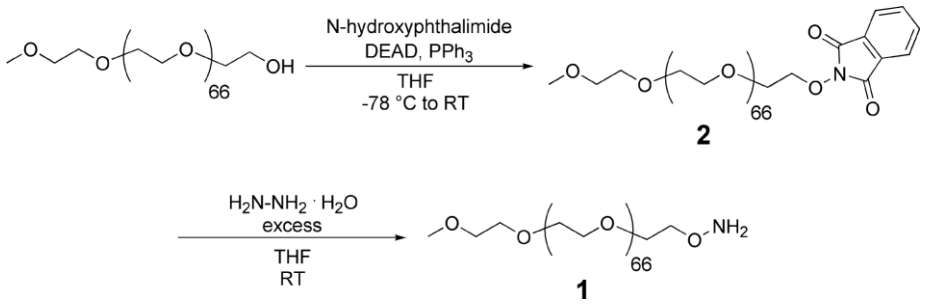

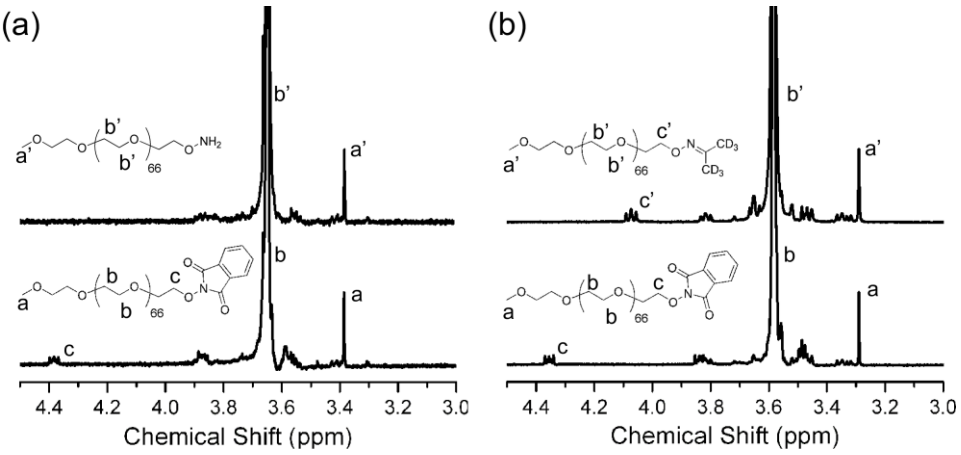

Figure 3-7 (a) ^{1}H NMR (300 MHz) spectra of α-methoxy-ω-phthalimido-PEO, **2**, and α-methoxy-ω-aminooxy-PEO, **1**, in $CDCl_3$, and **(b)** ^{1}H NMR (300 MHz) spectra in acetone-d_6 of α-methoxy-ω-phthalimido-PEO, **2**, and a ketoxime ether derivative, **1'**, of α-methoxy-ω-aminooxy-PEO, **1**, formed through a reaction between the aminooxy chain end and acetone-d_6.

group and the methylene protons of the –C***H***$_2$-O-Phth group, respectively; the proton signal arising from the methoxy chain end was observed as a singlet at 3.38 ppm (**Figure 3-1(a)**). Integration of the resonances belonging to the methoxy terminus and the multiplet corresponding to the –C***H***$_2$-O-Phth methylene protons indicated quantitative conversion of the hydroxyl group to the phthalimide. Upon transformation to the aminooxy group of **1**, the signal for the methylene protons at 4.38 ppm disappeared, however, direct confirmation of their resonance frequency could not be made. As it was difficult to discern the signal corresponding to the chain end -C***H***$_2$-O-NH_2 protons, a ^{1}H NMR spectrum of **1** was obtained in acetone-d_6 (**Figure 3-1(b)**). In this case, the acetone-d_6 acted not only as the NMR solvent, but also as a derivatizing agent, used to produce the corresponding ketoxime ether conjugate. Through the formation of the oxime, the methylene protons shifted upfield from 4.35 ppm when adjacent to the phthalimide of **2** to 4.10 ppm when adjacent to the ketoxime of **1'**, well resolved from the broad -OC***H***$_2$C***H***$_2$- signal of the PEO chain.

Examination of the ^{1}H NMR spectrum of the aminooxy compound in acetone-d_6 indicated complete removal of the phthalimide through comparison of the integration of the singlet corresponding to the methoxy end group at 3.29 ppm to the multiplet at 4.10 ppm, which is the resonance attributed to the $-CH_2$-O-N=C$(CD_3)_2$ methylene protons (**Figure 3-1(b)**). In addition to providing better resolution of the chain end protons, the reaction of **1** with acetone-d_6 chemically confirmed the presence of the terminal aminooxy functionality.

A P(CL-*co*-OPD) polymer, **3**, containing an average of 45 reactive OPD repeat units per polymer chain was used as the parent polymer substrate for the conjugation of α-methoxy-ω-aminooxy-PEO, **1**, to yield the PCL-*g*-PEO block graft copolymer , **4** (**Scheme 3-2**). Additionally, as part of a strategy to work towards the synthesis of multi-functional, water-dispersible PCL materials, the α-methoxy-ω-aminooxy-PEO, **1**, and *p*-methoxy-*O*-benzylhydroxylamine, a small molecule designed to act as an analog for a chromophore or other imaging agent, were allowed to undergo reaction in a single-step, one-pot reaction with P(CL-*co*-OPD) to produce the graft block copolymer, **5**, containing both hydrophilic PEO grafts and functional small molecule

Scheme 3-4. Synthesis of PCL-*g*-PEO graft block copolymers, **4** and **5**.

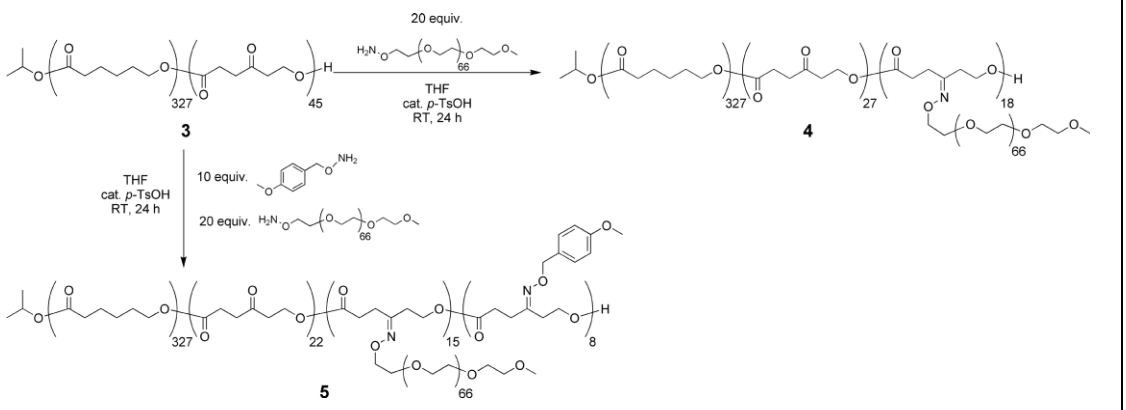

side chains (**Scheme 3-2**). In both cases, the reactions were conducted in THF for 24 h using a catalytic amount of *p*-toluenesulfonic acid; the resulting grafting efficiencies of the aminooxy-terminated PEO and the *p*-methoxy-*O*-benzylhydroxylamine were found to be remarkably high.

^{1}H NMR spectra were collected for **4** and **5** in $CDCl_3$ to confirm their structures and to determine the number of grafts incorporated onto the P(CL-*co*-OPD) backbone (**Figure 3-2**). The ^{1}H NMR spectrum of the PCL-*g*-PEO graft block copolymer, **4**, had proton signals indicating the conversion of a portion of the ketones to ketoxime ethers (blue spectrum in **Figure 3-2(a)**). The resonance at 4.25 ppm corresponds to protons on the methylene adjacent to the oxygens of the ester groups in functionalized OPD repeat units (blue f' in **Figure 3-2(a)**). In addition, an intense signal from the PEO chain at 3.6-3.7 ppm, the protons on the methoxy end group at 3.39 ppm, and the appearance of a quartet at 4.15 ppm corresponding to the –C***H***$_2$-ON=C methylene (blue g' in **Figure 3-2(a)**), each supported the covalent attachment of PEO chains onto the PCL backbone. The ^{1}H NMR spectrum of the bi-

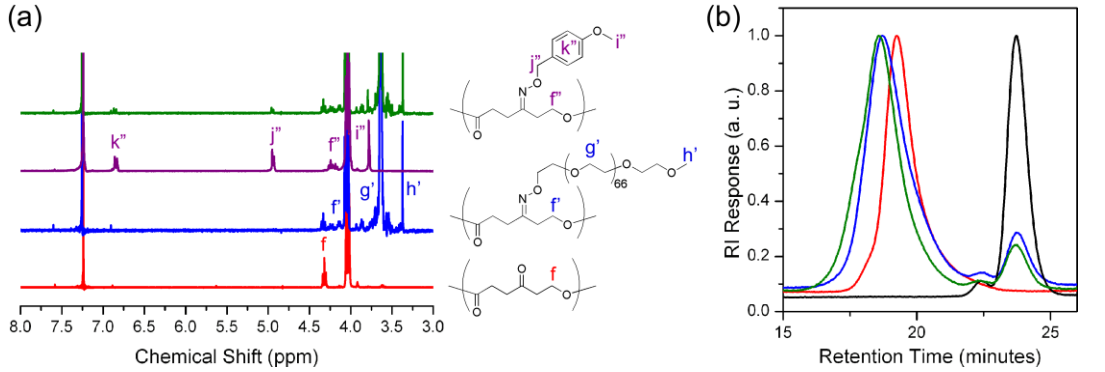

Figure 3-8 **(a)** ^{1}H NMR spectra (300 MHz, $CDCl_3$) of the parent P(CL-*co*-OPD) polymer, **3** (red), P(CL-*co*-OPD-*co*-(OPD-*g*-PEO)), **4** (blue), a fully functionalized P(CL-*co*-OPD-*co*-(ODP-*g*-*p*MeOBn)) (purple), and P(CL-*co*-OPD-*co*-(OPD-*g*-PEO)-*co*-(OPD-*g*-*p*MeOBn)), **5** (green). **(b)** An overlay of GPC RI traces of the parent P(CL-*co*-OPD) polymer, **3** (red), P(CL-*co*-OPD-*co*-(OPD-*g*-PEO)), **4** (blue), P(CL-*co*-OPD-*co*-(OPD-*g*-PEO)-*co*-(OPD-*g*-*p*MeOBn)), **5** (green), and 3 kDa PEO (black).

functionalized graft block copolymer, **5**, had diagnostic signals associated with the conversion of ketones to ketoxime ether linkages at 4.25 ppm (purple f" **Figure 3-2(a)**); the presence of PEO-grafts was confirmed by the strong signal for the PEO chain at 3.6-3.7 ppm and a multiplet corresponding to –C***H***$_2$-ON=C protons at 4.15 ppm (green spectrum, **Figure 3-2(a)**). The incorporation of *p*-methoxybenzyl (*p*-MeOBn) grafts was confirmed by the appearance of aromatic resonances at 6.85 ppm, two signals indicative of the benzylic protons at 4.96 ppm, and a singlet corresponding to the methoxy protons at 3.75 ppm (purple and green spectra, **Figure 3-2(a)**). To assist with the confirmation of the assignments of the proton signals responsible for the *p*-MeOBn functionalities, a sample that resulted from reaction only between P(CL-*co*-OPD) and *p*-methoxy-*O*-benzylhydroxylamine was prepared and analyzed (purple spectrum of **Figure 3-2(a)**).

The reaction between P(CL-*co*-OPD), **3**, and 20 equivalents of α-methoxy-ω-aminooxy-PEO, **1**, resulted in the grafting of 18 PEO chains, giving a grafting efficiency of 90%, based upon the integration of signals representing the remaining OPD repeat units relative to those signals associated with the CL repeat units. It is important to note that the equivalents used here are relative to the P(CL-*co*-OPD) (20 mol:1 mol, **1**:**3**), not relative to the ketone stoichiometry (0.4 mol:1 mol, **1**:ketones on **3**). The grafting efficiency for the conjugation of α-methoxy-ω-aminooxy-PEO, **1**, and *p*-methoxy-*O*-benzylhydroxylamine to the PCL backbone in a single step, though slightly lower, was also highly efficient at 75% and 80% grafting efficiency for the PEO and the *p*-methoxybenzyl compounds, respectively.

GPC analysis of the resulting PCL-*g*-PEO block graft copolymers **4** and **5**,

showed a marked increase in the molecular weight of the graft copolymer relative to the parent P(CL-*co*-OPD) polymer. There was not a substantial increase in the polydispersity of the graft copolymer products, suggesting that little to no degradation of the polyester backbone occurred during the coupling reaction (**Figure 3-2(b)**). Interestingly, in the case of both graft copolymers, a small amount of free PEO remained present in the isolated precipitate, as observed in the GPC traces. This free PEO could not be removed with subsequent precipitations or fractional precipitation techniques, and dialysis was found to be an unsuitable method for removal of excess PEO due to the resulting degradation of the graft copolymer backbone.

Thermal characterization of PCL-*g*-PEO ketoxime ether conjugates

Differential scanning calorimetry (DSC) experiments were performed to compare the thermal characteristics of the PCL-*g*-PEO ketoxime ether conjugates to the parent P(CL-*co*-OPD) and PEO polymers. Substantial differences in the melting transition temperatures of **4** and **5** relative to the peak melting temperature transition of the P(CL-*co*-OPD) parent copolymer and the 3 kDA PEO were observed, and are illustrated in **Figure 3-3(a)** as DSC traces of the third heating cycle so that each sample had undergone similar thermal annealing. The grafting of 3 kDa α-methoxy-ω-aminooxy-PEO onto the PCL backbone *via* ketoxime ether formation resulted in a polymeric material diplaying a single melting transition—rather than two transitions corresponding to the melting temperatures of the PEO and the P(CL-*co*-OPD)—with a peak melting temperature of 48 °C for the P(CL-*co*-OPD-*co*-(OPD-*g*-PEO)) copolymer, **4** (**Figure 3-3 (a)**, blue). In the case of the multifunctional, amphiphilic

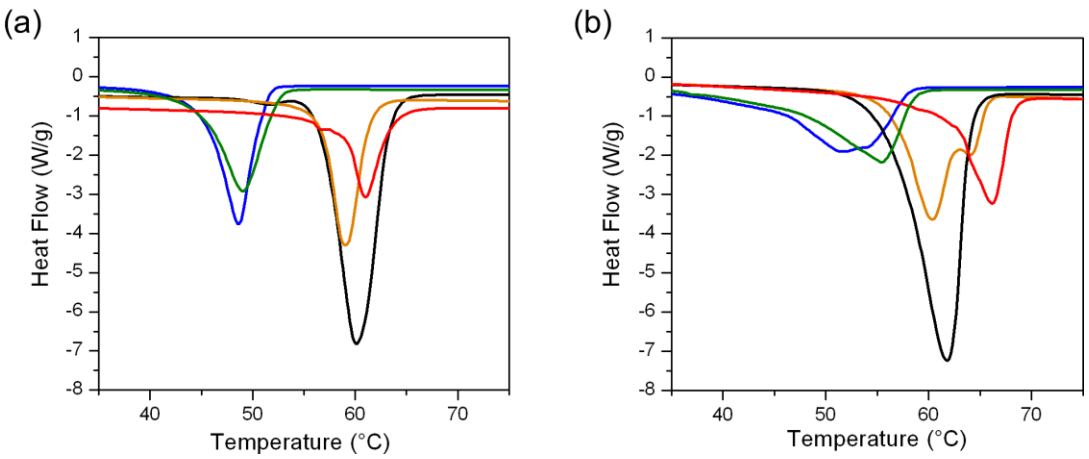

Figure 9-3 (a) DSC thermograms from the third heating cycle of the melting transition region of the parent P(CL-*co*-OPD) polymer, **3** (red); 3 kDA PEO (black); a physical mixture of the parent P(CL-*co*-OPD) polymer, **3**, and 3 kDA PEO (orange); P(CL-*co*-OPD-*co*-(OPD-*g*-PEO)), **4** (blue); and P(CL-*co*-OPD-*co*-(OPD-*g*-PEO)-*co*-(OPD-*g*-*p*MeOBn)), **5** (green), and **(b)** DSC thermograms from the first heating cycle of the melting transition region of the parent P(CL-*co*-OPD) polymer, **3** (red); 3 kDA PEO (black); a physical mixture of the parent P(CL-*co*-OPD) polymer, **3**, and 3 kDA PEO (orange); P(CL-*co*-OPD-*co*-(OPD-*g*-PEO)), **4** (blue); and P(CL-*co*-OPD-*co*-(OPD-*g*-PEO)-*co*-(OPD-*g*-*p*MeOBn)), **5** (green).

graft copolymer, **5**, the incorporation of 3 kDa PEO and *p*-methoxy-benzyl ketoxime ether grafts also yielded a material with a single transition having a peak melting point of 49 °C (**Figure 3-3 (a)**, green). In both cases, the addition of grafts onto the polymer backbone resulted in a melting transition that was significantly lower than the temperature observed for the parent PCL copolymer and the PEO composing the grafts. This result is consistent with previously reported melting transitions observed in PCL materials with small molecule ketoxime ether grafts that disrupted the crystallinity.[38] To demonstrate that the depression in melting temperature was caused by both compositional and structural changes resulting from the covalent attachment of PEO to the PCL backbone, the melting transition temperatures, T_m's, of the PCL-*g*-PEO ketoxime ether conjugates were compared to a physical mixture, 1:1 by mass of the parent P(CL-*co*-OPD) polymer, **3**, and 3 kDA PEO, which is a comparable mass ratio to that found in both graft copolymers. The resulting T_m for the physical blend

was a single peak at 59 °C (**Figure 3-3 (a)**, orange). This temperature is approximately ten degrees higher than the melting transitions observed for **4** and **5**, and is comparable to the peak melting transition temperatures of 61 and 60 °C obtained for P(CL-*co*-OPD) and 3 kDA PEO, respectively (**Figure 3-3 (a)**, red and black).

While all of the melting transitions observed in the third heating cycle display a single peak, suggesting a single melting transition for each of the polymer samples characterized, thermograms from the first heating cycles provide additional insight into the unique behavior of the PCL-*g*-PEO ketoxime ether conjugates relative to their parent polymers (**Figure 3-3 (b)**). In both cases, neat P(CL-*co*-OPD) and 3 kDA PEO present a well defined transition, with the peak T_m of the PEO appearing at 61 °C and the peak T_m of the parent polyester, **3**, occuring at 66 °C (**Figure 3-3 (b)**, red and black). In the first heating cycle, a two stage melt was observed for the physical mixture of the P(CL-*co*-OPD) copolymer, **3**, and 3 kDA PEO (**Figure 3-3(b)**, orange), with one stage having a peak T_m at 60 °C, which matches the T_m for PEO, and a second less intense transition appearing at 64 °C, corresponding to a slightly depressed T_m for P(CL-*co*-OPD). Observation of two melting transitions for physical mixtures containing two crystalline polymers is not uncommon, and has been previously observed in investigations studying the melting transitions of PCL and PEO blends.[39] Similarly, the thermogram from the first heating cycle for the P(CL-*co*-OPD-*co*-(OPD-*g*-PEO)) copolymer, **4** (**Figure 3-3(b)**, blue), exhibits a peak T_m at 52 °C associated with the melting transition of the PEO grafts and a slight shoulder at 55 °C, likely corresponding to the T_m of the P(CL-*co*-OPD) backbone. The

multifunctional, amphiphilic graft copolymer, **5**, (**Figure 3-3(b)**, green) has a peak T_m at 55 °C, but does not clearly display two obvious stages or a shoulder that would suggest two unique melting points.

The differences observed in the first and third heating cycles are due to the different thermal histories of the polymer samples; the first heating cycle was heated from room temperature with no annealing, but in the case of the third heating cycle the polymer samples had been crystallized nonisothermally twice at a rate of 10 °C/min. Despite the differences in thermal history, in both the first and third heating cycles, the PCL-*g*-PEO ketoxime ether conjugates, **4** and **5**, exhibited significantly lower melting temperatures than the parent polymers and the mixture of P(CL-*co*-OPD) with 3 kDA PEO. These results suggest that the covalent attachment of PEO grafts onto the polyester backbone disrupts the crystallinity present in both polymer species, and that the thermal profiles of the of the PCL-*g*-PEO ketoxime ether conjugates can be correlated to chemical and structural changes in the polymer architecture.

Self assembly of PCL-*g*-PEO ketoxime ether conjugates in aqueous solution

The amphiphilic block graft copolymers, when transitioned from organic solvent (tetrahydrofuran, THF) to water, undergo multi-molecular aggregation to afford nanostructures having interesting morphologies. The P(CL-*co*-OPD-*co*-(OPD-*g*-PEO)) copolymer, **4**, having a 55 wt % of PEO was allowed to undergo assembly in an aqueous solution. This particular block graft copolymer formed micellar aggregates with an intensity-averaged hydrodynamic diameter, D_h, of 225 ± 21 nm, a

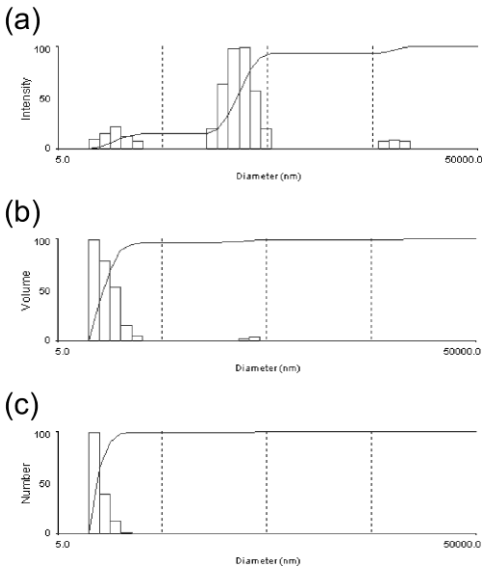

Figure 3-10 **(a)** Intensity-averaged DLS histogram showing the bimodal size distribution of the aggregates **(b)** volume-averaged DLS histogram **(c)** and the number-averaged DLS histogram of the aggregates present in a 0.3 mg/mL solution of P(CL-*co*-OPD-*co*-(OPD-*g*-PEO)), **4**, a block graft copolymer containing 55 wt % PEO.

volume-averaged D_h of 29 ± 4 nm, and a number-averaged D_h of 16 ± 1 nm, as measured by dynamic light scattering (DLS). DLS analysis reveals that the aggregates exhibited a bimodal distribution with population size maxima at approximately 19 nm and 285 nm, which can both be observed in the intensity-averaged DLS histogram of **Figure 3-4**. Such bimodal distributions of aggregates have been observed previously for block graft copolymers where PEO has been grafted onto PCL backbones *via* other chemical coupling methods.[28]

AFM and TEM were used to analyze the size and also the shape of the aggregates formed by P(CL-*co*-OPD-*co*-(OPD-*g*-PEO)) copolymer **4**, with the heights being determined by AFM and the diameters by TEM, each after deposition of the aqueous solutions onto solid substrates. The aggregates visualized by tapping-mode AFM appear globular in shape with a fairly broad height distribution (**Figure 3-5(a)**). Calculation of the particle sizes over a 5 x 5 μm area gave an average height of 2 ± 1

nm, with the height of the observed aggregates ranging from 1 to 7 nm. The TEM image obtained from a 0.2 mg/mL solution of **4** in 9:1 water/THF (v/v) showed circular, particle-like aggregates with an average diameter of 116 ± 35 nm (**Figure 3-5(b)**). There is clearly a broad distribution of particle diameters in the micrograph, which is comparable to the broad size distributions observed by DLS and AFM. The low height value observed through AFM, relative to the large diameter, suggests a reorganization of the aggregates to cause flattening upon adsorption onto the solid substrates (mica (AFM) or carbon-coated copper grid (TEM)). Furthermore, the large, unusual aggregates observed in the TEM image suggest significant reorganization events. As opposed to our past experience with hydrophilic nanoparticles, these new materials presented difficulties in the preparation of samples for AFM and TEM imaging. In many cases, cooling was necessary and deposition conditions required optimization (see Experimental details). Each of these results illustrates the unique characteristics of these amphiphilic and crystalline block graft copolymers in water as well as the challenges in working with these systems.

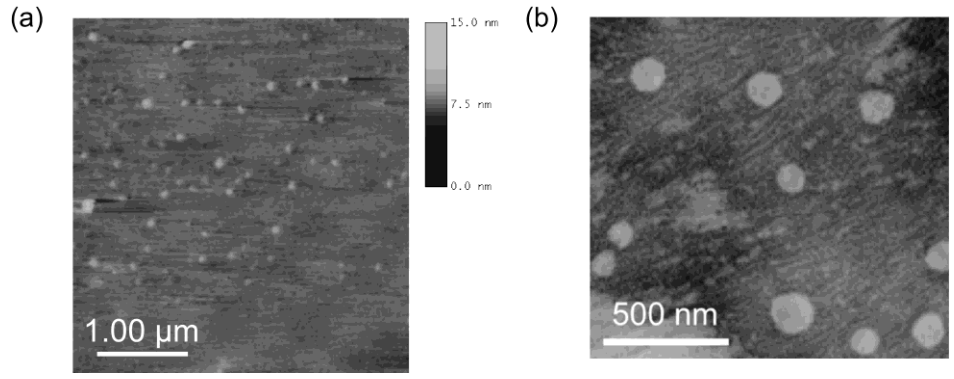

Figure 3-11 (a) Height image of tapping mode AFM image of P(CL-*co*-OPD-*co*-(OPD-*g*-PEO)), **4** (concentration 0.1 mg/mL) **(b)** TEM image of the micellar aggregates formed by P(CL-*co*-OPD-*co*-(OPD-*g*-PEO)), **4** (0.3 mg/mL solution).

The PCL-PEO graft block copolymer with pendant *p*-methoxybenzyl groups, **5**, having 49 wt % PEO, showed unique self assembly behavior upon being dispersed in aqueous solution. Unlike the graft copolymer **4**, which has only PEO grafts, TEM images obtained after drop deposition of a solution of **5** onto a carbon-coated copper grid, indicated that the copolymer having both PEO grafts and dangling *p*MeOBn side chains forms cylindrical or rod-like aggregates having an average diameter of 12 ± 2 nm and an average length of 190 ± 37 nm when dispersed in aqueous solution at the same block graft copolymer concentrations as used for **4** (**Figure 3-6**).

The reason for the observed differences in the solution-state aggregates formed by **4** and **5** is not obvious at this time and warrants additional study. One potential characteristic that may generate differences in the observed aggregates is the change in the overall weight percent of PEO present in the block graft copolymer samples; specifically the reduced number of PEO grafts present on **5** relative to **4**, may be influencing the morphology of the solution state aggregates. Previous research on PCL-*b*-PEO copolymer systems indicates that these block copolymer systems form cylindrical and wire-like aggregates with certain ratios of PCL to PEO and block

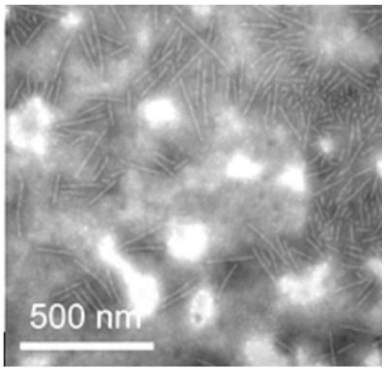

Figure3-12 TEM image of the cylindrical aggregates formed by P(CL-*co*-OPD-*co*-(OPD-*g*-PEO)-*co*-(OPD-*g*-*p*MeOBn)), **5**, at 50000x magnification (0.3 mg/mL solution).

copolymer concentrations.[40, 41] A preference for cylindrical or worm-like micelles was noted to occur when the hydrophobic PCL block was longer, while a preference for spherical aggregates was observed when the amount of PEO was increased,[41] or if the block length of PEO was held constant while the PCL block length was reduced.[40, 42, 43] At this time, it is unclear whether the formation of the cylindrical aggregates in this graft copolymer system results from a diminished density of PEO grafts in **5** relative to **4**, or if the self assembly process and the rod-like aggregates are a consequence of having *p*MeOBn side chains covalently attached to the PCL backbone. In order to better understand this system and the self assembly of PCL-*g*-PEO copolymers in general, further investigation pertaining to the self assembly of these rod-like aggregates and the characteristics that influence aggregate shape is ongoing.

Experimental

Materials

The synthesis of 1,4,8-trioxaspiro-9-undecanone (TOSUO) has been described elsewhere.[32, 44-48] ε-Caprolactone (CL) (Aldrich Chemical Company) was distilled from CaH_2 and stored under argon. Toluene (Aldrich Chemical Company) was dried by heating at reflux over sodium and distilled under argon prior to use. Aluminum triisopropoxide $Al(OiPr)_3$ (Aldrich Chemical Company) was purified by sublimation and dissolved in dry toluene prior to use. Polyethylene oxide (3 kDA PEO) was purchased from Nektar and was dried by azeotropic distillation of toluene (3 x) to dryness to remove residual water. All other reagents (solvents, *p*-toluenesulfonic acid

(*p*-TsOH), diethyl azodicarboxylate (DEAD), triphenylphosphene, *etc*.) were purchased from Aldrich and used as received.

Instrumentation

^{1}H NMR (300 MHz) and ^{13}C NMR (75 MHz) spectra were acquired in $CDCl_3$ unless otherwise noted on a Varian Mercury 300 spectrometer using the residual solvent signal as the internal reference. Infrared spectra were recorded on a Perkin-Elmer Spectrum RX FT-IR system by film deposition onto NaCl salt plates. Differential scanning calorimetry was performed under nitrogen atmosphere using 40 μL aluminum pans on a Mettler Toledo DSC822 with heating and cooling at 10 °C/min from –100 °C to 100 °C. T_m values were obtained from the third heating scan as the peak values from the thermogram. Gel permeation chromatography was performed on a Waters Chromatography, Inc., 1515 isocratic HPLC pump equipped with an inline degasser, a model PD2020 dual-angle (15° and 90°) light scattering detector (Precision Detectors, Inc.), a model 2414 differential refractometer (Waters, Inc.), and four PL_{gel} polystyrene-*co*-divinylbenzene gel columns (Polymer Laboratories, Inc.) connected in series: 5 μm Guard (50 × 7.5 mm), 5 μm Mixed C (300 × 7.5 mm), 5 μm 10^4 (300 × 7.5 mm), and 5 μm 500 Å (300 × 7.5 mm) using the Breeze (version 3.30, Waters, Inc.) software. The instrument was operated at 35 °C with THF as eluent. Data collection was performed with Precision Acquire 32 Acquisition program (Precision Detectors, Inc.) and analyses were carried out using Discovery32 software (Precision Detectors, Inc.) with a system calibration curve generated from plotting molecular weight as a function of retention time for a series

of broad polydispersity poly(styrene) standards. The height measurements (H_{av}) for the aggregates formed by the PCL-*g*-PEO ketoxime ether conjugates were determined by tapping-mode atomic force microscopy (AFM) under ambient conditions in air. The AFM instrumentation consisted of a Nanoscope III BioScope system (Digital Instruments, Veeco Metrology Group; Santa Barbara, CA) and standard silicon tips (type, OTESPA-70; L, 160 μm; normal spring constant, 50 N/m; resonance frequency, 246-282 kHz). The sample solutions were drop cast (50-100 μL) onto freshly-cleaved mica and allowed to settle freely for 60 seconds, after which the excess solution was removed by wicking with filter paper and the mica surface was allowed to dry in air. Hydrodynamic diameters (D_h) and distributions for the PCL-*g*-PEO ketoxime ether aggregates in aqueous solution were determined by dynamic light scattering (DLS). The DLS instrumentation consisted of a Brookhaven Instruments Limited (Worcestershire, U.K.) system, including a model BI-200SM goniometer, a model BI-9000AT digital correlator, a model EMI-9865 photomultiplier, and a model 95-2 Ar ion laser (Lexel, Corp.; Farmindale, NY) operated at 514.5 nm. Measurements were made at 25 ± 1 °C. Scattered light was collected at a fixed angle of 90°. The digital correlator was operated with 522 ratio spaced channels and initial delay of 2.4 μs, a final delay of 250 ms, and a duration of 2 min. A photomulitplier aperture of 400 μm was used, and the incident laser intensity was adjusted to obtain a photon counting greater than 75 kcps. Only measurements in which the measured and calculated baselines of the intensity autocorrelation function agreed to within 0.3% were used to calculate particle size. Particle size distributions were performed with the ISDA software package (Brookhaven Instruments Company), which employed

single-exponential fitting, cumulant analysis, and nonnegatively constrained least-squares particle size distribution analysis routines. Samples for transmission electron microscopy (TEM)) measurements were pre-cooled (*ca*. 5 °C) and drop deposited onto pre-chilled (*ca*. 0 °C) carbon coated-copper grids, were diluted with with a 1 % phosphotungstic acid (PTA) stain (v/v, 1:1), and then the excess solution was removed by wicking with filter paper. The samples were allowed to dry under ambient conditions and then were imaged on a Hitachi H-600 TEM instrument. The number average particle diameters (D_{av}) and standard deviations were generated from the analysis of 40 particles.

Synthesis

***O*-(*p*-methoxybenzyl)-*N*-hydroxyphthalimide.**

N-hydroxyphthalimide (5.71 g, 35.0 mmol, 1.41 eq) was dissolved in 100 mL of dry THF followed by addition of triethylamine (5.0 mL, 36 mmol, 1.4 eq) to yield a deep red solution. *p*-Methoxybenzylbromide (5.00 g, 24.9 mmol, 1.0 eq Br) was added to the reaction mixture drop wise. The reaction was allowed to proceed at reflux for 18 h and monitored by TLC and ^{1}H NMR spectroscopy. CH_2Cl_2 was added and the solution was washed with H_2O (3×), dried over Na_2SO_4, and concentrated *in vacuo* to afford the crude product (91% conversion by ^{1}H NMR spectroscopy). Flash column chromatography of the crude product yielded *O*-(*p*-methoxybenzyl)-*N*-hydroxyphthalimide as white crystals. Yield: 6.11 g, 87 %. IR (NaCl) 3037, 2960-2840, 2037, 2962, 2839, 1783, 1726, 1612, 1516, 1463, 1387, 1253, 1174, 1142, 1027, 972, 877, 822, 697 cm^{-1}. ^{1}H NMR (300 MHz, $CDCl_3$) δ 7.7-7.9 (two m, 4H,

aromatic of phthalimide), 7.45 (dt, J = 9, 2 Hz, 2H, aromatic of *p*-MeO-Bn), 6.9 (dt, J = 9, 2 Hz, 2H, aromatic of *p*-MeO-Bn), 5.15 (s, 2H, -OC***H***$_2$-), 3.8 (s, 3H, -OC***H***$_3$) ppm. ^{13}C NMR (75 MHz, $CDCl_3$) δ 163.7, 160.6, 134.6, 131.8, 129.1, 126.0, 114.1, 79.7, 55.4 ppm.

_O_-(_p_-methoxybenzyl)hydroxylamine.

O-(*p*-methoxybenzyl)-*N*-hydroxyphthalimide (0.985 g, 3.48 mmol, 1.0 eq) was dissolved in 35 mL of dry THF. Hydrazine monohydrate (0.5 mL, 10 mmol, 3 eq) was added and the reaction was allowed to proceed at room temperature for 18 h, monitored by ^{1}H NMR spectroscopy. The reaction mixture; a clear solution containing a white solid, was dissolved into 100 mL CH_2Cl_2, extracted with 1.0 M KOH (2 × 50 mL) and H_2O (2 × 50 mL), dried over Na_2SO_4, and concentrated *in vacuo* to afford the product, *O*-(*p*-methoxybenzyl)hydroxylamine, as a clear, colorless oil. Yield: 0.55 g, >98 %. IR (NaCl) 3314, 3235, 3100-3000, 2950-2840, 1611, 1585, 1512, 1464, 1362, 1301, 1247, 1174, 1032, 814 cm^{-1}. ^{1}H NMR (300 MHz, $CDCl_3$) δ 7.3 (dt, J = 9, 2 Hz, 2H, aromatic of *p*-MeO-Bn), 6.9 (dt, J = 9, 2 Hz, 2H, aromatic of *p*-MeO-Bn), 5.3 (s, 2H -CH_2-ON***H***$_2$), 4.6 (s, 2H, -C***H***$_2$-ONH_2) ppm, 3.8 (s, 3H, -OC***H***$_3$) ppm. ^{13}C NMR (75 MHz, $CDCl_3$) δ 159.5, 130.5, 130.1, 129.5, 113.9, 77.6, 71.5, 55.3 ppm.

P(CL-*co*-OPD) Copolymer Synthesis [32, 44, 45]

Random copolymers of ε-caprolactone (CL) and 2-oxepane-1,5-dione (OPD) were prepared by ring opening polymerization of CL and the synthetic monomer TOSUO

by initiation with $Al(OiPr)_3$, and the resulting P(CL-*co*-TOSUO) was subsequently deprotected using triphenylcarbenium tetrafluoroborate as previously reported.

P(CL_{327}–*co*-OPD_{49}) (**3**). GPC: $M_{n,\ PS}$ = 38700 Da, $M_{w,\ PS}$ = 50400 Da, PDI_{PS} = 1.3. M_n (^{1}H NMR) = 43600 Da. T_m = 61 °C. IR (NaCl) 3600-3000, 2940-2860, 1732 (str, multiple modes), 1595, 1470, 1437, 1420, 1397, 1367, 1295, 1244, 1191, 1108, 1065, 1046, 962, 933, 903, 841 cm^{-1}. ^{1}H NMR (300 MHz, $CDCl_3$) δ 5.0 (septet, J = 6.3 Hz, 1 H of initiated chain end, $(CH_3)C\boldsymbol{H}O$), 4.25 (t, J = 7.2 Hz, 2 H of OPD units, $C\boldsymbol{H}_2OCO$), 4.05 (t, J = 6.6 Hz, 2 H of CL units, $C\boldsymbol{H}_2OCO$), 3.65 (t, J = 6.3 Hz, 2 H of terminated chain end, $C\boldsymbol{H}_2OH$), 2.82 (t, J = 7.2 Hz, 2 H of OPD units, $C(O)C\boldsymbol{H}_2CH_2CO$), 2.75 (t, J = 7.2 Hz, 2 H of OPD units, C(O)CH2CH2), 2.62 (t, J = 7.5 Hz, 2 H of OPD units, , $C(O)C\boldsymbol{H}_2CH_2OCO$), 2.30(t, J = 7.5 Hz, 2 H of CL units, $C\boldsymbol{H}_2COOCH_2$), 1.65 (m, 4 H of CL units, $OCH_2C\boldsymbol{H}_2$ and $C\boldsymbol{H}_2CH_2COO$), 1.45 (m, 2 H of CL units, $C\boldsymbol{H}_2CH_2CH_2COO$), 1.25 (d, J = 6.3 Hz, 6 H of initiated chain end, $(C\boldsymbol{H}_3)_2CHO$) ppm. ^{13}C NMR (75 MHz, CDCl3) δ 205.9, 173.4, 172.7, 64.6, 64.2, 59.2, 41.6, 37.5, 34.2, 34.0, 28.4, 27.9, 25.6, 24.7, 24.5 ppm.

α-methoxy-ω-phthalimidoxy-poly(ethylene oxide), 2.

A solution of triphenyl phosphine (4.4 g, 17 mmol) in THF (70 mL) was cooled to -78 °C under argon. A 40 wt. % solution of diethyl azodicarboxylate in toluene (7.5 mL, 17 mmol) was added to the reaction dropwise *via* syringe, and the reaction was stirred under argon and allowed to warm to room temperature over 1 h. The reaction mixture was again cooled to -78 °C under argon, a solution of 3 kDa α-methoxy-poly(ethylene oxide) (5.0 g, 1.7 mmol) in THF (50 mL) was added dropwise by syringe, and the

reaction was allowed to warm to room temperature over 30 min. A solution of *N*-hydroxy phthalimide (2.8 g, 17 mmol) in THF (50 mL) was added to the reaction by syringe over a 30 min period, and the reaction was allowed to stir at room temperature under argon for 18 h. The resulting phthalimidoxy-terminated PEO was isolated and purified by two precipitations into diethyl ether (3.9 g, 75 % yield). IR (NaCl) 2950-2690, 1789, 1734, 1466, 1359, 1342, 1280, 1241, 1147, 1113, 1060, 962, 842 cm^{-1}. ^1H NMR (300 MHz, $CDCl_3$) δ 7.7-7.9 (m, 4H of phthalimido chain end), 4.39 (dd, J = 4, 5 Hz, 2H, C***H***$_2$-O-Phth chain end), 3.65 (bs, 4H of PEO repeat unit), 3.39 (s, 3H of –OC***H***$_3$ chain end). ^{13}C NMR (75 MHz, $CDCl_3$) δ 163.5, 134.5, 129.1, 123.6, 70.7, 59.1 ppm.

α-methoxy-ω-aminooxy-poly(ethylene oxide), 1.

Hydrazine monohydrate (1.0 mL, 20 mmol) was added in a single portion to a solution of α-methoxy-ω-phthalimidoxy-poly(ethylene oxide) (2.1 g, 0.67 mmol) in THF (50 mL). The reaction was capped and stirred at room temperature for 96 h. The resulting polymer was isolated by precipitation into diethyl ether (1.55 g, 76 % yield). T_m = 60 °C. IR (NaCl) 2950-2800, 1466, 1359, 1342, 1280, 1240, 1148, 1109, 1060, 962, 842 cm^{-1}. ^1H NMR (300 MHz, $CDCl_3$) δ 3.85 (m, 2H of -CH_2-ON***H***$_2$ chain end), 3.65 (bs, 4H of PEO repeat unit), 3.39 (s, 3H of –OC***H***$_3$ chain end). ^{13}C NMR (75 MHz, $CDCl_3$) δ 74.7, 70.5, 59.0 ppm.

P(CL$_{327}$-*co*-OPD$_{27}$-*co*-(OPD-*g*-PEO)$_{18}$), 4.

A solution of α-methoxy-ω-aminooxy(poly(ethylene oxide)), **1**, (118 mg, 0.39 mmol)

in THF (1.0 g) was added to a solution of P(CL_{327}-*co*-OPD_{45}), **3**, (73 mg, 0.0015 mmol) in THF (0.5 g). The reaction mixture was allowed to stir at RT for 1 min, after which four drops of a solution of *p*-TsOH (7.5 mg) in THF (20 mL) was added. The reaction was stirred at RT for 24 h. The polymer was purified by precipitation into hexanes, the stringy white solid was isolated *via* vacuum filtration with a coarse glass frit, and was dried *in vacuo* for 12 h (166 mg, 91% yield). GPC: $M_{n,\ PS}$ = 60000 Da, $M_{w,\ PS}$ = 78500 Da, PDI_{PS} = 1.3. M_n (^{1}H NMR) = 97800 Da. T_m = 48 °C. IR (NaCl) 2950-2800, 1733, 1726, 1465, 1456, 1384, 1357, 1342, 1278, 1239, 1193, 1145, 1109, 1064, 961, 842 cm^{-1}. ^{1}H NMR (300 MHz, $CDCl_3$) δ 4.33 (t, J = 6.2 Hz, 2H of OPD units, C***H***$_2$OCO), 4.3-4.1 (pair of multiplets, 2H of ketoxime ether isomers of OPD-*g*-PEO units, CH_2OCO), 4.05 (t, J = 6.7 Hz, 2H of CL units, C***H***$_2$OCO), 3.64 (bs, 4H of PEO repeat unit), 3.37 (s, 3H of OC***H***$_3$ PEO end group), 2.79 (t, J = 6.6 Hz, 2H of OPD units, C(O)C***H***$_2$ CH_2COO), 2.74 (t, J = 6.6 Hz, 2H of OPD units, C(O)C***H***$_2$$CH_2$OCO), 2.62-2.50 (2H OPD, C***H***$_2$$COOCH_2$; m, 6H of OPD-*g*-PEO), 2.30 (t, J = 7.4 Hz, 2H of CL units, C***H***$_2$$COOCH_2$), 1.64 (m, 4H of CL units, OCH_2C***H***$_2$ and C***H***$_2$$CH_2$COO), 1.37 (m, 2H of CL units, C***H***$_2$ CH_2 CH_2COO), 1.22 (d, J = 6.3 Hz, 6H of initiated chain end (CH_3)CHO) ppm. ^{13}C NMR (75 MHz, $CDCl_3$) δ 205.9, 173.7, 173.4, 172.8, 156.4, 155.7, 77.4, 72.1, 70.7, 69.7, 64.7, 64.3, 59.2, 41.6, 37.7, 34.3, 34.2, 33.9, 30.4, 30.3, 30.2, 28.5, 28.0, 25.7, 24.7, 24.5, 24.4 ppm.

P(CL_{327}-*co*-OPD_{27}-*co*-(OPD-*g*-PEO)$_{15}$-*co*-(OPD-*g*-MeOBn)$_8$), 5.

A solution of α-methoxy-ω-aminooxy(poly(ethylene oxide)), **1**, (128 mg, 0.042 mmol) in THF (1.2 g) was added to a solution of P(CL_{327}-*co*-OPD_{45}) (66 mg, 0.0017

mmol) in THF(0.5 g). The reaction mixture was stirred at RT for 1 min. to ensure the dissolution of both polymer species. A solution of *O*-(4-methoxybenzyl)hydroxylamine (2.6 mg, 0.017 mmol) in THF (0.5 g) was added to the reaction mixture, and then four drops of a solution of *p*-TsOH (7.5 mg) in THF (20 mL) was added. The reaction was stirred at RT for 24 h and the polymer was purified by precipitation into hexanes. The stringy white solid was isolated *via* vacuum filtration with a coarse glass frit, and was dried *in vacuo* for 12 h (180 mg, 89% yield). GPC: $M_{n,\ PS}$ = 74900 Da, $M_{w,\ PS}$ = 97600 Da, PDI_{PS} = 1.3. M_n (^{1}H NMR) = 89700 Da. T_m = 49 °C. IR (NaCl) 2950-2800, 1733, 1466, 1456, 1360, 1342, 1280, 1240, 1149, 1110, 1061, 963, 842 cm^{-1}. ^{1}H NMR (300 MHz, $CDCl_3$) δ 6.86 (d, J = 8.8 Hz, 4H, aromatic), 4.94-4.96 (two singlets, 2H, Ph-CH_2), 4.33 (t, J = 6.2 Hz, 2H of OPD units, C***H***$_2$OCO), 4.3-4.1(pair of multiplets, 2H of ketoxime ether isomers of OPD-*g*-PEO units, C***H***$_2$OCO, and pair of multiplets, 2H of ketoxime ether isomers of OPD-*g*-*p*MeOBn units), 4.05 (t, J = 6.7 Hz, 2H of CL units, C***H***$_2$OCO), 3.80 (s, 3H, C***H***$_3$O-Ph) 3.64 (bs, 4H of PEO repeat unit), 3.37 (s, 3H of OC***H***$_3$ PEO end group), 2.79 (t, J = 6.3 Hz, 2H of OPD units, C(O)CH_2 C***H***$_2$COO), 2.74 (t, J = 6.6 Hz, 2H of OPD units, C(O)C***H***$_2$$CH_2$OCO), 2.62-2.50 (t, J = 6.6 Hz, 2H OPD, C***H***$_2$$COOCH_2$; m, 6H of OPD-*g*-PEO; m, 6H of OPD-*g*-*p*MeOBn), 2.30 (t, J = 7.5 Hz, 2H of CL units, C***H***$_2$$COOCH_2$), 1.64 (m, 4H of CL units, OCH_2C***H***$_2$ and C***H***$_2$$CH_2$COO), 1.37 (m, 2H of CL units, C***H***$_2$ CH_2 CH_2COO), 1.22 (d, J = 6.3 Hz, 6H of initiated chain end (CH_3)CHO) ppm. ^{13}C NMR (75 MHz, $CDCl_3$) δ 205.9, 173.7, 173.4, 172.8, 157.8, 156.2, 129.5, 113.8, 77.4, 72.2, 71.0, 70.7, 69.5, 64.7, 64.5, 64.3, 59.1, 41.6, 37.6, 34.3, 34.1, 28.5, 27.9, 25.7, 24.6, 24.5 ppm.

Self Assembly Procedure

Approximately 15 mg of polymer was massed into a 5 mL volumetric flask, and tetrahydrofuran was added to the flask until a final volume of 5 mL was achieved. A 1 mL aliquot of the polymer solution was transferred to a small vial, and nanopure water (pH 6, 18 MΩ·cm) was added to the polymer solution at a rate of 10 mL/h until a total volume of 10 mL was obtained. The resulting solutions were used subsequently in DLS, TEM, and AFM studies without further purification, as dialysis against nanopure water was found to result in degradation of the graft copolymers.

Conclusions

An efficient strategy for the functionalization of a ketone-containing polyester, taking advantage of stable ketoxime ethers with enhanced reaction conditions for their formation, was employed to yield a functional amphiphilic graft copolymer system, with up to 90% grafting efficiencies. Specifically, this methodology was used for the incorporation of both hydrophilic poly(ethylene oxide) grafts and *p*-methoxybenzyl side chains onto the backbone of poly((ε-caprolactone)-*co*-(2-oxepane-1,5-dione)) allowing for the creation of functional PCL-*g*-PEO ketoxime ether conjugates that were shown to be capable of undergoing self assembly in aqueous solution. The graft block copolymer system containing only PEO grafts formed spherical aggregates in aqueous solution, whereas the copolymer system with both PEO and *p*-MeOBn grafts was found to form rod-like aggregates.

The ability to form a variety of self-assembled architectures based upon the degree

of PEO grafting or the incorporation of small molecule side chains onto a PCL backbone is a powerful tool for the efficient synthesis of well-defined multifunctional degradable materials. Consequently, it is of great importance to continue to explore the chemistries involving the grafting of polymer chains and small molecule ligands onto P(CL-*co*-OPD) copolymers since this system provides a modular platform for the creation of a variety of complex hydrolytically-degradable nanostructures. Efforts to better understand the way in which the density of PEO grafts and the incorporation of small, hydrophobic side chains affects the self-assembly process are also currently under investigation. Due to the potential of this copolymer system, we continue to extend this work through the incorporation of other functional grafts—including chromophores for imaging and ligands for tissue-selective targeting—for the creation of more complex polyester nanoobjects.

Acknowledgements

This material is based upon work supported in part by the National Science Foundation under Grant No. DMR-0451490 and Grant No. DMR-0906815, by the Department of Energy under Grant No. DE-FG02-08ER64671, and by the National Heart Lung and Blood Institute of the National Institutes of Health as a Program of Excellence in Nanotechnology (HL080729). Transmission electron microscopy images were obtained in part using the equipment and facilities at Washington University in St. Louis, Department of Otolaryngology, Research Center for Auditory and Visual Studies funded by NIH P30 DC004665. The authors would also like to thank Mr. G. Veith (Washington

University Electron Microscopy Laboratory) and Yun (Lily) Lin for assistance with TEM, and Nam S. Lee for assistance with DLS.

References

1. Iha, R. K.; Wooley, K. L.; Nyström, A. M.; Burke, D. J.; Kade, M. J.; Hawker, C. J., Applications of orthogonal "Click" chemistries in the synthesis of functional soft materials. *Chemical Reviews* **2009,** *109* (11), 5620-5686.

2. Hawker, C. J.; Fokin, V. V.; Finn, M. G.; Sharpless, K. B., Brining efficiency to materials synthesis: The philosophy of click chemistry. *Austrailian Journal of Chemistry* **2007,** *60*, 381-383.

3. Takizawa, K.; Nulwala, H. H.; Thibault, R. J.; Lowenhielm, P.; Yoshinaga, K.; Wooley, K. L.; Hawker, C. J., Facile syntheses of 4-vinyl-1,2,3-triazole monomers by click azide/acetylene coupling. *Journal of Polymer Science Part A: Polymer Chemistry* **2008,** *46*, 2897-2912.

4. Hang, H. C.; Bertozzi, C. R., Chemoselective approaches to glycoprotein assembly. *Accounts of Chemical Research* **2001,** *34*, 727-736.

5. Francis, M. B., New methods for protein bioconjugation. *Chemical Biology* **2007,** *2*, 593-634.

6. Li, R. C.; Broyer, R. M.; Maynard, H. D., Well-defined polymers with acetal side chains as reactive scaffolds synthesized by atom transfer radical polymerization. *Journal of Polymer Science Part A: Polymer Chemistry* **2006,** *44*, 5004-5013.

7. Hwang, J.; Li, R. C.; Maynard, H. D., Well-defined polymers with activated ester and protected aldehyde side chains for bio-functionalization. *Journal of Controlled Release* **2007,** *122*, 279-286.

8. Fulton, D. A., Dynamic Combinatorial Libraries Constructed on Polymer Scaffolds. *Organic Letters* **2008,** *10*, 3291-3294.

9. Yang, S. K.; Weck, M., Modular covalent multifunctionalization of copolymers. *Macromolecules* **2008,** *41*, 346-351.

10. Barrett, D. G.; Yousaf, M. N., Preparation of a class of versatile, chemoselective, and amorphous polyketoesters. *Biomacromolecules* **2008,** *9* (2029-2035).

11. Barrett, D. G.; Yousaf, M. N., Poly(triol alpha-ketoglutarate) as biodegradable, chemoselective, and mechanically tunable elastomers. *Macromolecules* **2008,** *41*, 6347-6352.

12. Timbart, L.; Amsden, B. G., Functionalizable biodegradable photocrosslinked elastomers based on 2-oxepane-1,5-dione. *Journal of Polymer Science Part A: Polymer Chemistry* **2008,** *46*, 8191-8199.

13. Jérôme, C.; Lecomte, P., Recent advances in the synthesis of aliphatic polyesters by ring opening polymerization. *Advanced Drug Delivery Reviews* **2008,** *60*, 1056-1076.

14. Takizawa, K.; Nulwala, H.; Hu, J.; Yoshinaga, K.; Hawker, C. J., Molecularly defined (L)-lactic acide oligomers and polymers: Synthesis and characterization. *Journal of Polymer Science Part A: Polymer Chemistry* **2008,** *46*, 5977-5990.

15. Odelius, K.; Albertsson, A.-C., Precision synthesis of microstructures in star-shaped copolymers of epsilon-caprolactone, L-lactide, and 1,5-dioxepan-2-one. *Journal of Polymer Science Part A: Polymer Chemistry* **2008,** *46*, 1249-1264.

16. Höglund, A.; Albertsson, A.-C., Spontaneous crosslinking of poly(1,5-dioxepane-2-one) originating from ether bond fragmentation. *Journal of Polymer Science Part A: Polymer Chemistry* **2008,** *46*, 7258-7267.

17. Ozturk, G.; Long, T. E., Michael addition for crosslinking of poly(caprolactone)s. *Journal of Polymer Science Part A: Polymer Chemistry* **2009,** *47*, 5437-5447.

18. Albertsson, A.-C.; Varma, I. K., Recent developments in ring opening polymerization of lactones for biomedical applications. *Biomacromolecules* **2003,** *4*, 1466-1486.

19. Höglund, A.; Odelius, K.; Hakkarainen, M.; Albertson, A.-C., Controllable degradation product migration from cross-linked biomedical polyester-ethers through predetermned alterations in copolymer composition. *Biomacromolecules* **2007,** *8*, 2025-2032.

20. Höglund, A.; Hakkarainen, M.; Kowalczuk, M.; Adamus, G.; Albertson, A.-C., Fingerprinting the degradation products patterns of different polyester-ether networks by electrospray ionization mass spectrometry. *Journal of Polymer Science Part A: Polymer Chemistry* **2008,** *46*, 4617-4629.

21. Hu, X.; Chen, X.; Liu, S.; Shi, Q.; Jing, X., Novel aliphatic poly(ester-carbonate) with pendant allyl ester groups and its folic acid functionalization. *Journal of Polymer Science Part A: Polymer Chemistry* **2008,** *46*, 1852-1861.

22. Hu, X.; Chen, X.; Xie, Z.; Cheng, H.; Jing, X., Aliphatic poly(ester-carbonate)s bearing amino groups and its RGD peptide grafting. *Journal of Polymer Science Part A: Polymer Chemistry* **2008,** *46* (7022-7032).

23. Xu, N.; Wang, R.; Du, F.-S.; Li, Z.-C., Synthesis of amphiphilic biodegradable glycopolymers based on poly(epsilon-caprolactone) by ring opening polymerization and click chemistry. *Journal of Polymer Science Part A: Polymer Chemistry* **2009,** *47*, 3583-3594.

24. El Habnouni, S.; Blanquer, S.; Darcos, V.; Coudane, J., Aminated PCL-based copolymers by chemical modification of poly(alpha-iodo-epsilon-caprolactone-*co*-epsilon-caprolactone). *Journal of Polymer Science Part A: Polymer Chemistry* **2009,** *47*, 6104-6115.

25. Prime, E. L.; Cooper-White, J. J.; Qiao, G. G., Coupling hydrophilic amine-containing molecules to the backbone of poly(epsilon-caprolactone). *Austrailian Journal of Chemistry* **2006,** *59*, 534-538.

26. Prime, E. L.; Hamid, Z. A. A.; Cooper-White, J. J.; Qiao, G. G., Addition of biological funtionality to poly(epsilon-caporlactone) films. *Biomacromolecules* **2007,** *8*, 2416-2421.

27. Huang, M. H.; Coudane, J.; Li, S.; Vert, M., Methylated and pegylated PLA-PCL-PLA block copolymers via the chemical modification of di-hydroxy PCL combined with ring opening polymerization of lactide. *Journal of Polymer Science Part A: Polymer Chemistry* **2005,** *43*, 4196-4205.

28. Riva, R.; Rieger, J.; Jérôme, R.; Lecomte, P., Heterograft copolymers of poly(epsilon-caprolactone) prepared by combination of ATRA "grafting onto" and ATRP "grafing from" processes. *Journal of Polymer Science Part A: Polymer Chemistry* **2006,** *44*, 6015-6024.

29. Parrish, B.; Breitenkamp, R. B.; Emrick, T., PEG- and peptide grafted aliphatic polyesters by click chemistry. *Journal of the American Chemical Society* **2005,** *127*, 7404-7410.

30. Riva, R.; Schmeits, S.; Stoffelbach, F.; Jérôme, C.; Jérôme, R.; Lecomte, P., Combination of ring-opening polymerization and "click" chemistry towards functionalization of aliphatic polyesters. *Chemical Communications* **2005,** *5334-5336*.

31. Lee, R.-S.; Huang, Y.-T., Synthesis and characterization of amphiphilic block-graft MPEG-*b*-(PN3CL-*g*-alkyne) degradable copolymers by ring-opening polymerization and click chemistry. *Journal of Polymer Science Part A: Polymer Chemistry* **2008,** *46*, 4320-4331.

32. Tian, D.; Dubois, P.; Jérôme, R., Poly(2-oxepane-1,5-dione): A highly crystalline modified poly(epsilon-caprolactone) of a high melting temperature. *Macromolecules* **1998,** *31*, 924-927.

33. Van Horn, B. A.; Wooley, K. L., Toward cross-linked degradable polyester materials: investigations into the compatability and use of reductive amination chemistry for crosslinking. *Macromolecules* **2007,** *40*, 1480-1488.

34. Van Horn, B. A.; Iha, R. K.; Wooley, K. L., Sequential and single-step, one-pot strategies for the transformation of hydrolytically degradable polyesters into multifunctional systems. *Macromolecules* **2008,** *41*, 1618-1626.

35. Taniguchi, I.; Mayes, A. M.; Chan, E. W.; Griffith, L. G., A Chemoselective approach to grafting biodegradable polyesters. *Macromolecules* **2005,** *38*, 216-219.

36. Taniguchi, I.; Kuhlman, W. K.; Mayes, A. M.; Griffith, L. G., Functional modification of biodegradable polyesters through a chemoselective approach: application to biomaterial surfaces. *Polymer International* **2006,** *55*, 1385-1397.

37. Gajewiak, J.; Cai, S.; Shu, X. Z.; Prestwich, G. D., Aminooxy pluronics: Synthesis and preparation of glycosaminoglycan adducts. *Biomacromolecules* **2006,** *7*, 1781-1789.

38. Van Horn, B. A.; Wooley, K. L., Crosslinked and functionalized polyester materials constructed using ketoxime ether linkages. *Soft Matter* **2007,** *3*, 1032-1040.

39. Qui, Z.; Ikehara, T.; Nishi, T., Miscibility and crystallization of poly(ethylene oxide) and poly(epsilon-caprolactone) blends. *Polymer* **2003,** *44*, 3101-3106.

40. Geng, Y.; Discher, D. E., Hydrolytic degradation of poly(ethylene oxide)-*block*-polycaprolactone worm micelles. *Journal of the American Chemical Society* **2005,** *127*, 12780-12781.

41. Fairley, N.; Hoang, B.; Allen, C., Morphological control of poly(ethylene glycol)-*block*-poly(epsilon-caprolactone) copolymer aggregates in aqueous solution. *Biomacromolecules* **2008,** *9* (2283-2291).

42. Geng, Y.; Discher, D. E., Visualization of degradable worm micelle breakdown in relation to drug release. *Polymer* **2006,** *47*, 2519-2525.

43. Cai, S.; Vijayan, K.; Cheng, D.; Lima, E. M.; Discher, D. E., Micelles of different morphologies--advantages of worm-like filomicelles of PEO-PCL in paclitaxel delivery. *Pharmaceutical Research* **2007,** *24*, 2099-2108.

44. Tian, D.; Dubois, P.; Grandfils, C.; Jérôme, R., Ring-opening polymerization of 1,4,8-trioxospiro[4.6]-9-undecanone: A new route to aliphatic polyesters bearing functional pendant groups. *Macromolecules* **1997,** *30,* 406-409.

45. Tian, D.; Dubois, P.; Jérôme, R., Macromolecular engineering of polylactones and polylactides 23. Synthesis and characterization of biodegradable and biocompatible homopolymers and block Copolymers based on 1,4,8-trioxa[4.6]spiro-9-undecanone. *Macromolecules* **1997,** *30,* 1947-1954.

46. Tian, D.; Dubois, P.; Jérôme, R., Macromolecular engineering of polylactones and polylactides. 22. Copolymerization of 1,4,8-trioxaspiro[4.6]-9-undecanone initiated by aluminum isopropoxide. *Macromolecules* **1997,** *30,* 2575-2576.

47. Latere, J.-P.; Lecomte, P.; Dubois, P.; Jérôme, R., 2-Oxepane-1,5-dione: A precursor of a novel class of versatile semicrystalline biodegradable (co)polyesters. *Macromolecules* **2002,** *35,* 7857-7859.

48. Latere Dwan'Isa, J.-P.; Lecomte, P.; Dubois, P.; Jérôme, R., Synthesis and characterization of random copolyesters of epsilon-caprolactone and 2-oxepane-1,5-dione. *Macromolecules* **2003,** *36,* 2609-2615.

CHAPTER 4

AN INVESTIGATION INTO THE UNIQUE SHORT-TERM HYDROLYTIC DEGRADATION BEHAVIOR OF PCL-PEO KETOXIME ETHER CONJUGATES

CHAPTER FOUR

An investigation into the unique short-term hydrolytic degradation behavior of PCL-PEO ketoxime ether conjugates

[This work was conducted in collaboration with Ritu Shrestha]

Abstract

Poly(ε-caprolactone)-*g*-poly(ethylene oxide) (PCL-*g*-PEO) copolymers synthesized from poly(ε-caprolactone)-*co*-(2-oxepane-1,5-dione), (PCL-*co*-OPD), that still contained free OPD units were found to undergo an early and rapid degradation upon being dispersed in aqueous solution. P(CL_{92}-*co*-OPD_5-*co*-(OPD-*g*-$PEO)_9$), **1**, showed immediate signs of degradation upon being dispersed in aqueous solution based upon both ^{1}H NMR spectroscopy and gel permeation chromatography (GPC) analysis. Additional GPC analysis of the polymer as it remained in aqueous solution over 24 h revealed unique behavior indicating changes not only in molecular weight but possibly in polymer architecture. The solution state aggregates showed a minimal increase in aggregate size moving from a number-averaged hydrodynamic diameter (D_h) of 13 ± 3 nm at 0 h to 17 ± 3 nm at 24 h based upon analysis by dynamic light scattering (DLS). An increase in diameter upon degradation was corroborated by transmission electron microscopy (TEM) images showing circular particles that had a D_{av} of 15 ± 4 nm and 22 ± 5 nm at 0 and 24 h respectively. P(CL_{92}-*co*-(OPD-*g*-$PEO)_8$-*co*-(OPD-*g*-*p*$MeOBn)_6$), **2**, a polyester analogous to P(CL_{92}-*co*-OPD_5-*co*-(OPD-*g*-$PEO)_9$), **1**, but having no free OPD units, showed no similar signs of rapid degradation over 24 h by ^{1}H NMR or GPC analysis. Characterization of the solution state aggregates by DLS and TEM indicated that the

circular particles formed by the PCL-*g*-PEO copolymer, **2**, maintained both their size and morphology while being dispersed in aqueous solution for 24 h. P(CL_{327}-*co*-OPD_{22}-*co*-$(OPD\text{-}g\text{-}PEO)_{15}$-*co*-$(OPD\text{-}g\text{-}p\text{MeOBn})_8$), **3**, a significantly larger PCL-PEO ketoxime ether conjugate possessing free OPD units, also showed signs of backbone degradation by ^{1}H NMR and GPC upon being transitioned into aqueous solution. DLS analysis, of the solution state aggregates formed by the graft copolymer, **3**, in solution showed no significant changes in the hydrodynamic diameter of the aggregates over time. However, characterization by TEM showed a transition from circular to rod-like or cylindrical aggregates as the polyester backbone was hydrolyzed.

Introduction

Degradable polymers have become a fundamental polymer component used in numerous fields, and have potential applications ranging from the production of environmentally friendly materials to employment in nanoscale biomedical devices.[1] Aliphatic polyesters like polyglycolide (PGA), polylactide (PLA), and polycaprolactone (PCL) that can be precisely synthesized by ring opening polymerization methods[2] comprise one class of degradable polymers that have received significant attention for use as biomaterials[3] due to their promising mechanical properties[4], known biocompatibility,[5] and production of benign products upon hydrolytic degradation.[6] The effectiveness of synthetic materials in biological settings for use as drug delivery, imaging, and tissue engineering applications is often determined by the timely or controlled break down of the material, a characteristic that is intrinsic to aliphatic polyesters. However, the utility of these polyesters is limited due to their lack of chemical handles and inherent

hydrophobicity, which respectively restricts their direct use as functional materials and retards both hydrolytic degradation and biodegradation.

The utility of aliphatic polyesters can be broadened upon incorporation of functionality and hydrophilicity. Therefore, the development of strategies focusing on the incorporation of functional groups and efficient chemistries that can be used to impart hydrophilicity, attach imaging agents, and conjugate biologically relevant molecules is an important area of research.[7, 8] One method that has been frequently employed to partially address the aforementioned shortcomings of aliphatic polyesters is to synthesize amphiphilic block copolymers consisting of a hydrophobic polyester block and a biocompatible hydrophilic block. These block copolymers undergo self assembly in aqueous solution to form core-shell micelles, which are relevant for use in drug delivery applications as the hydrophilic, biocompatible shell provides stability in a biological setting while the hydrophobic core allows for encapsulation of a therapeutic payload.[9] Due to the interest in biodegradable and biocompatible nansoscale assemblies, there has been a considerable effort devoted to investigating the synthesis, self-assembly, and degradation of micelles composed of degradable block copolymers; one of the most studied block copolymer systems is poly(ε-caprolactone)-*b*-poly(ethylene oxide) (PCL-*b*-PEO) due to the biocompatibility of PEO and the ability of PCL to undergo hydrolytic degradation. This amphiphilic copolymer system has been extensively researched to obtain an understanding of how composition influences self-assembly and solution state morphologies,[10-14] and there are numerous studies analyzing both the chemical[15-17] and enzymatic[18-21] degradation of PCL-*b*-PEO micelles. The chemical changes in the PCL-*b*-PEO copolymers, the effect of degradation on molecular weight, and the rate of

degradation have all been studied in depth. Studies addressing the morphological changes associated with degradation are less prevalent, but no less important since the degradation of the hydrophobic regime of these solution state aggregates leads not only to changes in morphology and size,[22] but also affects the uptake and release characteristics of the polymeric assemblies.[23, 24]

While block copolymers composed of PCL and PEO have been the subject of extensive investigation, the self-assembly and degradation of amphiphilic block graft copolymers consisting of a PCL backbone with PEO grafts have not been explored as thoroughly. PCL-*g*-PEO copolymers comprise a unique class of amphiphilic degradable copolymers with the potential to form a variety of self-assembled architectures.[25] Aggregates resulting from the self-assembly in aqueous solution of PCL-*g*-PEO made by atom transfer radical addition (ATRA),[26] click cycloadditon,[27, 28] and ketoxime ether formation[25] have been documented, but changes in the nanoscale morphologies due to degradation induced reassembly and hydrolysis of the polyester backbone have not been examined. As such, the early and rapid degradation of PCL-PEO ketoxime ether conjugates synthesized from a poly(ε-caprolactone)-*co*-(2-oxepane-1,5-dione) (P(CL-*co*-OPD)) platform was investigated to obtain a better understanding of the mechanism behind this rapid backbone degradation. Additionally, experiments were conducted to assess the effect of polyester backbone hydrolysis on the morphologies of the resulting solution-state aggregates.

Results and discussion

Solution state behavior of capped *vs*. uncapped PCL-PEO ketoxime ether conjugates

It has been previously reported that PCL-PEO graft copolymers containing unfunctionalized OPD repeat units were unable to be purified by dialysis due to rapid degradation of the polyester backbone under aqueous conditions.[25] This behavior indicated that these block graft copolymers possessed unique short term degradation characteristics, as PCL—even in cases where it is incorporated into an amphiphilic block copolymer with PEO—degrades over a period of weeks and not hours.[17] Studies focusing on the degradation of the statistical polyester, P(CL-*co*-OPD), in bulk indicated that the presence of OPD repeat units resulted in an increase in the rate of hydrolytic degradation relative to rate of degradation observed for bulk PCL samples of similar molecular weight, and it was determined that the greater hydrophilicity of the OPD unit played a key role in the enhancement of backbone hydrolysis.[29] Since the presence of OPD was identified as being a critical factor affecting the rate and mechanism of

Scheme 4-1. Synthesis of P(CL_{92}-*co*-OPD_5-*co*-(OPD-*g*-$PEO)_9$), **1**.

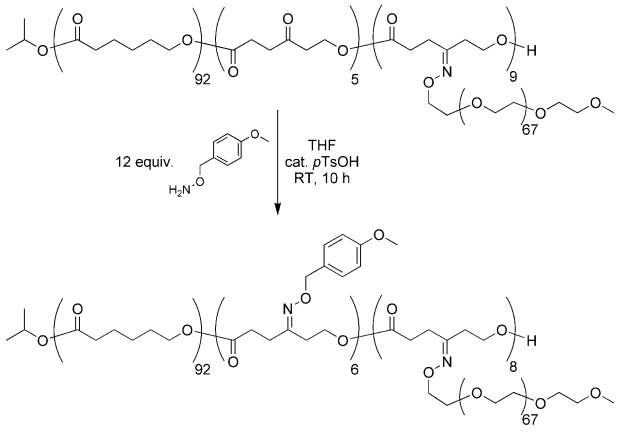

degradation in the statistical copolymer in bulk, it is likely that the presence of the more hydrophilic OPD units contributes to the rapid hydrolysis observed in PCL-PEO ketoxime ether conjugates.

To study the dependence of early degradation behavior on the presence of free OPD units, an amphiphilic graft copolymer P(CL_{92}-*co*-OPD_5-*co*-(OPD-*g*-PEO)$_9$), **1**, bearing only PEO grafts and containing free OPD units was synthesized by reacting P(CL-*co*-OPD) with α-methoxy-ω-aminooxy-poly(ethylene oxide) using previously reported methods.[25, 30, 31] A comparable graft copolymer bearing a similar number of PEO grafts but containing no free ketone units was prepared by reacting **1** with *p*-methoxy-*O*-benzylhydroxylamine to produce P(CL_{92}-*co*-(OPD-*g*-PEO)$_8$-*co*-(OPD-*g*-*p*MeOBn)$_6$), **2** (**Scheme 4-1**). ^{1}H NMR spectroscopy of **2** confirmed that all OPD units had been capped *via* ketoxime ether formation, indicated by the absence of a signal at 4.33 ppm corresponding to the C***H***$_2$OCO methylene protons in the non-derivatized OPD subunit as well as the absence of the signals at 2.74 ppm corresponding to the C(O)C***H***$_2$and C***H***$_2$COO protons on the methylenes β to the unfunctionalized ketone (**Figure 4-1 (b)**).

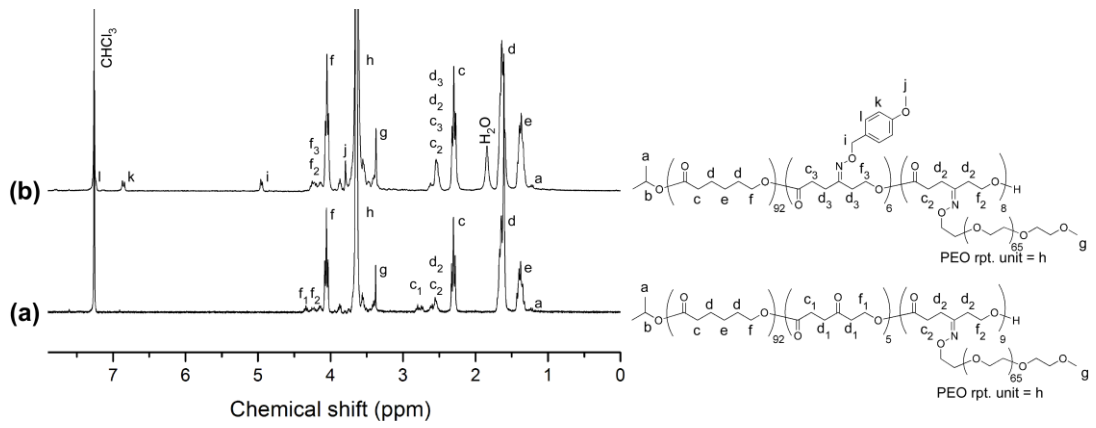

Figure 4-1. ^{1}H NMR spectra of **(a)** P(CL_{92}-*co*-OPD_5-*co*-(OPD-*g*-PEO)$_9$), **1**, in $CDCl_3$, and **(b)** P(CL_{92}-*co*-(OPD-*g*-PEO)$_8$-*co*-(OPD-*g*-*p*MeOBn)$_6$), **2**, a PCL-PEO ketoxime ether conjugate with no free OPD units present along the backbone.

GPC analysis revealed a slight increase in the molecular weight of polymer **2** relative to polymer **1** with no marked change in the PDI after the free ketone units were completely derivatized.

^{1}H NMR and GPC characterization of the capped and uncapped PCL-PEO graft copolymers in aqueous solution

^{1}H NMR was used to investigate chemical changes in the structures of P(CL_{92}-*co*-(OPD-*g*-PEO)$_8$-*co*-(OPD-*g*-*p*MeOBn)$_6$), **2**, and P(CL_{92}-*co*-OPD_5-*co*-(OPD-*g*-PEO)$_9$), **1**, after they were dispersed in aqueous solution. **Figure 4-2 (a)** (red) shows the ^{1}H NMR spectrum of the fully derivatized amphiphilic graft copolymer, **2**, dispersed in D_2O immediately after the self-assembly procedure had been completed (t = 0 h). The

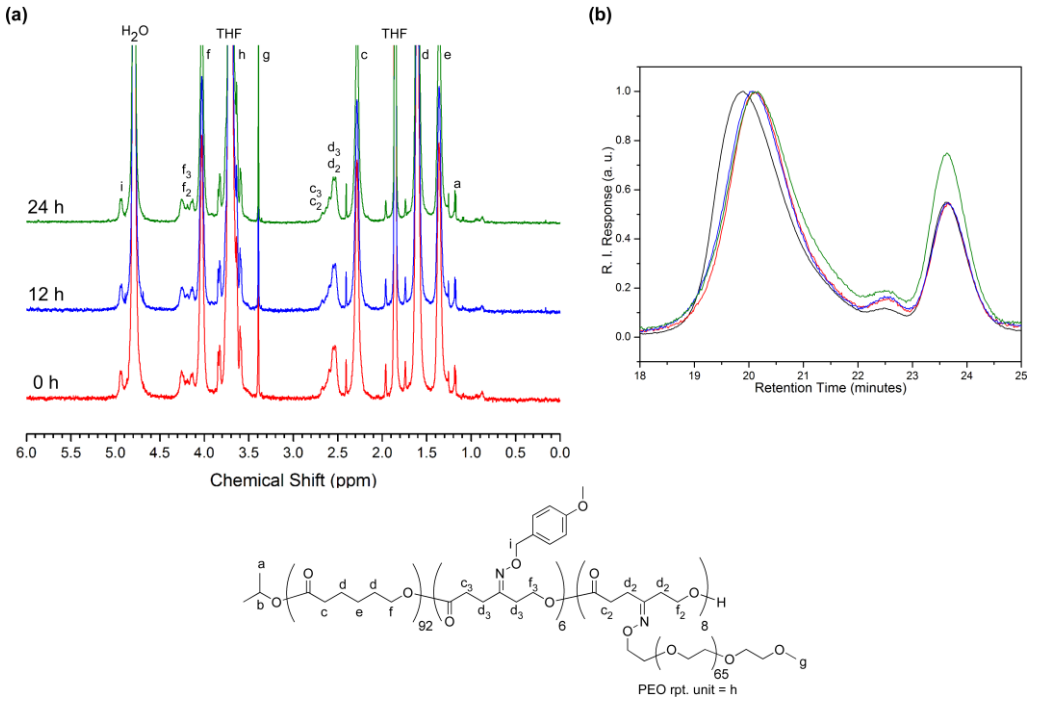

Figure 4-2. (a)^{1}H NMR spectra of a 0.6 mg/mL solution of P(CL_{92}-*co*-(OPD-*g*-PEO)$_8$-*co*-(OPD-*g*-*p*MeOBn)$_6$), **2**, in 9:1 D_2O/*d6*-THF (v/v) at 0 h (red), 12 h (blue) and 24 h (green) and **(b)** GPC chromatograms of P(CL_{92}-*co*-(OPD-*g*-PEO)$_8$-*co*-(OPD-*g*-*p*MeOBn)$_6$), **2** (black), and lyophilized aliquots of a 0.6 mg/mL solution of P(CL_{92}-*co*-(OPD-*g*-PEO)$_8$-*co*-(OPD-*g*-*p*MeOBn)$_6$), **2**, in 9:1 D_2O/ *d6*-THF (v/v) taken at 0 h (red), 12 h (blue) and 24 h (green).

spectrum showed signals representative of the PCL-PEO graft copolymer similar in chemical shift to those observed in the ^{1}H NMR spectrum taken in $CDCl_3$ (**Figure 4-1 (b)**). ^{1}H NMR spectra of **2** in D_2O were also obtained after the polymer had been dispersed in aqueous solution at 25 °C for 12 and 24h, and the spectra at 0, 12, and 24 h incubation time do not show any significant differences in signals or signal intensities (**Figure 4-2 (a)).** Additionally, the ^{1}H NMR spectra of **2** are absent of resonances typically associated with backbone degradation. For example, a signal corresponding to the methylene protons adjacent to a terminal alcohol group, which appear upfield of the C***H***$_2$OCO resonances of the CL and OPD groups—a sign indicative of polyester backbone degradation—is absent.[15, 32] The series of ^{1}H NMR spectra also illustrated that the derivatized OPD backbone units remain functionalized over a 24 h time period, with signals at 4.4 to 4.1 ppm corresponding to the C***H***$_2$OCO protons of the functionalized OPD unit, peaks at 2.5 to 2.7 ppm representative of the C***H***$_2$CH$_2$COO and CH$_2$C***H***$_2$COO protons in the functionalized OPD units being present in all spectra (**Figure 4-1 (a)**). Furthermore, over the duration of this study, of resonances representative of OPD repeat units bearing an unreacted ketone remained absent. The lack of a signal at 2.7 ppm diagnostic of the CH$_2$C***H***$_2$COO protons in the OPD repeat unit demonstrated that the ketone moieties remained functionalized after self assembly and dispersion in aqueous solution. As the ketoxime ether linkages were stable at room temperature under aqueous conditions over 24 h, previously observed degradation of PCL-PEO block graft copolymers was likely not occurring *via* hydrolysis of the ketoxime ether groups. It is important to note, however, that due to polymer self assembly and the solvent environment used for the experiment, that some proton resonances may not be observable

by ^{1}H NMR spectroscopy. Consequently, an absence of signals diagnostic of backbone degradation cannot absolutely confirm a lack of polyester hydrolysis. However, over a 24 h duration, polyester degradation in this sample was not extensive or widespread enough to be observed by NMR spectroscopy; to further confirm the absence of backbone degradation, additional analyses were performed.

In order to further evaluate the behavior of P(CL_{92}-*co*-(OPD-*g*-$PEO)_8$-*co*-(OPD-*g*-*p*$MeOBn)_6$), **2**, in an aqueous solution, GPC analysis was performed on lyophilized aliquots of a 0.6 mg/mL solution of **2** in 9:1 D_2O/*d6*-THF (v/v). GPC chromatograms of the capped graft copolymer, **2**, showed very little change over the 24 h period and showed no signs of significant degradation—changes in the polymer molecular weight—over the 24 h period. The *p*-methoxybenzyl-capped graft copolymer **2** displayed a peak molecular weight that was similar to that of the polymer prior to dispersion in aqueous solution. The peak molecular weight of the lyophilized samples remained constant and the chromatograms of these samples presented narrow molecular weight distributions at 0, 12 and 24 h (**Figure 4-2 (b)**). Some low molecular weight tailing was observed in the 24 h GPC trace suggesting that some degradation of the backbone from the alcohol chain terminus was occurring. However, after being dispersed in aqueous solutions at 25 °C for 24 h there were no signs by GPC analysis or ^{1}H NMR spectroscopy of significant or rapid degradation taking place, and if degradation of the polyester backbone was occurring, it occurred at the polyester chain end, and not *via* random hydrolysis along the polyester backbone.[33]

As the fully capped amphiphilic graft copolymer P(CL_{92}-*co*-(OPD-*g*-$PEO)_8$-*co*-(OPD-*g*-*p*$MeOBn)_6$), **2**, showed no obvious chemical or molecular weight changes

signaling substantial polyester degradation, the PCL-PEO ketoxime ether conjugate, **1**, bearing unfunctionalized OPD units along the polyester back bone was transitioned from *d6*-THF to D_2O to afford a 0.6 mg/mL solution of **1** in 9:1 D_2O/*d6*-THF (v/v). The dispersion of **1** in aqueous solution was monitored by ^1H NMR spectroscopy and analyzed by GPC over a 24 h period to respectively observe chemical and molecular weight changes occurring in the polymer system over time.

The ^1H NMR spectra obtained immediately after the addition of D_2O was complete (t = 0 h) contains signals characteristic of the PEO-PCL graft copolymer, **1**, but also showed peaks diagnostic of polyester backbone degradation (**Figure 4-3 (a)** (red)). The resonance at 3.90 ppm had a chemical shift consistent with that of methylene protons adjacent to an alcohol group, and there are shoulders or small peaks at 2.15, 1.55, and 1.30 ppm, slightly upfield of signals associated with the ε-caprolactone (CL) repeat units at 2.30, 1.60, and 1.55 ppm respectively (**Figure 4-3 (a)** (red)). Subsequent ^1H NMR spectra taken at t =12 and 24 h showed no appreciable changes over time, but each spectrum contained resonances characteristic of the graft copolymer and indicative of polyester backbone degradation (**Figure 4-3 (a)** (blue) and (green)). The presence of peaks at 3.90, 2.15, 1.55, and 1.30 ppm is consistent with resonances observed by ^1H NMR spectroscopy for the monomer unit 6-hydroxycaproic acid as well as terminal CL repeat units observed in other studies investigating PCL backbone degradation.[15, 32] While NMR resonances demonstrating backbone degradation were observed, the signals did not significantly increase in intensity between t = 0 h and t = 24 h indicating that chemical changes to the polymer structure caused by degradation was negligible or not quantifiable by NMR spectroscopy under these experimental conditions. Resonances

indicative of degradation were present at t = 0 h, which established that the chemical mechanism contributing to backbone degradation occurred rapidly upon dispersion of the amphiphilic block graft copolymer in aqueous solution (**Figure 4-3 (a)** (red)). Since PCL is known to take a considerable amount of time to degrade and produce monomers units (on the order of weeks and months in bulk or in micellar assemblies with PEO),[17, 34] it is unlikely that the peaks in the ^{1}H NMR spectra representative of polyester degradation are caused solely by the formation of 6-hydroxycaproic acid, and are instead the result of hydrolytic cleavage at OPD subunits in the backbone resulting in lower molecular weight amphiphilic graft copolymers with terminal CL repeat units possessing a hydroxyl end group.

GPC analysis of the aqueous solution of polyester **1** over time further supports the

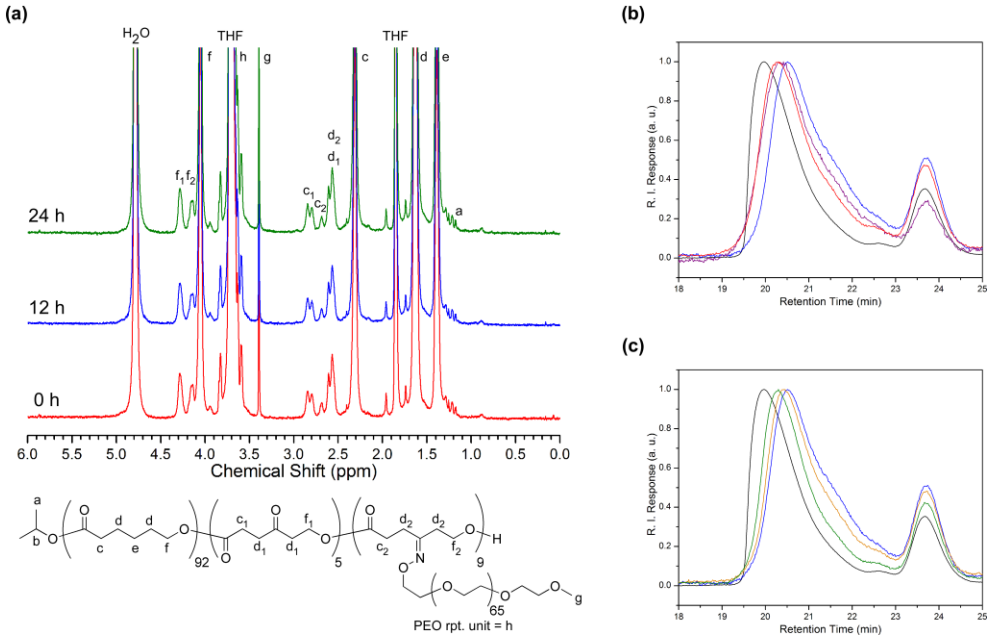

Figure 4-3. **(a)**^{1}H NMR spectra of a 0.6 mg/mL solution of P(CL_{92}-*co*-OPD_5-*co*-(OPD-*g*-$PEO)_9$), **1**, in 9:1 D_2O/ *d6*-THF/ (v/v) at 0 h (red), 12 h (blue) and 24 h (green); **(b)** GPC chromatograms of P(CL_{92}-*co*-OPD_5-*co*-(OPD-*g*-$PEO)_9$), **1** (black), and lyophilized aliquots of a 0.6 mg/mL solution of P(CL_{92}-*co*-OPD_5-*co*-(OPD-*g*-$PEO)_9$), **1**, in 9:1 D_2O/*d6*-THF (v/v) taken at 0 h (red), 6h (purple), and 12 h (blue); and **(c)** GPC chromatograms of P(CL_{92}-*co*-OPD_5-*co*-(OPD-*g*-$PEO)_9$), **1** (black), and lyophilized aliquots of a 0.6 mg/mL solution of P(CL_{92}-*co*-OPD_5-*co*-(OPD-*g*-$PEO)_9$), **1**, in 9:1 D_2O/ *d6*-THF (v/v) taken at 12 h (blue), 18 h (orange), and 24 h (green).

hypothesis that that degradation occured predominately at the free OPD subunits along the backbone. The hydrolysis of the amphiphilic graft copolymer, **1**, was monitored by removing and lyophilizing aliquots from a 0.6 mg/mL solution of **1** in 9:1 D_2O/*d6*-THF (v/v) followed by GPC characterization of the aliquots in THF. The GPC chromatograms taken at 0, 6, and 12 h show a successive decrease in peak molecular weight relative to the GPC trace of P(CL_{92}-*co*-OPD_5-*co*-(OPD-*g*-$PEO)_9$), **1**, prior to dispersion in aqueous solution (**Figure 4-3 (b)**). An observable increase in the PDI moving from 0 to 12 h was also observed, and a low molecular weight shoulder appeared causing the chromatogram to take on an asymmetric shape that suggested a bimodal molecular weight distribution. Chromatograms of polyesters possessing these characteristics is an analytical indicator signaling that degradation is occurring by hydrolysis at random locations along the polyester backbone (**Figure 4-3 (b)**).[33] Since previous studies have shown that the rapid initial hydrolysis of bulk P(CL-*co*-OPD) was a result of the enhanced hydrophilicity of the OPD repeat unit relative to the CL repeat unit,[29] this initial degradation in conjunction with ^{1}H NMR analysis is consistent with hydrolysis occurring at the OPD units randomly dispersed throughout the polyester backbone.

After being dispersed in water at 25 °C for times greater than 12 h, the degradable block graft copolymer, **1**, displayed a successive increase in the apparent peak molecular weight by GPC, and the low molecular weight shoulder observed at 12 h began to disappear giving way to a more symmetric chromatogram by 24 h incubation time (**Figure 4-3 (c)**). The behavior observed in the GPC traces from 12 to 24 h is counterintuitive for polyesters undergoing hydrolytic degradation. However, an apparent increase in molecular weight by GPC can be correlated to a change in the architecture of

the polymer transitioning from a morphology with a smaller hydrodynamic volume (like a grafted or highly branched polymer) to a morphology with a larger hydrodynamic volume (a linear or star-shaped polymer).[35, 36] An example of this phenomenon has been demonstrated in the hydrolytic degradation of cyclic PCL where the initial hydrolysis of the PCL backbone resulted in a change in morphology from a cyclic to linear architecture; this morphological change was accompanied by an apparent increase in molecular weight by GPC analysis due to an increase in the hydrodynamic volume of the polyester upon transition to a linear polymer chain.[37] It is plausible that hydrolysis of the polymer backbone in the PCL-PEO ketoxime ether conjugates resulted in the initial decrease in the peak molecular weight and increase in molecular weight distribution observed during the first 12 h, and was caused by the random breakage along the polyester backbone affording degradation products that strongly resemble the architecture of the original graft copolymer. However, after being dispersed in water for times greater than 12 h, the polyester continued to hydrolyze at the remaining OPD units, and the resulting polymeric degradation products became amphiphilic copolymers that more closely resembled amphiphilic star or block copolymers, thus producing a chromatogram that exhibited an apparent increase in molecular weight due to a change in morphology accompanied by an increase in e hydrodynamic volume and not an increase in the actual molecular weight of the polymer.

GPC analysis of the degradable polyester, **1,** after 48 h incubation time (not shown) produced a trace with the same peak molecular weight and distribution as that observed at t = 24 h. Since no clear change was observed in the GPC traces between 24 h and 48 h, no additional degradation resulting in an observable molecular weight occurred after 24

h, suggesting that the chemical process contributing to the short-term degradation was complete after approximately 24 h. Since no further signs associated with degradation were observed and because the polymer solution contained amphiphilic polymer species of high molecular weight, it is unlikely that the degradation mechanism was a result of hydrolysis at purely random locations along the backbone as the polyester would have continued to undergo rapid degradation at times greater than 24 h. Instead, the observations support rapid cleavage of the backbone at the free OPD subunits present in the polyester backbone, and, once hydrolysis had occurred at these sites, the rapid degradation observed by GPC over 24 was complete and no additional degradation by this mechanism occurred.

DLS and TEM characterization of the solution state aggregates formed by the capped and uncapped PCL-PEO ketoxime ether conjugates

Investigations analyzing PCL-*b*-PEO assemblies have shown that the aggregates formed in aqueous solution can undergo changes in size and morphology as a result of PCL degradation.[12, 15] Additionally, previous reports have shown that amphiphilic block graft copolymers composed of PCL with PEO grafts undergo multi-molecular self-assembly to afford nanoobjects with interesting and varied morphology when dispersed in water.[25]

As such, the fully functionalized P(CL_{92}-*co*-(OPD-*g*-$PEO)_8$-*co*-(OPD-*g*-*p*$MeOBn)_6$), **2**, was allowed to undergo self assembly in aqueous solution, by transitioning from THF to water. Light scattering measurements performed immediately after the addition of water was complete (t = 0 h) showed that this polymer formed micellar aggregates with a

bimodal distribution observed in the intensity- and volume-averaged histograms (**Figure 4-4 (a)**). A bimodal distribution of this sort is not uncommon and has been previously observed in the DLS characterization of aggregates formed from PCL-*g*-PEO copolymers synthesized by various routes and techniques.[25, 26] At t = 0 h, the smaller aggregates displayed an intensity-averaged D_h of 28 ± 9 nm, a volume-averaged D_h of 22 ± 6 nm, and a number-averaged D_h of 18 ± 4 nm; the assemblies corresponding to the larger diameter distribution had an intensity-averaged D_h of 293 ± 109 nm a volume-averaged D_h of 201 ± 70 nm, but was not present in the number-averaged histogram (**Table 4-1**, **Figure 4-4 (a)**).

Table 4-1. Particle analysis of aggregates formed from **2** in aqueous solution.

Time (h)	D_h (intensity)[a] (nm)		D_h (volume)[a] (nm)		D_h (number)[a] (nm)	D_{av}[b] (nm)
0	28 ± 9	293 ± 109	22 ± 6	201 ± 70	18 ± 4	16 ± 3
12	27 ± 9	380 ± 194	20 ± 6	200 ± 88	17 ± 4	15 ± 3
24	25 ± 8	281 ± 104	20 ± 6	194 ± 66	17 ± 4	17 ± 3

[a] Hydrodynamic diameters of aggregates in aqueous solution as determined by DLS analysis.
[b] Average diameters of particles measured by TEM from the values for 250 particles.

This solution was analyzed after incubating for 12 and 24 h in aqueous solution at 25 °C. DLS analysis at these time points revealed that there was essentially no change in the intensity averaged, volume-averaged, and number averaged D_h of the smaller aggregates over 24 hours. Though there were changes in the intensity- and volume-averaged D_h corresponding to larger solution state assemblies, these changes were not significant given the large standard deviation in aggregate size (**Table 4-1 and Figure 4-4 (b) and**

(c)). The regularity of the hydrodynamic diameter over 24 h as measured by DLS combined with the consistency observed in the ^{1}H NMR and GPC measurements performed on aqueous dispersions of the fully derivatized amphiphilic graft copolymer, **2**, further confirmed that no rapid degradation of the polyester backbone was occurring.

Transmission electron microscopy (TEM) was employed to analyze the size and shape of the aggregates formed by the PCL-PEO ketoxime ether conjugate, **2**. Immediately after addition of water was complete (t = 0 h), TEM samples were prepared by drop deposition of a 0.6 mg/mL solution of **2** in 9:1 water/THF (v/v) onto a glow treated carbon-coated copper grid. The TEM images obtained at t = 0 h showed globular, particle-like aggregates with an average diameter of 16 ± 3 nm posessing a narrow size distribution observable in both the micrograph and the histogram analysis (**Table 4-1** and **Figure 4-5 (a)**). The average diameter calculated from TEM measurements agreed with the number-averaged hydrodynamic diameter obtained at t = 0 h by DLS measurements.

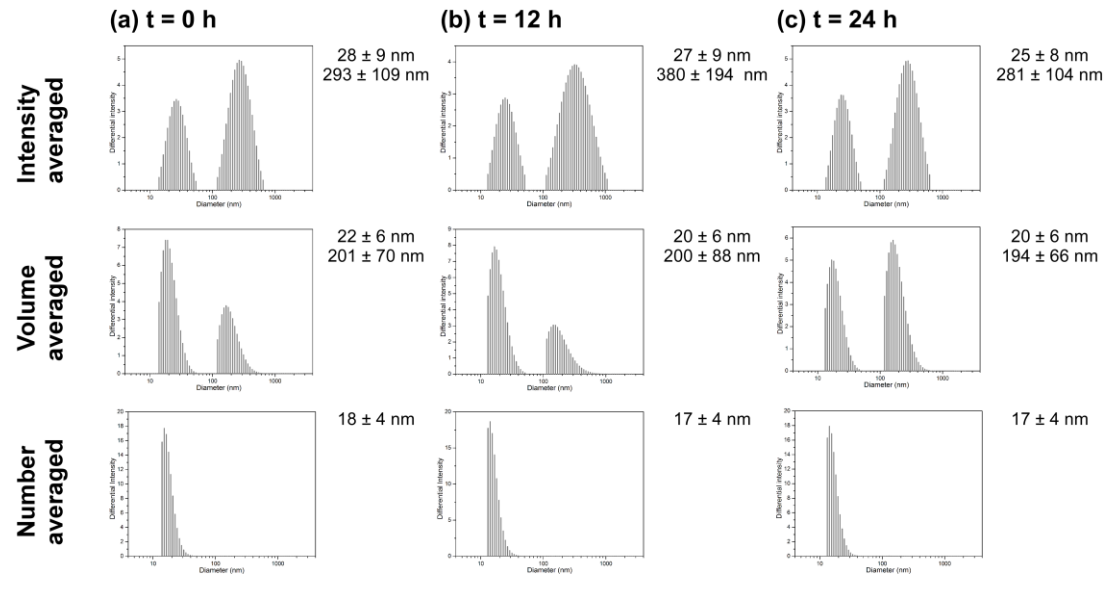

Figure 4-4. Intensity averaged, volume averaged, an number averaged histograms from dynamic light scattering analysis of a 0.6 mg/mL solution of P(CL_{92}-*co*-(OPD-*g*-PEO)$_8$-*co*-(OPD-*g*-*p*MeOBn)$_6$), **2**, in 9:1 water/THF (v/v) at **(a)** 0 h incubation time, **(b)** 12 h incubation time and **(c)** 24 h incubation time.

Similarly sized particle diameters and narrow distribution were observed in TEM micrographs prepared at t = 12 and 24 h, and showed aggregates with a D_{av} of 15 ± 3 nm and 17 ± 3 nm respectively. While the size and shape of the aggregates remain relatively constant during the duration of this study, the aggregates present in the TEM images obtained at 24 h possess a more defined and distinctly circular shape when compared to the aggregates visualized at 0 and 12 h.The PCL-PEO graft copolymer with unfunctionalized ketone moieties, **1**, was dispersed in water to afford a 0.6 mg/mL solution of 2 in 9:1 water/THF (v/v), and was immediately analyzed (t = 0 h) by DLS. DLS analysis of the self-assembled nanostructures at t = 0 h, revealed a bimodal distribution of aggregate sizes (**Figure 4-6(a)**). The resulting nanostructures corresponding to the smaller diameter distribution had an intensity-averaged D_h of 25 ± 8 nm, a volume-averaged D_h of 17 ± 6 nm, and a number-averaged D_h of 13 ± 3 nm. The assemblies possessing a larger diameter displayed an intensity-averaged D_h of 513 ± 218 nm, a volume-averaged D_h of 248 ± 116 nm, and were not observable in the number-averaged histogram (**Table 4-2** and **Figure 4-6 (a)**).

Table 4-2. Particle analysis of aggregates formed from **1** in aqueous solution.

Time (h)	D_h (intensity)[a] (nm)		D_h (volume)[a] (nm)		D_h (number)[a] (nm)	D_{av}[b] (nm)
0 h	25 ± 8	513 ± 218	17 ± 6	248 ± 116	13 ± 3	15 ± 4
12 h	26 ± 9	574 ± 376	19 ± 6	226 ± 115	16 ± 6	18 ± 7
24 h	27± 9	491 ± 245	20 ± 6	269 ± 114	17 ± 4	22 ± 5

[a] Hydrodynamic diameters of aggregates in aqueous solution as determined by DLS analysis.
[b] Average diameters of particles measured by TEM from the values for 250 particles.

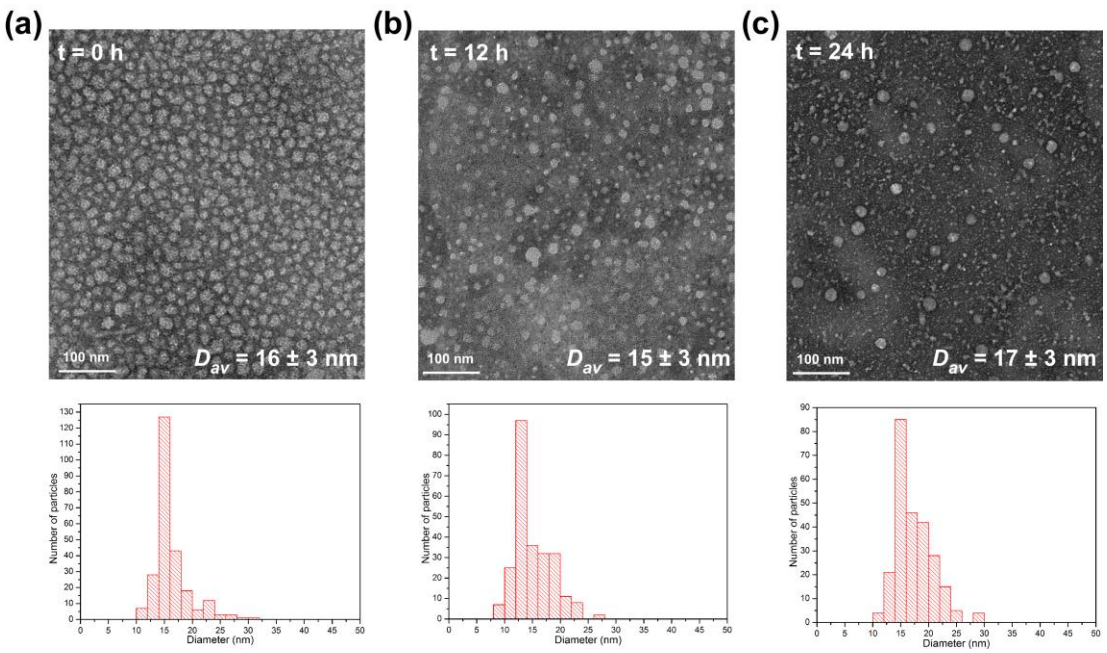

Figure 4-5. TEM images and corresponding histograms for solution state aggregates formed in a 0.6 mg/mL solution of P(CL_{92}-*co*-(OPD-*g*-PEO)$_8$-*co*-(OPD-*g*-*p*MeOBn)$_6$), **2**, in 9:1 water/THF (v/v) at **(a)** 0 h incubation time, **(b)** 12 h incubation time and **(c)** 24 h incubation time. All samples were drop deposited onto glow treated TEM grids and were stained with a 2 % solution of uranyl acetate.

DLS analysis of the polymer solution after it had incubated at 25 °C for 12 and 24 h shows a small increase in the hydrodynamic diameter of the smaller micellar aggregates. At 12 h the intensity- volume- and number-averaged diameters increased to 16 ± 6, 19 ± 6, and 26 ± 9 nm respectively (**Table 4-1** and **Figure 4-6 (b)**). The assemblies present at 24 h were larger still and displayed diameters of 27 ± 9 nm for the intensity-averaged D_h, 20 ± 6 nm for the volume-averaged D_h, and 17 ± 4 nm for the number-averaged D_h (**Table 4-1** and **Figure 4-6 (c)**). The diameters of the larger aggregates do not appear to change significantly over the duration of analysis, but the standard deviation of the larger diameter aggregates by DLS were substantial, making it difficult to assess whether any changes in the average diameter corresponding to these larger aggregates is significant.

TEM images obtained after drop deposition of a 0.6 mg/mL solution of the degradable graft copolymer, **1,** onto a carbon coated copper grid immediately after water addition was complete (t = 0 h) showed globular nanostructures with a D_{av} of 15 ± 4 nm (**Table 4-2** and **Figure 4-6(a)**). TEM analysis of this sample over time showed a distinct and significant increase in the diameter of the aggregates, which increase from 15 ± 4 nm, to 18 ± 7 nm, to 22 ± 5 nm at 0, 12, and 24 h respectively (**Table 4-2** and **Figure 4-7**). The histograms corresponding to particle diameters measured at each time point illustrated an increase in particle size over time; additionally, these histograms showed a transition from smaller aggregates to larger aggregates occurring over 24 h (**Figure 4-7**). The histogram and micrograph for the self-assembled nanostructures present in solution at 12 h incubation time displayed a broad distribution that appeared bimodal in nature (**Figure 4-7 (b)**). Both the histogram and TEM image representing the nanostructures present in solution at 12 h showed two different sizes of particles where the smaller

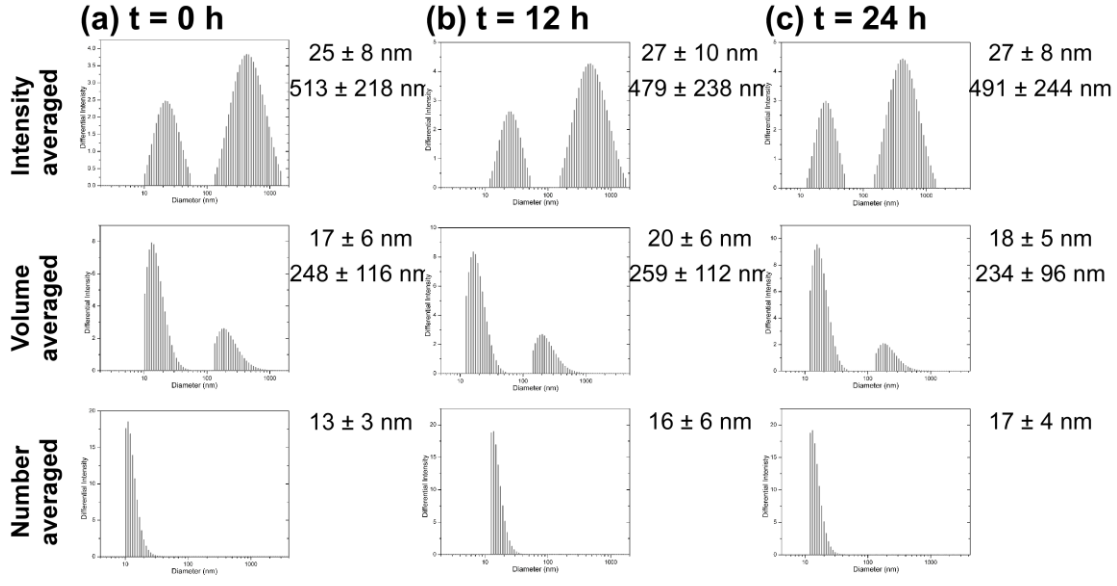

Figure 4-6. Intensity averaged, volume averaged, an number averaged histograms from dynamic light scattering analysis of a 0.6 mg/mL solution of P(CL_{92}-*co*-OPD_5-*co*-(OPD-*g*-$PEO)_9$), **1,** in 9:1 water/THF (v/v) at **(a)** 0 h incubation time, **(b)** 12 h incubation time, and **(c)** 24 h incubation time.

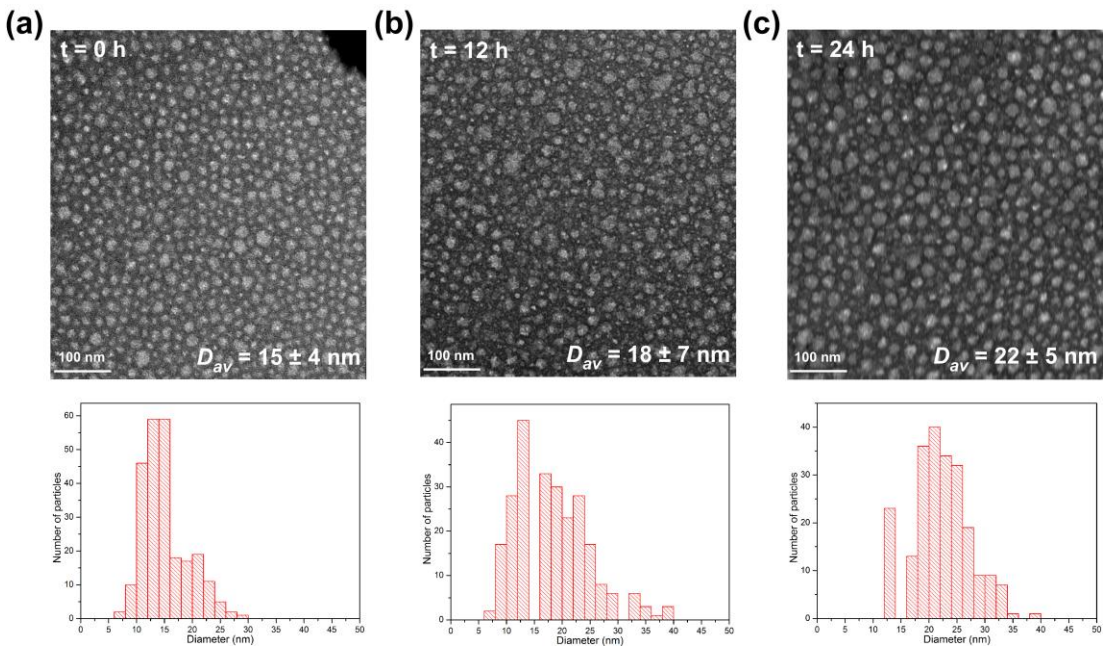

Figure 4-7. TEM images and corresponding histograms for solution state aggregates formed in a 0.6 mg/mL solution of P(CL_{92}-*co*-OPD_5-*co*-(OPD-*g*-$PEO)_9$), **1**, in 9:1 water/THF (v/v) at **(a)** 0 h incubation time, **(b)** 12 h incubation time and **(c)** 24 h incubation time. All samples were drop deposited onto glow treated TEM grids and were stained with a 2% solution of uranyl acetate.

aggregates were comparable in diameter to those observed at 0 h and the larger aggregates were similar in size to those observed at 24h, approximately 15 and 22 nm in diameter respectively (**Figure 4-7**).

The diameter of the assemblies formed showed an increase in diameter over time by both TEM and DLS measurements when the degradable PCL-PEO graft copolymer, **1**, was dispersed and stored in aqueous solution. The D_{av} of the particles observed in the TEM at 0, 12, and 24 h were comparable to the number-averaged diameters measured by DLS analysis at the same time points. However, at every time point, the D_{av} observed in the TEM micrograph was greater than those observed by DLS, which suggested that some deformation or flattening of the self-assembled structures occurred as a function of deposition and drying. This difference in diameter is most clear at 24 h, as the number-

averaged D_h was 17 ± 4 nm while the D_{av} by TEM was 22 ± 5 nm. This difference is not entirely unexpected since amphiphilic PCL-PEO graft copolymers have been observed to reorganize and deform when deposited and dried on a surface.[25] As degradation of the hydrophobic core occurred over time, only minor changes in the hydrodynamic diameter were observed by DLS, which is most likely due to the fact that the PCL core was swollen by the THF present in solution. However, after deposition and drying on the TEM grid, the aggregates deforedm to give a D_{av} greater than the number-averaged D_h observed while the particles were still dispersed in solution. This increase in diameter has been observed in previous studies investigating PCL-PEO block copolymers, where an increase in particle size early in investigation was attributed to polyester degradation.[15]

Degradation of a PCL-ketoxime ether conjugate known to form cylindrical assemblies

While slight changes in the diameter of the globular aggregates formed by P(CL_{92}-*co*-OPD_5-*co*-(OPD-*g*-$PEO)_9$), **1**, could be observed by DLS and TEM, the changes caused by degradation in these particles were almost undetectable by DLS, and only small changes (ca. 7 nm) in diameter could be ascertained by TEM measurements. Additionally, these changes only appeared significant when compared to the solution state aggregates formed by the fully functionalized graft copolymer, **2**, which effectively showed no changes in aggregate morphology or size over 24 h. In this class of amphiphilic block graft copolymers, as is also the case with spherical micelles composed of PCL-*b*-PEO, degradation only caused subtle changes in particle size, which made it more difficult to assess degradation.[12, 38] To further probe the degradation of amphiphilic block graft

copolymers prepared from a PCL-co-OPD platform, the degradation behavior of P(CL_{327}-*co*-OPD_{22}-*co*-(OPD-*g*-PEO)$_{15}$-*co*-(OPD-*g*-*p*MeOBn)$_8$), **3**—a polymer known to form cylindrical or rod-like aggregates in aqueous solution—was investigated.

^{1}H NMR and GPC analysis

^{1}H NMR was used to detect changes in the chemical structure of P(CL_{327}-*co*-OPD_{22}-*co*-(OPD-*g*-PEO)$_{15}$-*co*-(OPD-*g*-*p*MeOBn)$_8$), **3**, during degradation. **Figure 4-8 (a)** shows the ^{1}H NMR spectra of the amphiphilic degradable graft copolymer, **3**, dispersed in D_2O immediately after the self-assembly procedure was complete (t = 0 h), and after being dispersed in aqueous solution at 25 °C for 12 and 24 h. All of the ^{1}H NMR spectra looked very similar, and contained resonances diagnostic of the graft copolymer as well as signals that can be attributed to polyester degradation (**Figure 4-8 (a)**). ^{1}H NMR analysis indicated that the PCL-PEO graft copolymer **3**, displayed degradation characteristics similar to that of P(CL_{92}-*co*-OPD_5-*co*-(OPD-*g*-PEO)$_9$), **1,** when dispersed in aqueous solution**.** The ^{1}H NMR spectra of **3** included signals indicative of polyester backbone degradation at 3.90 ppm, a resonance having a chemical shift consistent with that of a methylene adjacent to a hydroxyl group, and signals at 2.15, 2.55, and 1.30 ppm that match resonances for a terminal CL repeat unit. The peaks indicative of backbone degradation were present in the ^{1}H NMR spectrum of **3** at all time points and did not significantly increase or change in intensity between 0 and 24 h. These results are consistent with a rapid hydrolysis mechanism that predominately occurs while the graft copolymer is being transitioned from organic to aqueous solution and is undergoing self assembly. Changes due to degradation after t = 0 h, based on the absence of change over

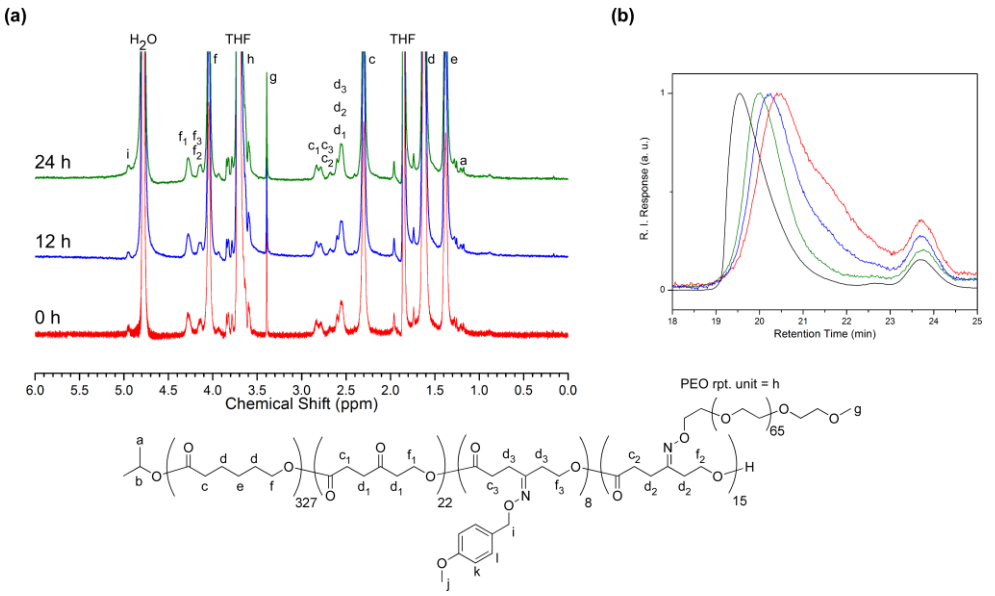

Figure 4-8. **(a)** ^{1}H NMR spectra of a 0.4 mg/mL solution of P(CL_{327}-*co*-OPD_{22}-*co*-(OPD-*g*-PEO)$_{15}$-*co*-(OPD-*g*-*p*MeOBn)$_8$), **3**, in 9:1 D_2O/*d6*-THF (v/v) at 0 h (red), 12 h (blue) and 24 h (green); **(b)** GPC chromatograms of P(CL_{327}-*co*-OPD_{22}-*co*-(OPD-*g*-PEO)$_{15}$-*co*-(OPD-*g*-*p*MeOBn)$_8$), **3**, (black), and lyophilized aliquots of a 0.6 mg/mL solution of P(CL_{327}-*co*-OPD_{22}-*co*-(OPD-*g*-PEO)$_{15}$-*co*-(OPD-*g*-*p*MeOBn)$_8$), **3** in 9:1 D_2O/*d6*-THF (v/v) taken at 0 h (red), 12 h (blue); and 24 h (green).

time, were either negligible or undetectable by ^{1}H NMR spectroscopy due to the conditions under which the experiment was performed.

GPC analysis of the degradable graft copolymer, **3**, further confirmed rapid degradation occurring at sites along the PCL backbone. The GPC trace obtained from an aliquot removed and lyophilized immediately after completion of D_2O addition (t = 0 h), displayed a peak molecular weight lower than that of the PCL-PEO conjugate, **3**, prior to dispersion in aqueous solution; additionally, the chromatogram was asymmetric in shape, displayed a large molecular weight distribution, and possessed a low molecular weight shoulder (**Figure 4-8 (b)** (red)). The characteristics observed in the t = 0 h GPC trace are all qualities indicative of PCL degradation by hydrolysis at random locations along the backbone, and since degradation was so significant t = 0 h, this trace also suggested that hydrolysis was very rapid.

Subsequent GPC analysis of aliquots removed from the solution at t = 12 and 24 h presented traces that exhibited a successive increase in the apparent peak molecular weight along with a transition to a more symmetric shape with a less pronounced low molecular weight shoulder (**Figure 4-8 (b)** (blue) and (green))..This same phenomenon was observed in the GPC analysis of P(CL_{92}-*co*-OPD_5-*co*-(OPD-*g*-$PEO)_9$), **1**, and was probably caused by highly branched or graft-like structures with possessing a smaller hydrodynamic volume present early in the degradation process transitioning to architectures that were less branched and more strongly resembled amphiphilic star or block copolymers with a larger hydrodynamic volume.

The GPC trace obtained for the PCL-PEO graft copolymer, **3**, after being dispersed in aqueous solution for 48 h, was identical in shape, peak molecular weight, and molecular weight distribution to the GPC analysis performed at 24h (not shown). Consequently, it appeared that the rapid chemical process contributing to early degradation was completed at 24 h, and that no significant hydrolysis of the PCL backbone that affected molecular weight occurred between 24 and 48 h. This initial degradation was rapid, and the chromatographic data supported degradation by random chain scission. The results were very similar to be the behavior observed in the degradation of the shorter PEO-PCL ketoxime ether conjugate, **1**. These data in conjunction with previous literature implicating free OPD units in PCL-*co*-OPD polymers as a site of enhanced degradation, support a mechanism whereby the PCL backbone breaks apart rapidly at the OPD units, and, once hydrolysis has occurred at these sites, degradation of the remaining ester moieties along the PCL backbone proceeds at a significantly slower rate.

TEM and DLS analysis

P(CL_{327}-*co*-OPD_{22}-*co*-(OPD-*g*-$PEO)_{15}$-*co*-(OPD-*g*-*p*$MeOBn)_8$), **3**, was allowed to undergo assembly in aqueous solution, and immediately after the micellization process was complete, DLS measurements were performed. A 0.4 mg/mL solution of **3** in 9:1 water/THF (v/v) produced a bimodal distribution of nanoscale aggregates where the smaller structures had an intensity-averaged D_h of 29 ± 10 nm, a volume-averaged D_h of 21 ± 7 nm, and a number-averaged D_h, of 17 ± 4 nm, while the intensity- and volume-averaged D_h for the larger aggregates were 429 ± 186 nm and 260 ± 103 nm respectively (**Figure 4-9 (a)**). Over an 18 h period, the DLS measurements showed the same bimodal distribution and no obvious change in diameter (**Figure 4-9**). While GPC and ^{1}H NMR analysis clearly demonstrated that the amphiphilic graft copolymer, **3**, was undergoing degradation, no noticeable changes in the hydrodynamic diameter of the smaller aggregates due to degradation were observed, and changes in the size of the larger self-assembled structures were not conclusive due to the broad size distribution.

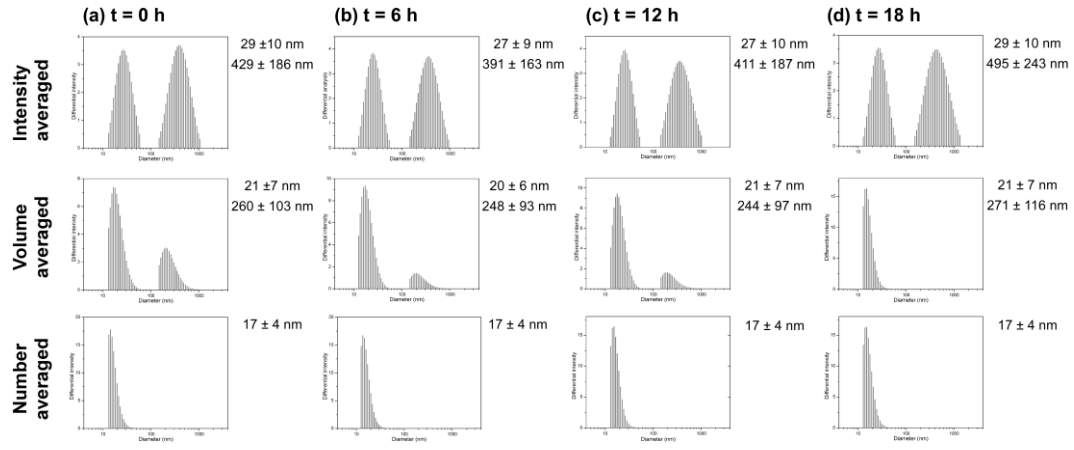

Figure 4-9. Intensity averaged, volume averaged, an number averaged histograms from dynamic light scattering analysis of a 0.4 mg/mL P(CL_{327}-*co*-OPD_{22}-*co*-(OPD-*g*-$PEO)_{15}$-*co*-(OPD-*g*-*p*$MeOBn)_8$), **3**, in 9:1 THF/H_2O (v/v) at **(a)** 0 h incubation time, **(b)** 6 h incubation time, **(c)** 12 h incubation time, and **(d)** 18 h incubation time.

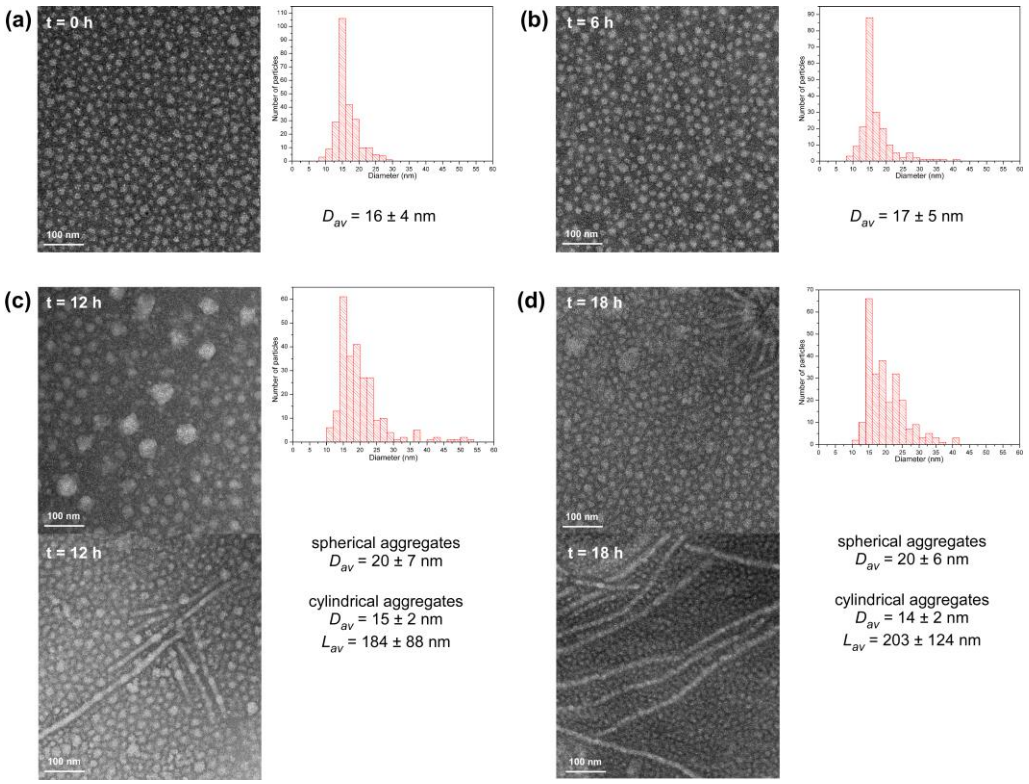

Figure 4-10. TEM images of the solution state aggregates and corresponding histograms for the spherical particles present in a 0.4 mg/mL solution of P(CL_{327}-*co*-OPD_{22}-*co*-(OPD-*g*-$PEO)_{15}$-*co*-(OPD-*g*-*p*$MeOBn)_8$), **3** in 9:1 water/THF (v/v) **(a)** 0 h incubation time, **(b)** 6 h incubation time **(c)** 12 h incubation time, and **(d)** 18 h incubation time. All samples were drop deposited onto glow treated TEM grids and were stained with a 2 % solution of uranyl acetate.

As larger changes for the assemblies formed by P(CL_{92}-*co*-OPD_5-*co*-(OPD-*g*-$PEO)_9$), **1**, were noted by TEM analysis, samples were prepared from a 0.4 mg/mL solution of **3** in 9:1 water/THF (v/v) by drop deposition onto a carbon coated copper grid immediately after water addition was complete (t = 0 h). The nanoscale aggregates visualized by TEM at t = 0 h were globular and possessed a D_{av} of 16 ± 4 nm (**Figure 4-10 (a)**). The aqueous solution of P(CL_{327}-*co*-OPD_{22}-*co*-(OPD-*g*-$PEO)_{15}$-*co*-(OPD-*g*-*p*$MeOBn)_8$), **3**, in 9:1 water/THF (v/v) was stored at 25 °C, and subsequent TEM analysis showed a transition from spheres to rods over an 18 h period. The solution state assemblies of polymer **3** at 6 h were globular and possessed a D_{av} of 17 ± 5 nm, the histogram of particle sizes at this

time point displayed a large population of particles with a diameter of approximately 15 nm, but also indicated the apresenence of pareticle-like aggregates with a larger diameter (**Figure 4-10 (b)**). At t = 12 h, the TEM images displayed circular aggregates of two different sizes; additionally, cylindrical aggregates that appear to be forming from the globular aggregates were also present at t = 12 h (**Figure 4-10 (c)**). The circular aggregates at t =12 h displayed a larger D_{av} of 20 ± 6 nm due to the presence of two different populations of globular aggregates, which is clearly illustrated in the histogram analysis, and the rod-like aggregates had a D_{av} of 15 ± 2 nm—similar to the diameter of the smaller particle-like aggregates observed at 0 and 6 h—and an L_{av} of 184 ± 88 nm (**Figure 4-10 (c)**). After being dispersed in aqueous solution at room temperature for 18 h, the TEM micrograph showed the both globular nanostructures with a D_{av} of 20 ± 6 nm and cylindrical aggregates with a D_{av} of 14 ± 2 nm and an L_{av} of 203 ± 124 nm (**Figure 4-10 (d)**).

While the DLS measurements showed no changes in size over an 18 h period, TEM analysis showed that the self-assembled structures changed dramatically in both shape and size (**Figure 4-10**). The D_{av} of the globular aggregates by TEM analysis were similar in diameter to the number-averaged D_h. However, the D_{av} was greater than the diameter of the micellar aggregates observed in the solution state by DLS indicating that the assemblies deformed or reorganized upon deposition and drying. The presence of both the cylindrical and circular aggregates in the TEM micrographs is consistent with the bimodal distributions present in the DLS analysis as the L_{av} and the distribution of lengths amongst the cylindrical aggregates by TEM corresponded to the volume-and intensity-averaged D_h of the larger assemblies present in solution.

Experimental

Materials

The synthesis of 1,4,8-trioxaspiro-9-undecanone (TOSUO)[39, 40], and PCL-*co*-OPD[41-43] has been described elsewhere. ε-Caprolactone (CL) (Aldrich Chemical Company) was distilled from CaH_2 and stored under argon. Toluene (Aldrich Chemical Company) was dried by heating at reflux over sodium and distilled under argon prior to use. Aluminum triisopropoxide $Al(OiPr)_3$ (Aldrich Chemical Company) was purified by sublimation and dissolved in dry toluene prior to use. Polyethylene oxide (3 kDA PEO) was purchased from Nektar and was dried by azeotropic distillation of toluene (3 x) to dryness to remove residual water. All other reagents (solvents, *p*-toluenesulfonic acid (*p*-TsOH), *etc*.) were purchased from Aldrich and used as received.

Instrumentation

^1H NMR (300 MHz) and ^{13}C NMR (75 MHz) spectra for characterization of synthesized polymers were acquired in $CDCl_3$ on a Varian Mercury 300 spectrometer using the residual solvent signal as the internal reference unless otherwise noted. ^1H NMR (600 MHz) spectra to monitor polymer degradation were acquiree in 9:1 D_2O/*d6*-THF (v/v) on a Varian Unity-Inova 600 spectrometer using the residual water pead as the internal reference. Infrared spectra were recorded on a Perkin-Elmer Spectrum RX FT-IR system by film deposition onto NaCl salt plates. Differential scanning calorimetry was performed under nitrogen atmosphere using 40 μL aluminum pans on a Mettler Toledo DSC822 with heating and cooling at 10 °C/min

from –100 °C to 100 °C. T_m values were obtained from the third heating scan as the peak values from the thermogram. Gel permeation chromatography was performed on a Waters Chromatography, Inc., 1515 isocratic HPLC pump equipped with an inline degasser, a model PD2020 dual-angle (15° and 90°) light scattering detector (Precision Detectors, Inc.), a model 2414 differential refractometer (Waters, Inc.), and four PL_{gel} polystyrene-*co*-divinylbenzene gel columns (Polymer Laboratories, Inc.) connected in series: 5 μm Guard (50 × 7.5 mm), 5 μm Mixed C (300 × 7.5 mm), 5 μm 10^4 (300 × 7.5 mm), and 5 μm 500 Å (300 × 7.5 mm) using the Breeze (version 3.30, Waters, Inc.) software. The instrument was operated at 35 °C with THF as eluent. Data collection was performed with Precision Acquire 32 Acquisition program (Precision Detectors, Inc.) and analyses were carried out using Discovery32 software (Precision Detectors, Inc.) with a system calibration curve generated from plotting molecular weight as a function of retention time for a series of broad polydispersity poly(styrene) standards.

DLS sample preparation and analysis

Samples for light scattering analysis were performed without filtration and without centrifugation in order to maintain counts high enough for analysis. Hydrodynamic diameters (D_h) and distributions for the PCL-*g*-PEO ketoxime ether aggregates in aqueous solution were determined using a Beckman Coulter Delsa Nano C particle sizer with a pinhole of 50 μm. Measurements were made at 25 °C. Scattered light was collected at a fixed angle of 165° and the digital correlator was operated with 440 ratio spaced channels. Only measurements in which the measured and calculated baselines of

the intensity autocorrelation function agreed to within 0.5% were used to calculate particle size. Particle size distributions were performed with the Delsa Nanoversion 2.31 software package (Beckman Coulter, Inc.), which calculated size based upon the time domain method using cumulant analysis and the CONTIN method for determining particle size and distributions.

TEM sample preparation and analysis

Samples for transition electron microscopy (TEM) measurements were prepared under ambient conditions by drop depositing 5 μL of sample onto glow discharged carbon coated copper grids. The sample was allowed to incubate for 3 min, excess sample was removed by wicking the liquid away with filter paper, and the grids were allowed to dry in air for 1 min. Following that process, the grids were stained with 5 μL of 2% uranyl acetate for 15 sec. Excess stain was wicked away using filter paper and the grids were allowed to dry in air in a desiccator. Specimens were observed on a JEOL 1200EX transmission electron microscope operating at 100 kV and micrographs were recorded at calibrated magnifications using an SIA-15C CCD camera. The final pixel size was 0.42 nm/pixel. The number average particle diameters (D_{av}) and standard deviations for spherical aggregates were generated from the analysis of 250 particles. The number average diameters (D_{av}), lengths (L_{av}) and standard deviations for cylindrical aggregates were generated from the analysis of 100 aggregates.

Polymer synthesis

P(CL_{92}-*co*-OPD_5-*co*-(OPD-*g*-PEO)$_9$) (1). A solution of α-methoxy-ω-aminooxy(poly(ethylene oxide)), (237 mg, 0.083 mmol) in THF (1.0 g) was added to a solution of P(CL_{92}-*co*-OPD_{14}), (104 mg, 0.0086 mmol) in THF (0.5 g). The reaction mixture was allowed to stir at RT for 1 min, after which four drops of a solution of *p*-TsOH (75 mg) in THF (20 mL) was added. The reaction was stirred at RT for 24 h. The polymer was purified by precipitation into hexanes, the stringy white solid was isolated *via* vacuum filtration with a coarse glass frit, and was dried *in vacuo* for 12 h (275 mg, 77% yield). GPC: $M_{n,\,PS}$ = 45,200 Da, $M_{w,\,PS}$ = 53,000 Da, PDI_{PS} = 1.2. M_n (^{1}H NMR) = 39700 Da. T_m = 53 °C. IR (NaCl) 2950-2800, 1733, 1726, 1465, 1456, 1384, 1357, 1342, 1278, 1239, 1193, 1145, 1109, 1064, 961, 842 cm^{-1}. ^{1}H NMR (300 MHz, $CDCl_3$) δ 4.34 (t, J = 6.9 Hz, 2H of OPD units, C***H***$_2$OCO), 4.3-4.1 (pair of multiplets, 2H of ketoxime ether isomers of OPD-*g*-PEO units, C***H***$_2$OCO), 4.06 (t, J = 6.6 Hz, 2H of CL units, C***H***$_2$OCO), 3.64 (bs, 4H of PEO repeat unit), 3.38 (s, 3H of OC***H***$_3$ PEO end group), 2.76 (t, J = 6.6 Hz, 2H of OPD units, C(O)C***H***$_2$$CH_2$COO), 2.74 (t, J = 6.1 Hz, 2H of OPD units, C(O)C***H***$_2$$CH_2$OCO), 2.62-2.50 (m, 2H OPD, C***H***$_2$$COOCH_2$; m, 6H of OPD-*g*-PEO), 2.31 (t, J = 7.4 Hz, 2H of CL units, C***H***$_2$$COOCH_2$), 1.65 (m, 4H of CL units, OCH_2C***H***$_2$ and C***H***$_2$$CH_2$COO), 1.38 (m, 2H of CL units, C***H***$_2$$CH_2CH_2$COO), 1.22 (d, J = 6.4 Hz, 6H of initiated chain end (CH_3)CHO) ppm. ^{13}C NMR (75 MHz, $CDCl_3$) δ 205.8, 173.5, 173.3, 172.6, 156.4, 155.5, 77.2, 71.8, 70.5, 69.5, 64.7, 64.5, 59.0, 41.4, 37.4, 34.1, 33.8, 30.0, 28.9, 27.7, 25.5, 24.5ppm.

P(CL$_{92}$-*co*-(OPD-g-*p*MeOBn)$_6$-*co*-(OPD-*g*-PEO)$_8$) (2) P(CL$_{92}$-*co*-OPD$_5$-*co*-(OPD-*g*-PEO)$_9$, **1** (63 mg, 0.0017 mmol), was dissolved in THF (0.50 mL). The solution was stirred at RT for 10 minutes to ensure complete dissolution of the polymer. A solution of *O*-(4-methoxybenzyl)hydroxylamine (3.3 mg, 0.022 mmol) in THF (1.0 mL) was added to the reaction mixture, and then four drops of a solution of *p*-TsOH (75 mg) in THF (20 mL) was added. The reaction progress was monitored by ^{1}H NMR spectroscopy, and was stirred at RT for 10 h to ensure the complete functionalization of all free OPD repeat units. The polymer was purified and isolated by precipitation into hexanes. The white solid was collected *via* vacuum filtration with a medium porosity glass frit, and was dried *in vacuo* for 12 h (54 mg, 86% yield). GPC: $M_{n,\ PS}$ = 43,600 Da, $M_{w,\ PS}$ = 52000 Da, PDI_{PS} = 1.2. M_n (^{1}H NMR) = 37,3000 Da. T_m = 52 °C. IR (NaCl) 2950-2800, 1726, 1466, 1456, 1360, 1342, 1280, 1240, 1149, 1110, 1061, 963, 842 cm^{-1}. ^{1}H NMR (300 MHz, $CDCl_3$) δ 6.86 (d, J = 7.7 Hz, 4H, aromatic), 4.97-4.95 (two singlets, 2H, Ph-C***H***$_2$), 4.3-4.1(pair of multiplets, 2H of ketoxime ether isomers of OPD-*g*-PEO units, C***H***$_2$OCO, and pair of multiplets, 2H of ketoxime ether isomers of OPD-*g*-*p*MeOBn units), 4.06 (t, J = 6.5 Hz, 2H of CL units, C***H***$_2$OCO), 3.80 (s, 3H, C***H***$_3$O-Ph) 3.65 (bs, 4H of PEO repeat unit), 3.38 (s, 3H of OC***H***$_3$ PEO end group), 2.63-2.50 (m, 6H of OPD-*g*-PEO; m, 6H of OPD-*g*-*p*MeOBn), 2.31 (t, J = 7.5 Hz, 2H of CL units, C***H***$_2$COOCH$_2$), 1.65 (m, 4H of CL units, OCH$_2$C***H***$_2$ and C***H***$_2$CH$_2$COO), 1.40 (m, 2H of CL units, C***H***$_2$ CH$_2$ CH$_2$COO), 1.22 (d, J = 6.3 Hz, 6H of initiated chain end (CH$_3$)CHO) ppm. ^{13}C NMR (75 MHz, $CDCl_3$) δ 173.7, 173.4, 172.8, 159.4, 156.4, 156.3 155.7, 155.3, 130.1, 130.0, 129.9, 128.7, 113.8, 77.4, 75.6, 74.2, 72.9, 72.1, 71.8, 70.5, 69.7, 64.6, 64.3,

61.1, 60.7, 59.2, 55.4, 59.0, 34.2, 33.9, 30.2, 30.0, 29.0, 28.5, 25.7, 24.7, 24.4 ppm.

P(CL$_{327}$-*co*-OPD$_{27}$-*co*-(OPD-*g*-PEO)$_{15}$-*co*-(OPD-*g*-MeOBn)$_8$ (3). A solution of α-methoxy-ω-aminooxy(poly(ethylene oxide)), (128 mg, 0.042 mmol) in THF (1.2 g) was added to a solution of P(CL$_{327}$-*co*-OPD$_{45}$) (66 mg, 0.0017 mmol) in THF(0.5 g). The reaction mixture was stirred at RT for 1 min. to ensure the dissolution of both polymer species. A solution of *O*-(4-methoxybenzyl)hydroxylamine (2.6 mg, 0.017 mmol) in THF (0.5 g) was added to the reaction mixture, and then four drops of a solution of *p*-TsOH (75 mg) in THF (20 mL) was added. The reaction was stirred at RT for 24 h and the polymer was purified by precipitation into hexanes. The stringy white solid was isolated *via* vacuum filtration with a coarse glass frit, and was dried *in vacuo* for 12 h (180 mg, 89% yield). GPC: $M_{n,\,PS}$ = 74900 Da, $M_{w,\,PS}$ = 97600 Da, PDI_{PS} = 1.3. M_n (^{1}H NMR) = 89700 Da. T_m = 49 °C. IR (NaCl) 2950-2800, 1733, 1466, 1456, 1360, 1342, 1280, 1240, 1149, 1110, 1061, 963, 842 cm^{-1}. ^{1}H NMR (300 MHz, $CDCl_3$) δ 6.86 (d, J = 8.8 Hz, 4H, aromatic), 4.94-4.96 (two singlets, 2H, Ph-CH_2), 4.33 (t, J = 6.2 Hz, 2H of OPD units, C***H***$_2$OCO), 4.3-4.1(pair of multiplets, 2H of ketoxime ether isomers of OPD-*g*-PEO units, C***H***$_2$OCO, and pair of multiplets, 2H of ketoxime ether isomers of OPD-*g*-*p*MeOBn units), 4.05 (t, J = 6.7 Hz, 2H of CL units, C***H***$_2$OCO), 3.80 (s, 3H, C***H***$_3$O-Ph) 3.64 (bs, 4H of PEO repeat unit), 3.37 (s, 3H of OC***H***$_3$ PEO end group), 2.79 (t, J = 6.3 Hz, 2H of OPD units, C(O)C***H***$_2$ CH_2COO), 2.74 (t, J = 6.6 Hz, 2H of OPD units, C(O)C***H***$_2$$CH_2$OCO), 2.62-2.50 (t, J = 6.6 Hz, 2H OPD, C***H***$_2$$COOCH_2$; m, 6H of OPD-*g*-PEO; m, 6H of OPD-*g*-*p*MeOBn), 2.30 (t, J = 7.5 Hz, 2H of CL units, C***H***$_2$$COOCH_2$), 1.64 (m, 4H of CL units, OCH_2C***H***$_2$ and

C***H***$_2$CH$_2$COO), 1.37 (m, 2H of CL units, C***H***$_2$ CH$_2$ CH$_2$COO), 1.22 (d, J = 6.3 Hz, 6H of initiated chain end (CH$_3$)CHO) ppm. ^{13}C NMR (75 MHz, CDCl$_3$) δ 205.9, 173.7, 173.4, 172.8, 157.8, 156.2, 129.5, 113.8, 77.4, 72.2, 71.0, 70.7, 69.5, 64.7, 64.5, 64.3, 59.1, 41.6, 37.6, 34.3, 34.1, 28.5, 27.9, 25.7, 24.6, 24.5 ppm.

Self assembly procedures

Preparation of solutions for ^{1}H NMR and GPC studies

Approximately 5 mg of the graft copolymer being analyzed was massed into a vial equipped with a magnetic stir bar. Tetrahydrofuran-d_6 (1.0g) was added to the flask, and the solution was stirred at RT for 10 min, after which, the reaction was cooled to approximately 0 °C in an ice/water bath. Using a syringe pump, D_2O was added to the polymer solution at a rate of 10 mL/h until a total volume of 10 mL was obtained. The resulting solutions were used subsequently in GPC and ^{1}H NMR studies without further purification. Upon warming to RT for ten minutes, A 1 mL aliquot was removed an transferred to an NMR tube for analysis every 6 h (the NMR sample and solution were kept next to each other to maintain a consistent temperature for both samples. Every 6 h, a ^{1}H NMR spectrum of the solution was obtained. Additionally, every 6 h, a 0.5 mL aliquot was removed, lyophilized for 3 h, dissolved in 0.60 mL of THF and analyzed by GPC.

Preparation of solutions for DLS and TEM measurements

Approximately 5 mg of the graft copolymer being analyzed was massed into a vial equipped with a magnetic stir bar. Unstabilized tetrahydrofuran (1.0 mL) was added to

the flask, and the solution was stirred at RT for 10 min, after which, the reaction was cooled to approximately 0 °C in an ice/water bath. Using a syringe pump, nanopure water was added to the polymer solution at a rate of 10 mL/h until a total volume of 10 mL was obtained. The solution was allowed to warm to room temperature for 10 minutes, and samples for the first analyses (t = 0 h)were prepared. The resulting solutions were used to prepare TEM samples and were used in DLS analysis without further purification. Every 6 h, the solutions were analyzed by DLS to obtain average hydrodynamic diameters in solution as a function of degradation, and every 6 h TEM samples were prepared to compare morphology and particle diameter as a function of degradation.

Conclusions

Rapid hydrolytic degradation of PCL-PEO ketoxime ether conjugates synthesized from a P(CL-*co*-OPD) platform was found to occur as a function of having OPD units along the polyester backbone. Two different PCL-PEO graft copolymers of differing lengths, P(CL_{92}-*co*-OPD_5-*co*-(OPD-*g*-$PEO)_9$), **1**, and P(CL_{327}-*co*-OPD_{22}-*co*-(OPD-*g*-$PEO)_{15}$-*co*-(OPD-*g*-*p*$MeOBn)_8$), **3**, displayed degradation behavior that was consistent with rapid hydrolysis at various points along the polyester backbone. GPC analysis of the degradable graft copolymers as they remained in aqueous solution over 24 h also revealed unique behavior (an initial decrease followed by an apparent increase in peak molecular weight) that indicated that the polyester back bone was not only undergoing hydrolytic degradation, but that changes associated with molecular architecture had also occurred.

By comparison, no degradation was observed over a 24 h period for, P(CL_{92}-*co*-(OPD-*g*-PEO)$_8$-*co*-(OPD-*g*-*p*MeOBn)$_6$), **2,** a PCL-PEO graft copolymer where all of the OPD units had been derivatized. This investigation in conjunction with prior studies that described OPD as a site of enhanced degradation strongly supports a mechanism whereby the PCL backbone of the graft copolymer undergoes a rapid and selective chain scission at the more hydrophilic OPD units statistically dispersed throughout the backbone.

Morphological changes associated with degradation were also observed in the amphiphilic block graft copolymers possessing unfunctionalized OPD units. P(CL_{92}-*co*-OPD_5-*co*-(OPD-*g*-PEO)$_9$), **1**, formed spherical aggregates that increased in size as a result of hydrolytic degradation of the hydrophobic PCL-based core. More interestingly, P(CL_{327}-*co*-OPD_{22}-*co*-(OPD-*g*-PEO)$_{15}$-*co*-(OPD-*g*-*p*MeOBn)$_8$), **3**, displayed a change in morphology shape as a result of the degradation occurring at the OPD units. This particular polyester exhibited a transition from spherical aggregates to self-assembled structures possessing rod-like or cylindrical morphology as hydrolysis of the PCL backbone progressed.

The ability to control and manipulate both the degradation and the micellar morphology of polyester-based materials through the incorporation or derivatization of OPD units is a valuable tool for altering the physical and chemical characteristics of the resulting nanoobjects. This unique degradability provides a compelling approach for the creation and application of unique hydrolytically degradable materials based upon PCL-PEO ketoxime ether conjugates synthesized from a P(CL-*co*-OPD) platform. Further exploration of PCL-*g*-PEO copolymers produced from this system and the specific mechanism of micellar degradation resulting in morphological changes should be

investigated further as these materials provide a modular method for the creation of a variety of complex functional nanostructures with the potential for tunable degradability.

Acknowledgements

This material is based upon work supported in part by the National Science Foundation under Grant No. DMR-0451490 and Grant No. DMR-0906815, by the Department of Energy under Grant No. DE-FG02-08ER64671, and by the National Heart Lung and Blood Institute of the National Institutes of Health as a Program of Excellence in Nanotechnology (HL080729).

References

1. *Biodegradable Polymers and Plastics*. The Royal Society of Chemistry: Cambridge, 1992.

2. Jérôme, C.; Lecomte, P., Recent advances in the synthesis of aliphatic polyesters by ring opening polymerization. *Advanced Drug Delivery Reviews* **2008,** *60*, 1056-1076.

3. Vert, M., Aliphatic polyesters: Great degradable polymers that cannot do everything. *Biomacromolecules* **2005,** *6*, 538-546.

4. Engelberg, I.; Kohn, J., Physico-mechanical properties of degradable polymers used in medical applications: A comparative study. *Biomaterials* **1991,** *12*, 292-304.

5. Hutmacher, D. W., Scaffold design and fabrication technologies for engineering tissues—state of the art and future perspectives. *Journal of Biomaterials Design, Polymer Edition* **2001,** *12*, 107-124.

6. Albertsson, A.-C.; Varma, I. K., Recent developments in ring opening polymerization of lactones for biomedical applications. *Biomacromolecules* **2003,** *4* (1466-1486).

7. Lecomte, P.; Riva, R.; S., S.; Riegrr, J.; Van Butsels, K.; Jérôme, R., New prospects for the grafting of functional groups onto aliphatic polyesters. Ring-opening polymerization of alpha- or gamma-substituted epsilon-caprolactone followed by the chemical derivitization of the substituents. *Macromolecular Symposia* **2006,** *240*, 157-165.

8. Williams, C. K., Synthesis of functionalized biodegradable polyesters. *Chemical Society Reviews* **2007,** *36*, 1573-1580.

9. Soo, P. L.; Luo, L.; Maysinger, D.; Eisenberg, A., Incorporation and realease of hydrophobic probes in biocompatible polycaprolactone-*b*-poly(ethylene oxide) micelles: Implications for drug delivery. *Langmuir* **2002,** *18*, 9996-10004.

10. Vangeyte, P.; Leyh, B.; Henrich, M.; Grandjean, J.; Bourgaux, C.; Jérôme, R., Self-assembly of poly(ethylene oxide)-*b*-poly(epsilon-caprolactone) copolymers in aqueous solution. *Langmuir* **2004,** *20*, 8442-8451.

11. Vangeyte, P.; Gautier, S.; Jérôme, R., About the methods of preparation of poly(ethyleneoxide)-*b*-poly(epsilon-caprolactone) nanoparticles in water: Analysis by dynamic light scattering. *Colloids and Surfaces A: Physiochemical and Engineering Aspects* **2004,** *242*, 201-211.

12. Geng, Y.; Discher, D. E., Hydrolytic degradation of poly(ethylene oxide)-*block*-polycaprolactone worm micelles. *Journal of the American Chemical Society* **2005,** *127*, 12780-12781.

13. Du, Z.-X.; Xu, J.-T.; Fan, Z.-Q., Micellear morphologies of poly(epsilon-caprolactone)-*b*-poly(ethylene oxide) block copolymers in water with a crystalline core. *Macromolecules* **2007,** *40*, 7633-7637.

14. Fairley, N.; Hoang, B.; Allen, C., Morphological control of poly(ethylene glycol)-*block*-poly(epsilon-caprolactone) copolymer aggregates in aqueous solution. *Biomacromolecules* **2008,** *9* (2283-2291).

15. Hu, Y.; Zhang, L.; Cao, Y.; Ge, H.; Jian, X.; Yang, C., Degradation behavior of poly(epsilon-caprolactone)-*b*-poly(ethylene glycol)-*b*-poly(epsilon-caprolactone) micelles in aqueous solution. *Biomacromolecules* **2004,** *7*, 1756-1762.

16. Carstens, M. G.; van Nostrum, C. F.; Verrijk, R.; De Leede, L. G. J.; Crommelin, D. J. A.; Hennink, W. E., A mechanistic study on the chemical and ensymatic degradation of PEG-oliog-(epsilon-caprolactone) micelles. *Journal of Pharmaceutical Sciences* **2008,** *97*, 506-518.

17. Jiang, Z.; Zhu, Z.; Liu, C.; Hu, Y.; Wu, W.; Jiang, X., Non-enzymatic and enzymatic degradation of poly(ethylene glycol)-*b*-poly(epsilon-caprolactone) diblock copolymer micelles in aqueous solution. *Polymer* **2008,** *49*, 5513-5519.

18. Gan, Z.; Jim, T. F.; Li, M.; Yuer, Z.; Wang, S.; Wu, C., Enzymatic biodegradation of poly(ethylene oxide-*b*-epsilon-caprolactone) diblock copolymer and its potential biomedical applications. *Macromolecules* **1999,** *32*, 599-594.

19. Li, S.; Garreau, H.; Pauvert, B.; McGrath, J.; Toniolo, A.; Vert, M., Enzymatic degradation of block copolymers prepared from epsilon-caprolactone and poly(ethylene glycol). *Biomacromolecules* **2002,** *3*, 525-530.

20. Nie, T.; Zhao, Y.; Xie, Z.; Wu, C., Micellar formation of Poly(caprolactone-*block*-ethylene oxide-*block*-caprolactone) and its enzymatic biodegradation. *Macromolecules* **2003,** *2003* (36), 8825-8829.

21. Lam, H. F.; Gong, X.; Wu, C., Novel differential refractometry study of the enzymantic degradation kinetics of poly(ethylene oxide)-*b*-poly(epsilon-caprolactone) particles dispersed in water. *Journal of Physical Chemistry B* **2007,** *111*, 1531-1535.

22. Geng, Y.; Discher, D. E., Hydrolytic degradation of poly(ethylene oxide)-*block*-polycaprolactone worm micelles. *Journal of the Americal Chemical Society* **2005,** *127*, 12780-12781.

23. Geng, Y.; Discher, D. E., Visualization of degradable worm micelle breakdown in relation to drug release. *Polymer* **2006,** *47*, 2519-2525.

24. Cai, S.; Vijayan, K.; Cheng, D.; Lima, E. M.; Discher, D. E., Micelles of different morphologies--advantages of worm-like filomicelles of PEO-PCL in paclitaxel delivery. *Pharmaceutical Research* **2007,** *24*, 2099-2108.

25. Iha, R. K.; Van Horn, B. A.; Wooley, K. L., Complex, degradable polyester materials *via* ketoxime ether-based functionalization: Amphiphilic, multifunctional graft copolymers and their resulting solution-state aggregates
Journal of Polymer Science Part A: Polymer Chemistry **2010,** *accepted*.

26. Riva, R.; Rieger, J.; Jérôme, R.; Lecomte, P., Heterograft copolymers of poly(epsilon-caprolactone) prepared by combination of ATRA "grafting onto" and ATRP "grafing from" processes. *Journal of Polymer Science Part A: Polymer Chemistry* **2006,** *44*, 6015-6024.

27. Riva, R.; Schmeits, S.; Stoffelbach, F.; Jérôme, C.; Jérôme, R.; Lecomte, P., Combination of ring-opening polymerization and "click" chemistry towards functionalization of aliphatic polyesters. *Chemical Communications* **2005,** *5334-5336*.

28. Lee, R.-S.; Huang, Y.-T., Synthesis and characterization of amphiphilic block-graft MPEG-*b*-(P-alpha-N_3CL-*g*-alkyne) degradable copolymers by ring opening polymerizatons and click chemistry. *Journal of Polymer Science Part A: Polymer Chemistry* **2008,** *46*, 4320-4331.

29. Latere Dwan'Isa, J.-P.; Lecomte, P.; Dubois, P.; Jérôme, R., Hydrolytic and thermal degredation of random copolyesters of epsilon-caprolactone and 2-oxepane-1,5-dione. **2003,** *Macrmolecular Chemistry and Physics,* 1191-1201.

30. Taniguchi, I.; Mayes, A. M.; Chan, E. W.; Griffith, L. G., A Chemoselective approach to grafting biodegradable polyesters. *Macromolecules* **2005,** *38*, 216-219.

31. Van Horn, B. A.; Iha, R. K.; Wooley, K. L., Sequential and single-step, one-pot strategies for the transformation of hydrolytically degradable polyesters into multifunctional systems. *Macromolecules* **2008,** *41*, 1618-1626.

32. Wiltshire, J. T.; Qiao, G. G., Degradable core cross-linked star polymers *via* ring opening polymerization. *Macromolecules* **2006,** *39*, 4282-4285.

33. Pitt, C. G., Non-microbial degradation of polyesters: Mechanisms and Modifications. In *Biodegradable Polymers and Plastics*, Vert, M.; Feijen, J.; Albertson, A.; Scott, G.; Chiellini, E., Eds. The Royal Society of Chemistry: Cambridge, 1992; pp 7-19.

34. Höglund, A.; Hakkarainen, M.; Albertson, A.-C., Degradation profile of poly(epsilon-caprolactone)--the influence of macroscopic and macromolecular

biomaterial design. *Jounal of Macromolecular Science, Part A: Pure and Applied Chemistry* **2007,** *44*, 1041-1046.

35. Jackson, C.; Barth, H. G., Molecular weight sensitive detectors for size exclusion. In *Handbook of Size Exclusion Chromatography and Related Techniques*, Wu, C.-S., Ed. Marcel Dekker, Inc.: New York, 2004; Vol. 91, pp 99-138.

36. Hiemenz, P. C.; Lodge, T. P., *Polymer Chemistry*. 2nd ed.; CRC Press: New York, 2007.

37. Hoskins, J. N.; Grayson, S. M., Synthesis and degradation behavior of cyclic poly(epsilon caprolactone). *Macromolecules* **2009,** *42*, 6406-6413.

38. Hu, Y.; Jiang, Z.; Chen, R.; Wu, W.; Jiang, X., Degradation and degradation-induced re-assembly of PVP-PCL micelles. *Biomacromolecules* **2010,** *11*, 481-488.

39. Tian, D.; Dubois, P.; Grandfils, C.; Jérôme, R., Ring-opening polymerization of 1,4,8-trioxospiro[4.6]-9-undecanone: A new route to aliphatic polyesters bearing functional pendant groups. *Macromolecules* **1997,** *30*, 406-409.

40. Tian, D.; Dubois, P.; Jérôme, R., Macromolecular engineering of polylactones and polylactides 23. Synthesis and characterization of biodegradable and biocompatible homopolymers and block Copolymers based on 1,4,8-trioxa[4.6]spiro-9-undecanone. *Macromolecules* **1997,** *30*, 1947-1954.

41. Tian, D.; Dubois, P.; Jérôme, R., Poly(2-oxepane-1,5-dione): A highly crystalline modified poly(epsilon-caprolactone) of a high melting temperature. *Macromolecules* **1998,** *31*, 924-927.

42. Latere, J.-P.; Lecomte, P.; Dubois, P.; Jérôme, R., 2-Oxepane-1,5-dione: A precursor of a novel class of versatile semicrystalline biodegradable (co)polyesters. *Macromolecules* **2002,** *35,* 7857-7859.

43. Latere Dwan'Isa, J.-P.; Lecomte, P.; Dubois, P.; Jérôme, R., Synthesis and characterization of random copolyesters of epsilon-caprolactone and 2-oxepane-1,5-dione. *Macromolecules* **2003,** *36,* 2609-2615.

CHAPTER FIVE

CONCLUSIONS

Chapter 5

Conclusions

Using poly(ε-caprolactone-*co*-2-oxepane-1,5-dione) (P(CL-*co*-OPD)) as a platform polyester system, a series of functional, degradable polyester materials were synthesized and characterized. Taking advantage of the electrophilic ketone moiety present in the OPD units, a "grafting onto" approach using nitrogen-based nucleophiles was employed for the incorporation of chromophores, small molecules, and hydrophilic polymer grafts, and provided a versatile functionalization strategy for the creation of a diversity of materials. The work in this dissertation took advantage of hydrazone and ketoxime ether formation to create and study functional, degradable poly(ε-caprolactone)-based materials with unique solvatochromic, thermal, and hydrolytic degradation characteristics.

As a first step towards incorporating functionality onto a PCL backbone, multiple dansyl moieities were reacted with the electrophilic ketone units present along the backbone of P(CL-*co*-OPD) with a 58% grafting efficiency. Derivatization of the polyester backbone was confirmed by the appearance of aromatic resonances in the ^{1}H NMR and ^{13}C NMR spectra, which displayed resonances indicative of hydrazone formation. Analysis of the resulting fluorescent polymer by gel permeation chromatograpy equipped with an inline UV-visible detector, showed that chromophore absorption and the retention time of the polymer converged, thus verifying that covalently bound dansyl groups were the source of absorption and emission.

The dansyl-functionalized polymer was also characterized by fluorescence emission spectroscopy in a series of organic solvents, and displayed solvatochromic behavior with a general increase in the maximum emission wavelength (λ_{em}) with increasing solvent polarity. The λ_{em} of the dansylated P(CL-*co*-OPD) and the λ_{em} of a dansyl-derivatized small molecule analog were plotted against three solvent polarity parameters: the dielectric constant, Dimroth's $E_T(30)$, and π^*. From these analyses it was determined that the λ_{em} of the polymer-bound dansyl fluorophore did not display as marked a sensitivity to the polarity of the surrounding solvent as did the small molecule.

While hydrazone formation was not a highly efficient method for the derivatization of the P(CL-co-OPD) backbone, a highly efficient strategy taking advantage of ketoxime ether formation, was employed to yield a functional amphiphilic graft copolymer system, with up to 90% grafting efficiency. This methodology was used for the incorporation of both hydrophilic poly(ethylene oxide) (PEO) grafts and *p*-methoxybenzyl (*p*MeOBn) side chains onto the backbone of P(CL-*co*-OPD) allowing for the creation of functional PCL-*g*-PEO ketoxime ether conjugates that self assembled in aqueous solution. An amphiphilic block graft copolymer system bearing only PEO grafts formed spherical aggregates in aqueous solution, whereas a copolymer system derivatized with both PEO and *p*MeOBn grafts was found to form rod-like or cylindrical aggregates.

These same amphiphilic PCL-PEO ketoxime ether conjugates were found to undergo rapid hydrolysis upon dispersion in aqueous solution. The degradation of PCL-*g*-PEO polymer systems synthesized from a P(CL-*co*-OPD) platform was found to occur as a function of having uncapped OPD units present along the polyester backbone. Two different PCL-PEO graft copolymers of differing lengths, P(CL_{92}-*co*-OPD_5-*co*-(OPD-*g*-

PEO)$_9$), and P(CL$_{327}$-*co*-OPD$_{22}$-*co*-(OPD-*g*-PEO)$_{15}$-*co*-(OPD-*g*-*p*MeOBn)$_8$), displayed degradation behavior that was consistent with rapid hydrolysis at various points along the polyester backbone. GPC analysis of the degradable graft copolymers as they remained in aqueous solution at room temperature over 24 h also revealed unique behavior (an initial decrease followed by an apparent increase in peak molecular weight) that indicated that the polyester backbone was not only undergoing hydrolytic degradation, but that degradation resulted in an alteration in polymer architecture observable by GPC. By comparison, no degradation was observed over a 24 h period for P(CL$_{92}$-*co*-(OPD-*g*-PEO)$_8$-*co*-(OPD-*g*-*p*MeOBn)$_6$, a polyester where all of the ketone moieties had been derivatized. This investigation in conjunction with prior studies that described OPD as a site of enhanced degradation supports a mechanism whereby the PCL backbone of the graft copolymer undergoes a rapid and selective chain scission at the more hydrophilic OPD units statistically dispersed throughout the backbone.

Morphological changes associated with degradation were also observed in the amphiphilic block graft copolymers possessing unfunctionalized OPD units. P(CL$_{92}$-*co*-OPD$_5$-*co*-(OPD-*g*-PEO)$_9$) formed spherical aggregates that increased in size as a function of hydrolytic degradation of the hydrophobic PCL-based core. More interestingly, the larger P(CL$_{327}$-*co*-OPD$_{22}$-*co*-(OPD-*g*-PEO)$_{15}$-*co*-(OPD-*g*-*p*MeOBn)$_8$) displayed a change in the shape of the solution state aggregates as a consequence of degradation. A transition from spherical nanostructures to self-assembled aggregates possessing a rod-like or cylindrical morphology was observed as hydrolysis of the PCL backbone progressed.

The ability to control and manipulate both the degradation and the micellar morphology of polyester-based materials through the incorporation or derivatization of OPD units is a valuable tool for altering the physical and chemical characteristics of the resulting nanoobjects. This unique degradability provides a compelling approach for the creation and application of unique hydrolytically degradable materials based upon PCL-PEO ketoxime ether conjugates synthesized from a P(CL-*co*-OPD) platform. It is important to continue to explore the chemistries involving the grafting of polymer chains and small molecule ligands onto P(CL-*co*-OPD) copolymers, and efforts to better understand the way in which the density of PEO grafts and the incorporation of small hydrophobic side chains affect the self-assembly and degradation process should be pursued. Further exploration of PCL-*g*-PEO copolymers produced from this system and the specific mechanism of micellar degradation resulting in morphological changes should be investigated in more depth as these materials provide a unique modular platform for the creation of a variety of complex functional nanostructures with the potential for tunable degradability.